

# **Appendix A**

---

*Stratigraphic and Lithologic Descriptions*



## **A-1.0 CRIN-1 WELL**

### **Alluvium (0–100 ft below ground surface [bgs])**

The light brownish-gray alluvium consists of a mixture of minor devitrified tuff, pumice, dacite, and sandstone fragments in a tuffaceous matrix. The fragments are partially coated with silty matrix. The sediment is moderately sorted and unconsolidated. The mineral and sandstone contents appear to increase with depth. The lower part of the tuffaceous sediment is light pinkish gray, poorly sorted, and unconsolidated. With depth, abundant gray and pinkish pumice fragments and minor devitrified tuff and variable amounts of dacite lava fragments are noted. The crystal content also appears to be lower.

### **Otowi Member of the Bandelier Tuff (100–240 ft bgs)**

The cuttings consist of poorly sorted, clast-supported gray pumice with minor light brownish-gray wood-chip-like pumices. Variable amounts of dacite fragments are mixed with the pumices in the upper part of the ash-flow tuff. Abundant quartz and feldspar grains are also noted. The pumices, crystals, and dacite fragments are lightly coated with tuffaceous silt. Lithic-rich ash-flow tuff is dominant with depth, and in some cases, more dacite fragments are present than gray pumice in the cuttings. Some pumice clasts exhibit-rust like stains on the surface.

### **Guaje Pumice Bed of the Bandelier Tuff (240–260 ft bgs)**

The upper part of the pumice deposit is lithic-rich and contains more dacite lava fragments than white pumice and abundant coarse minerals. The lava fragments consist of light to medium gray and pale red dacite. It is poorly sorted, clast-supported, and unconsolidated. In contrast, the lower part is dominated by fallout of gravely white pumice of comparable clast sizes. Fewer medium-gray dacite and scoriaceous basalt fragments were noted within the lower cuttings.

### **Cerros del Rio Volcanic Rocks (260–675 ft bgs)**

No upper Puye Formation sediments were encountered below the Guaje Pumice Beds. Instead, a thick (40-ft) reddish to dark brown clast-supported and poorly to moderately sorted scoria deposit unconformably underlies the Guaje Pumice Bed. Medium-gray vesicular basalt mixed with reddish-brown scoria occurs beneath the scoria deposit. The lava sequence is dominated by porphyritic medium-gray flow that contains plagioclase and partially altered and fractured pyroxene and olivine mostly in the microcrystalline matrix. Porphyritic dark gray lava with abundant plagioclase, olivine, and pyroxene embedded in a microcrystalline matrix was intersected below the medium gray flow and above oxidized and partially altered lava. The lower half of the lava sequence (430–700 ft bgs) consists of medium-gray lava that is porphyritic and contains abundant pyroxene olivine phenocrysts within a microcrystalline matrix. The mafic minerals are coarse and partially fractured. A minor fraction of scoria and oxidized lava fragments occur with the medium-gray fragments.

Homogeneous cuttings of a medium-gray lava that is sparsely vesicular and porphyritic, devoid of scoria or oxidized fragments was encountered in the lowermost part of the volcanic sequence mixed with abundant light pinkish-gray siltstone (570–590 ft bgs). No cuttings were recovered from the interval 590 to 700 ft bgs. However, at 700 ft bgs, the cuttings consisted of medium-gray lava fragments mixed with light to medium-gray subrounded to rounded dacite clasts that are lightly coated with light grayish-brown silt.

### **Puye Formation (675–960 ft bgs)**

Mixture of abundant basalt fragments and minor sandstone and dacite clasts coated with silty matrix define the transition from the Cerro del Rio volcanic lava to the Puye Formation sedimentary deposit. The Puye Formation is dominated by gravely to coarse sand sediments with minor amounts of minerals and matrix fractions. The gravel to coarse sand fragments consist of mostly subangular to subrounded, clast-supported, and moderately to poorly sorted clasts. At least two types of lithic fragments with variable abundances are present within the sedimentary sequence. In most cases, light- to medium-gray dacite fragments are the dominant fractions but sometimes, pale red lava clasts are either of comparable abundance or more. Except for a few intervals, the Puye Formation sequence is dominated by gravely sand of light- to medium-gray and pale red dacite fragments. The sandy intervals that occur within the upper and lower parts of the sedimentary sequence also contain similar lithologic fragments and represent well-sorted fractions.

More pale red lava fragments than the light- to medium-gray dacite fractions are noted in the lowermost part of the sequence. White pumice fragments also occur in the lowermost part of the well. The pumice clasts are rounded and increase in abundance with depth even though the light- to medium-gray and pale red lava fragments are more abundant.

### **Miocene Pumiceous and Miocene Jemez Alluvial (960–1040 ft bgs)**

The Miocene pumiceous deposit is defined by pumiceous sand with minor dacite fragments up to 1 in. in diameter. The pumice fragments are lightly coated with light brownish-gray tuffaceous silt. Quartz and feldspar minerals are present but less abundant compared with the pumice clasts. The pumiceous sand deposits become coarser and gravely with depth. Two types of pumice fragments of comparable amounts are present in the lower part of the unit. The reworked pumice is subrounded to rounded and light brownish-gray on the outside and white inside. The white pumice clasts are angular to subangular. Some of the pumice fragments are up to 0.5 in. in length. The white pumice decreases with depth and is completely replaced with the reworked pumice in the lowermost part of the deposit. Minor lava fragments of dacite, basalt, and scoria were also noted. Quartz and feldspars are sparse.

## **A-2.0 CRIN-2 WELL**

### **Alluvium (0–60 ft bgs)**

The alluvium sequence consists of silty to sandy tuffaceous sediments containing abundant quartz and feldspar minerals mixed with minor sandstone, tuff, and lava fragments, which are lightly coated with tuffaceous silt. The sediments are generally sorted and unconsolidated. The crystal contents vary randomly with depth. In the middle part of the section, well-sorted quartz and feldspar grains that are lightly coated with pulverized silty glass mostly dominate the sediments. At the base of the sequence, the tuffaceous alluvium is medium-gray, matrix-supported, moderately sorted, and partially consolidated. Crystals are sparse within the silty tuffaceous sand but light- to medium-gray dacite clasts and pumice were noted.

### **Cerro Toledo Formation (60–110 ft bgs)**

The tuffaceous alluvium directly overlies light- to medium-gray pumice deposit that is well sorted and clast-supported. Minerals and lithic fragments are sparse. The pumice fragments are angular to subrounded and lightly coated with light brown and light pinkish-gray silty tuffaceous matrix. The lower

half of the sequence is crystal- and lithic-rich tuffaceous sand. It is matrix-supported. The pumice fragments are white to light gray and angular to subrounded. Lithic fragments and the mineral grains are lightly coated with silty glass fraction. The felsic lava fragments are subrounded and light pinkish to reddish gray. A few grains of obsidian and perlite fragment that are mostly present within the Cerro Toledo Formation were also noted.

#### **Otowi Member (110–270 ft bgs)**

The tuff is pinkish-gray, matrix-supported and poorly sorted. It contains abundant quartz and feldspar minerals, pumice and less abundant lava fragments. The minerals and lithic fragments are moderately coated with pinkish silt of glass shards. Lava fragments are less abundant compared with pumice fragments. The pinkish color may be the result of alteration.

The pinkish-gray ash-flow tuff transitions to gray, matrix-supported, poorly sorted pumice mixed with abundant quartz and feldspar grains. The pumice clasts are subrounded. The dacite fragments are gray to light pinkish-gray and light brown and are less abundant compared with the gray pumice fraction. The pumice, minerals, and lithic fragments are lightly coated with silty tuffaceous fraction. Some of the gray pumice fragments have isolated rusty patches that are more prevalent in the upper part of the lower half of the sequence. Also, the amount of dacite fragments randomly varies with depth.

#### **Guaje Pumice Bed of the Bandelier Tuff (270–300 ft bgs)**

The pumice fallout unit consists of well-sorted, clast-supported white pumice. It is mixed with abundant quartz and feldspar grains and minor amounts of lava fragments. Pumice fragments are mostly angular. The mineral grains, pumices, and the lava fragments are lightly coated with silty tuffaceous matrix. White pumice is the dominant fraction, but the amount of lava fragments appears to increase with depth.

#### **Cerros del Rio Volcanic Rocks (300–740 ft bgs)**

The upper Puye Formation is generally occurs beneath the Guaje Pumice Bed. However, in the CrIN-2 well, scoriaceous basaltic lava directly underlies the Gujae Pumice Bed. The lava flow is dark gray, vesicular, partially glassy, and fairly porphyritic with phenocrysts of olivine, pyroxene, and plagioclase. The lava flow becomes more scoriaceous and pulverized with depth and contains mixed reddish and medium-brown scoria fragments. The scoriaceous deposits transition with depth to medium-gray lava, which contains olivine, pyroxene, and plagioclase. In the middle section of the volcanic sequence, the medium-gray lava is mixed with light pinkish-gray claystone fragments (520–530 ft bgs) and a few glassy scoria fragments.

In the upper part of the lower half of the volcanic sequence, comparable amounts of medium gray and vesicular dark gray lava fragments were noted. The dark gray fraction appears more porphyritic. However, the medium-gray lava is the dominant lava flow in the lower half of the volcanic sequence. More light pinkish-gray claystone fragments (630–640 ft. bgs) were noted in the lower part of the section. Porphyritic and sparsely vesicular dark gray lava with minor palagonitized fragments defines the base of the Cerro del Rio section. Abundant pinkish-gray claystone and a few light gray dacite fragments were also noted.

#### **Puye Formation (740–990 ft bgs)**

In the uppermost part, the Puye Formation consists of fairly sorted coarse sand, containing light gray, angular to subrounded felsic fragments mixed with abundant basaltic and quartz and feldspar grains. Few

pumice fragments were also noted. The coarse sand transitions to clast-supported gravel ( $\leq 0.75$  in.) beds that are mostly sorted. The subrounded lithic fragments are mostly dacitic, but rhyolite clasts were also noted. The rest of the section contains alternating beds of gravel and coarse sand. The coarse sand to gravelly sand fractions are generally matrix-supported and fairly sorted, whereas the gravel beds are mostly sorted, clast-supported and lightly coated with light brownish-gray tuffaceous silt. Most fragments are  $\leq 1$  in. in diameter. Abundant quartz and feldspar grains plus minor mafic minerals occur within the sandy layers. Rendija Canyon dacite fragments were noted, starting at a depth of 900–910 ft. bgs. Gravel deposits that transition to gravelly sand dominate the lowermost part of the Puye Formation. Even though the lava fragments are clast-supported and matrix-free, all clasts are lightly coated with tuffaceous silt.

### **Miocene Pumiceous (990–1062 ft bgs)**

The Miocene pumiceous deposit is defined by pumiceous sand with minor dacite fragments up to 1 in. in diameter. The pumice fragments are lightly coated with light brownish-gray tuffaceous silt. Quartz and feldspar minerals are present but less abundant compared with the pumice clasts. The pumiceous sand deposits become coarser and gravelly with depth. Two types of pumice fragments of comparable amounts are present in the lower part of the unit. The reworked pumice is subrounded to rounded and light brownish-gray on the outside and white inside. The white pumice clasts are angular to subangular. Some of the pumice fragments are up to 0.5 in. in length. The white pumice decreases with depth and is totally replaced with the reworked pumice in the lowermost part of the deposit. Minor lava fragments of dacite, basalt, and scoria were also noted. Quartz and feldspars are sparse.

## **A-3.0 CRIN-3 WELL**

### **Alluvium, Qal (0–30 ft bgs)**

The cuttings consist of light brownish-gray sand that is poorly sorted and contains unconsolidated rock fragments of variable amounts of pumice, tuff, dacite lava plus abundant crystals and organic matter. With depth, the sediments transition to tuffaceous silty sand that is fairly consolidated and sorted. The rock fragments and minerals are lightly coated with tuffaceous silt. The lowermost part of the alluvium is gravelly silty sand, poorly sorted, and unconsolidated. Minerals and partially rounded pumice clasts are heavily coated with brownish silt.

### **Tshirege Member Unit 1g (30–70 ft bgs)**

The ash-flow tuff cuttings consist of light brownish-gray pumice clasts, coarse minerals, and minor dacite lava fragments that are lightly coated with pulverized glassy silt. The cuttings are poorly sorted and unconsolidated. More crystals and dacite lava fragments mixed with abundant pumice are noted in the lower part of the unit. The cuttings are mostly clast-supported with light coating of pulverized glass. A couple of perlite grains were noted in the lower part of the unit mixed with partially rounded pumice and dacite lava fragments.

### **Cerro Toledo Formation (70–110 ft bgs)**

The unit consists of lithic-rich, clast-supported reworked pumiceous sand containing abundant rounded to subrounded white to medium gray pumices that are moderately sorted and unconsolidated. Light- to medium-gray dacite lava fragments are less abundant compared with the amount of pumice. A few perlite and banded rhyolite fragments were also noted. Minerals are fine-grained and less abundant. The pumiceous sand transitions to poorly sorted gravelly coarse sand that is dominated by pumice with

variable amounts of light- to medium-gray and pale red dacite fragments. In some cases, the dacite fragments are coarser than the pumices. The crystal contents are also higher and variable in size. The cuttings from the basal section are light brownish-gray, moderately sorted and contain comparable amounts of pumice and dacite clasts that are lightly coated with tuffaceous glassy matrix. Minerals from the lowermost cuttings are coarser and more abundant and are also lightly coated with glassy silt. A few perlite grains were also noted.

#### **Otowi Member (110–330 ft bgs)**

The uppermost part of the unit consists of lightly weathered light-pinkish-gray ash-flow tuff, containing abundant pumices and crystals and minor light- to medium-gray and pale red dacite lava fragments that are partially covered with tuffaceous glassy matrix. More abundant pale red dacite fragments are noted than the light- to medium-gray fraction in deeper samples. The light pinkish-gray layer transitions with depth to light gray pumiceous coarse sand that is sorted, matrix-poor, and unconsolidated. Pumices and crystals are abundant, and more pale red dacite lava fragments are present. The minerals, pumices, and dacite fragments are lightly coated with glassy tuffaceous silt. In some cases, the cuttings (140–220 ft bgs) are pulverized, resulting in matrix-supported light gray fraction that is dominated by crushed pumice and crystals. In the lower part of the section, the Otowi Member cuttings are lithic-rich, clast-supported, and poorly to moderately sorted. Crystals are abundant and light- to medium-gray dacite lava clasts are more abundant than the pale red fraction. Pumice clasts are light gray to white.

#### **Guaje Pumice Bed of the Bandelier Tuff (330–340 ft bgs)**

The cuttings consist of clast-supported and moderately sorted equant fragments of white pumice mixed with abundant dark gray and pale red dacite fragments. Quartz and feldspar grains are fairly abundant. No matrix-glass coating was noted on the pumice, dacite lava fragments, or crystals.

#### **Upper Puye Formation (340–350 ft bgs)**

The clast-supported sediment is sorted and consists of abundant pumice and dacite lava fragments that are heavily coated with light reddish silty clay. The silt-coated pumice is from the overlying Guaje Pumice Bed that contaminated the underlying upper Puye Formation sediment during sampling.

#### **Cerros del Rio Volcanic Rocks (350–755 ft bgs)**

The uppermost cuttings consist of abundant fine-grained and dark gray basaltic lava fragments that are mixed with minor light to medium gray dacite and pumice clasts. Some basaltic fragments are scoriaceous and oxidized. With depth, the cuttings consist of partially oxidized medium- to dark-gray vesicular basalt with phenocrysts of plagioclase and fractured and weathered pyroxene and olivine. Most vesicle walls are coated with vapor-phase minerals and some are completely filled with secondary minerals. Medium-gray lava and minor dark gray vesicular basaltic fragments sparsely mixed with scoria are commonly noted in the cuttings from the upper and middle parts of the basaltic section. Generally the lower half of the lava sequence contains mostly medium-gray fragments and minor amounts of oxidized brown lava and scoria clasts. The medium-gray lava fragments are porphyritic and microcrystalline. Fractured and partially altered plagioclase, olivine, and pyroxene are the dominant phenocrysts. Moreover, minor light orange claystone fragments were encountered within the medium-gray lava-dominated cuttings (610–640 ft bgs).

### **Cerros del Rio Volcanic Rocks–Hydrovolcanic Sediment (745–755 ft bgs)**

The lowermost part of the Cerros del Rio volcanic sequence in CrIN-3 consists of microcrystalline and porphyritic medium-gray lava fragments that are mixed with minor fraction of medium gray, fine-grained, and platy clasts of weathered basaltic tuff deposit (Maar). The altered basaltic tuff appears similar to outcrops in Sandia and Los Alamos Canyons.

### **Puye Formation (755–1021 ft bgs)**

The cuttings from the Cerros del Rio volcanics and Puye Formation contact zone are heavily contaminated with medium gray basalt fragments (755–765 ft bgs). However, the next batch (765–770 ft bgs) contains very little or no basaltic lava fragment. Instead, the cuttings are dominated by a mixture of variable grain sizes and amounts of light to medium gray and pale red dacite fragments and a minor fraction of Rendija Canyon dacite fragments that are present throughout the Puye Formation. Fine- to coarse-grained and variable amounts of quartz, feldspar, and minor mafic minerals were mostly noted within the Puye Formation cuttings. In most cases, the cuttings are moderately sorted, clast-supported, and range in size from coarse to gravelly coarse sand. Fine-grained matrix fractions were insignificant or absent from the Puye Formation cuttings.

## **A-4.0 CRIN-4 WELL**

### **Tshirege Member Unit 2 (0–30 ft bgs)**

The partially pulverized and devitrified light brownish-gray ash-flow tuff consists of abundant nonwelded devitrified fragments mixed with significant amounts of quartz and feldspar that are lightly to heavily coated with pulverized tuffaceous silt. The pulverized fraction is poorly sorted and mostly clast-supported. The abundance of tuff fragments decreases with depth because of strong pulverization. Cuttings from the lower part of the unit are totally pulverized and are transformed to crystal-rich powdery fraction. The sandy fraction is light brownish-gray and sorted. Very few partially weathered lava fragments were noted within the pulverized cuttings.

### **Tshirege Member Unit 1v (30–150 ft bgs)**

The crystal-rich tuff is light to medium-gray, crystal-rich, and devitrified. The tuff fragments are nonwelded and mostly pulverized. Microcrystalline mineral aggregates are noted in cavities, and pumice clasts are totally replaced by fine-grained minerals. Abundant quartz and feldspars and minor lithic fragments are noted and are lightly coated with silty matrix of devitrified glass. The amount of the light- to medium-gray dacite lava fragments randomly varies within the unit.

### **Tshirege Member Unit 1g (150–230 ft bgs)**

The gray tuff is crystal- and lithic-rich and partially pulverized. The minerals and lithic fragments are lightly coated with silty matrix of pulverized glass shards. Angular to subrounded gray pumice clasts are commonly noted. In the middle part of the unit, the pumices and lithic fragments are coated with light pinkish-gray glassy matrix, whereas in the lower part, white and light pinkish-gray pumice clasts are present. A few grains of perlite were also noted.



### **Cerro Toledo Formation (230–250 ft bgs)**

The reworked pumices are clast-supported, poorly sorted, light pinkish to reddish-gray, subrounded to rounded, and are coated with tuffaceous silt. A few subrounded white pumice fragments are also present. Considerable amount of light- to medium-gray and minor pale red lava fragments are mixed with the pumices. Minerals are fine-grained and sparse, and a few rounded perlite clasts were also noted.

### **Otowi Member (250–500 ft bgs)**

The ash-flow tuff is poorly sorted, mostly clast supported, and contains abundant angular to subrounded light-pinkish-gray pumices and minor light- to medium-gray lava fragments. The amounts of the pumice and lava fragments randomly vary within the unit. The quartz and feldspar minerals are also variable. In the middle section of the unit, light to medium and pale red angular to subrounded lithic fragments are more abundant than the pumice contents. Unlike in the upper part of the unit, the pumices are mostly gray with rusty patches. The lithic and pumice contents vary with depth, and more white pumices are noted in the lower part of the unit.

### **Guaje Pumice Bed of the Bandelier Tuff (500–540 ft bgs)**

The pumice-rich deposit is moderately sorted, clast-supported, and contains minor medium- to dark-gray and pale red lava fragments that vary in abundance with depth. White pumice is the dominant fraction and the clasts are generally angular to subangular. Quartz and feldspar grains are fairly abundant. The mineral grains, pumices, and the lava fragments are lightly coated with silty glass shards matrix.

### **Upper Puye Formation (540–560 ft bgs)**

The sedimentary unit is poorly sorted and consists of abundant pinkish-gray silty sandstone mixed with medium- to dark-gray dacite and pumice clasts. The silty sandstone fragments are fine grained and indurated. The lava fragments and pumices are subrounded and are lightly coated with tuffaceous silty matrix.

### **Cerros del Rio Volcanic Rocks (560–900 ft bgs)**

Dark gray, fine-grained, and sparsely vesicular basalt underlies the upper Puye Formation. The vesicle walls are partially filled with secondary minerals. The underlying lava is medium-gray, fairly vesicular, and sparsely porphyritic, containing fractured and partially altered pyroxene, plagioclase, and olivine. Mixtures of medium-gray porphyritic lava and medium-brown scoriaceous fragments occur in the middle part of the volcanic sequence that transitions to underlying reddish-brown scoriaceous lava. The scoriaceous deposit is underlain by thick sequence of medium-gray porphyritic lava containing olivine, pyroxene, and plagioclase phenocrysts embedded in a matrix of microcrystalline mineral phases. The medium-gray lava fragments are vesicular, platy, and partially altered. A few pinkish-gray siltstone fragments were noted in the middle part of the lava sequence.

### **Puye Formation (900–1202 ft bgs)**

Mixture of abundant basalt fragments and minor sandstone and dacite clasts coated with silty matrix define the transition from the Cerro del Rio volcanic lava to the Puye Formation sedimentary deposit. The Puye Formation is dominated by gravely to coarse sand sediments with minor amounts of minerals and matrix fractions. The gravel to coarse sand fragments consist of mostly subangular to subrounded, clast-supported and moderately to poorly sorted clasts. At least two types of lithic fragments with variable

abundances are present within the sedimentary sequence. In most cases, light- to medium-gray dacite fragments are the dominant fractions, but sometimes pale red lava clasts are either of comparable abundance or more. Except for a few intervals, the Puye Formation sequence is dominated by gravely sand of light- to medium-gray and pale red dacite fragments. The sandy intervals that occur within the upper and lower parts of the sedimentary sequence also contain similar lithologic fragments and represent well-sorted fractions.

More pale red lava fragments than the light- to medium-gray dacite fractions are noted in the lowermost part of the sequence. White pumice fragments also occur in the lowermost part of the well. The pumice clasts are rounded and increase in abundance with depth even though the light- to medium-gray and pale red lava fragments are more abundant.

## **A-5.0 CRIN-5 WELL**

### **Tshirege Member, Unit Qbt 2 (0–40 ft bgs)**

The partially pulverized and devitrified light-brownish-gray ash-flow tuff consists of abundant nonwelded devitrified fragments mixed with significant amounts of quartz and feldspar that are lightly to heavily coated with pulverized tuffaceous silt. The pulverized fraction is poorly sorted and mostly clast-supported. The abundance of tuff fragments decreases with depth because of strong pulverization. Cuttings from the lower part of the unit are totally pulverized and are transformed to crystal-rich powdery fraction. The sandy fraction is light brownish-gray and sorted. Very few partially weathered lava fragments were noted within the pulverized cuttings.

### **Tshirege Member Unit Qbt 1v (40–160 ft bgs)**

The ash-flow tuff is nonwelded, poorly sorted, light- to medium-gray, devitrified, crystal-rich, and partially to mostly pulverized cuttings. The transition from Qbt 2 to Qbt 1v is marked by the appearance of devitrified or recrystallized well-preserved pumice morphology. The devitrified clasts form aggregates of clear, fine-grained crystals. In other cases, glassy matrix is recrystallized to microcrystalline groundmass. Dacite lava fragments are generally sparse. Cuttings from the lowermost part of the unit appear to contain more tuff fragments, crystals, and dacite lava fragments. The tuff fragments and the quartz and feldspar grains are lightly coated with light- to medium-gray powdery silt that is devitrified glass.

### **Tshirege Member Unit Qbt 1g (160–250 ft bgs)**

The ash-flow tuff consists of brick-red glassy pumice clasts mixed with minor medium- to dark-gray dacite lava fragments, and abundant clear quartz and feldspars. The tuff is sorted and clast-supported, and the fragments are not coated with matrix of pulverized glassy silt. The pumice clasts are subangular to subrounded and lava fragments are sparse. The brick-red pumices disappear with depth and are replaced by gray pumice, abundant crystals (i.e., feldspar and quartz), and lava fragments set within pulverized glassy matrix. A few obsidian fragments were also noted. The basal part of the unit consists of abundant clast-supported and sorted white to gray pumice mixed with minor dacite lava fragments and banded rhyolite.

### **Cerro Toledo Formation (250–280 ft bgs)**

The reworked pumice bed consists of mixed reddish-gray and rounded white pumices, minor dacite, few obsidian fragments, and crystals of variable grain sizes coated with tuffaceous silty matrix. Cuttings from the lowermost part of the unit is characterized by lithic-rich pumiceous sand of lithic-rich, clast-supported reworked pumiceous sand and few perlite grains coated with light reddish silt.

### **Otowi Member (280–560 ft bgs)**

The ash-flow tuff cuttings are crystal-rich, medium-gray, fairly sorted, clast-supported, and lightly coated with pulverized volcanic glass. Less abundant medium- to dark-gray lavas and other clasts are mixed with the crystals and pumices in the upper part of the unit. More varieties of lithic fragments, consisting of medium- to dark-gray and pale-red lavas, angular to subrounded light pinkish pumices, and less abundant crystals were noted in subsequent cuttings. With depth, more light brownish-gray pumices were encountered. In the middle part of the unit, the ash-flow tuff cuttings and pumices are mostly pulverized into sandy glassy matrix. A few grains of rounded obsidian and perlite grains mixed with abundant medium- to dark-gray lava clasts, gray pumices, and crystals occur in the lower half of the section. All fragments are lightly coated with pulverized glassy silt. The amounts of crystals and light to medium lava fragments appears to be more abundant than the coarse white to gray subrounded pumices in the lower half of the unit. The cuttings from the lower part of the unit contain variable amounts of pulverized glassy matrix.

### **Guaje Pumice Bed of the Bandelier Tuff (560–580 ft bgs)**

The cuttings are characterized by white, dense pumice clasts that are clast-supported and mixed with abundant coarse, clear crystals and medium- to dark-gray dacite lava fragments. The pumice clasts are moderately sorted and of comparable clast sizes. The crystals are also sorted and consist of quartz and feldspars. The cuttings are matrix-poor and unconsolidated.

### **Upper Puye Formation (580–610 ft bgs)**

The cuttings are dominated by reworked pumice sand that are coated with light brown silty matrix. Abundant lithic lava fragments that are similar to those noted in the overlying Guaje Pumice Bed are also present. With depth, the reworked pumiceous sand contains a mixture of white and light-brownish-gray pumice clasts and light- to dark-gray dacite fragments within light brown silty glassy matrix. In most cases, the upper Puye Formation consist of reddish-brown silty sandstone fragments that are massive and moderately indurated. The abundant pumice and lava fragments are most likely contaminants from the overlying Guaje Pumice Bed mixed during recovery of the cuttings.

### **Cerros del Rio Volcanic Rocks (610–970 ft bgs)**

Sparsely vesicular basaltic lava cuttings coated with silty tuffaceous glass matrix mixed with sandstone and pumice clasts were encountered directly below the upper Puye Formation (610–630 ft bgs). The basaltic fragments are porphyritic with microcrystalline matrix and are partially altered. Plagioclase and pyroxene were noted. Sparsely vesicular and partially weathered dark gray porphyritic lava, containing plagioclase, olivine, and fractured and altered pyroxene occurs below the contaminated cuttings. A few scoriaceous fragments were noted. At 660–690 ft bgs, sparsely vesicular, fine-grained, and medium-gray porphyritic lava with phenocrysts of plagioclase, olivine, and pyroxene was encountered. Vesicles walls are coated with microcrystalline vapor-phase minerals. A mixture of medium-gray and oxidized scoriaceous fragments were encountered about 30 ft (690–710 ft bgs) below the uppermost lava flow. Pulverized medium-gray porphyritic lava fragments with phenocrysts of plagioclase, olivine, and fractured pyroxene underlie the scoriaceous flow. The medium-gray lava is thick and persists with depth except for occasional dark gray lava fragments (850–860 ft bgs and 890–920 ft bgs) and minor contents of light pinkish-gray silty clay fragments (880–890 ft bgs). Medium-gray porphyritic lava fragments were intersected to the base of the Cerro del Rio lava sequence (960–970 ft bgs).

### **Puye Formation (970–1292 ft bgs)**

Clasts of light gray to pale red dacite, rounded quartzite, and sparse minerals in a coarse sandy fraction contaminated by abundant medium-gray lava fragments define the upper part of the Puye Formation. A few clasts of Rendija Canyon lava fragments were noted. More sorted and matrix-poor rounded to subangular dacite fragments are the dominant lithologic unit within the upper half (970–1140 ft bgs) of the formation. A layer of tuffaceous sand with dacite lava and minor Rendija Canyon clasts embedded in a silty matrix was intersected below the matrix-poor coarse sand. The silty sand transitioned back to sorted coarse sand with sparse mineral contents. The coarse fragments consisted of mixtures of light- to medium- and pale red dacite clasts. More dark gray rounded lava fragments and Rendija Canyon clasts were noted with depth. Crystal-poor and sorted coarse sand, consisting of light gray and light pale red dacite clasts mixed with Rendija Canyon lava fragments minor white pumice, were noted in the lower part of the drill hole (1240–1290 ft bgs).

## **Appendix B**

---

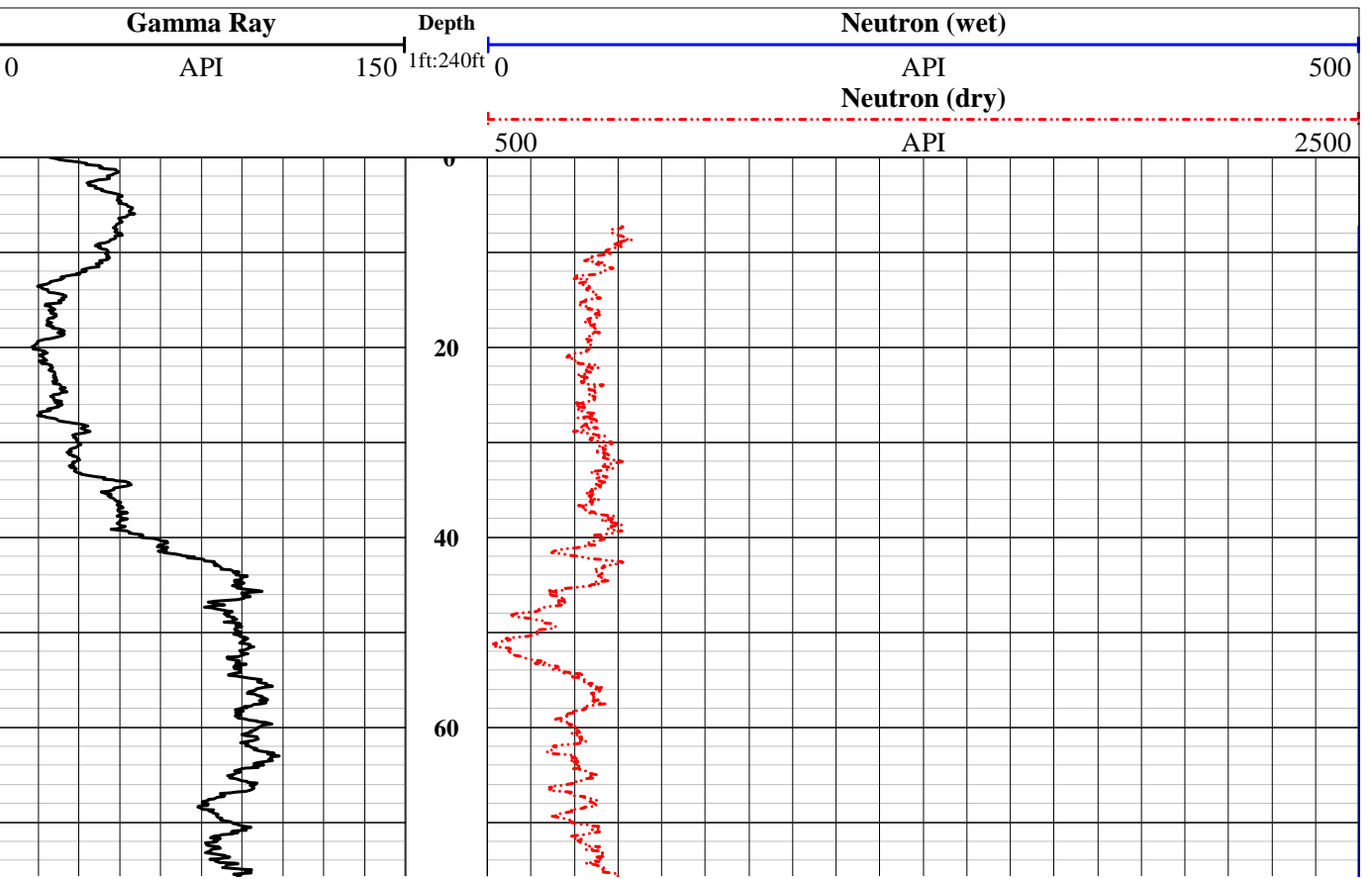
*Geophysical Logs*  
*(on CD included with this document)*

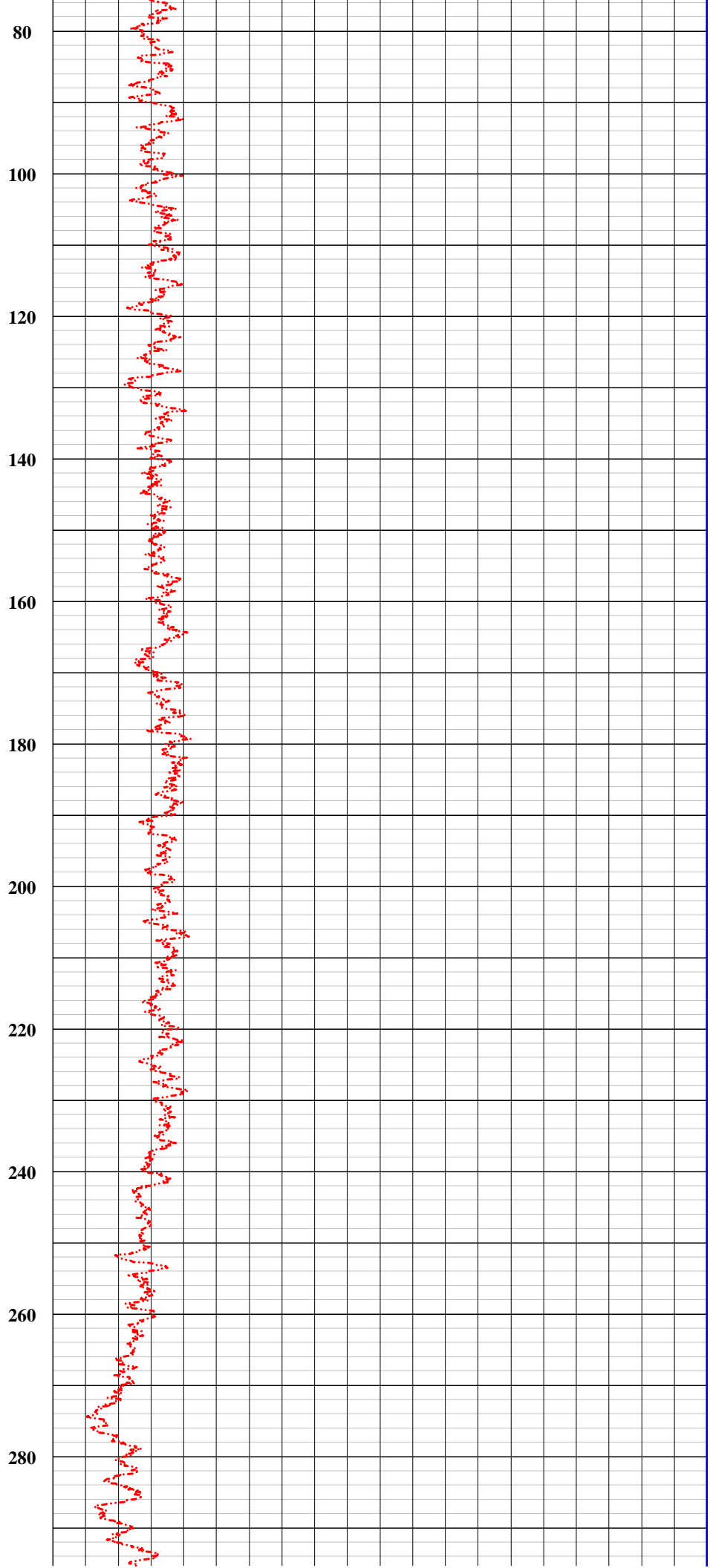
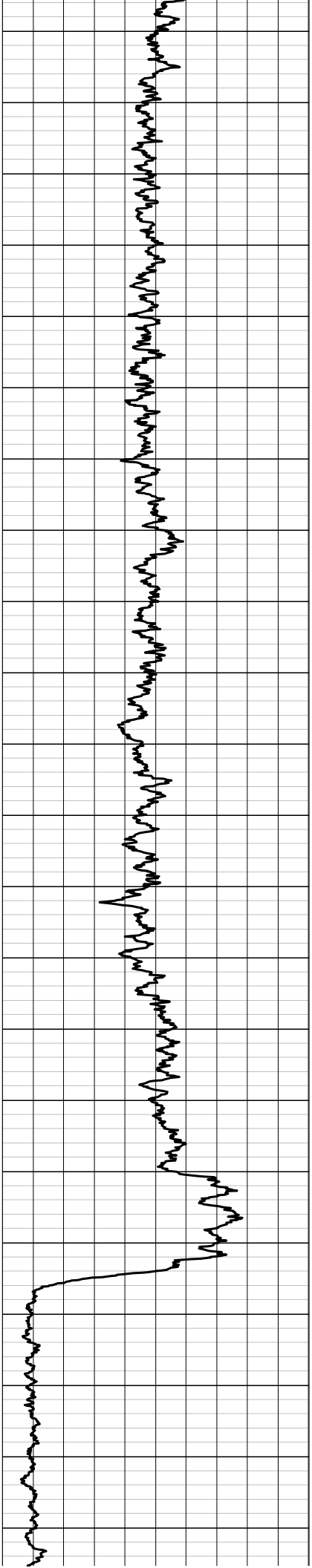


# JET WEST

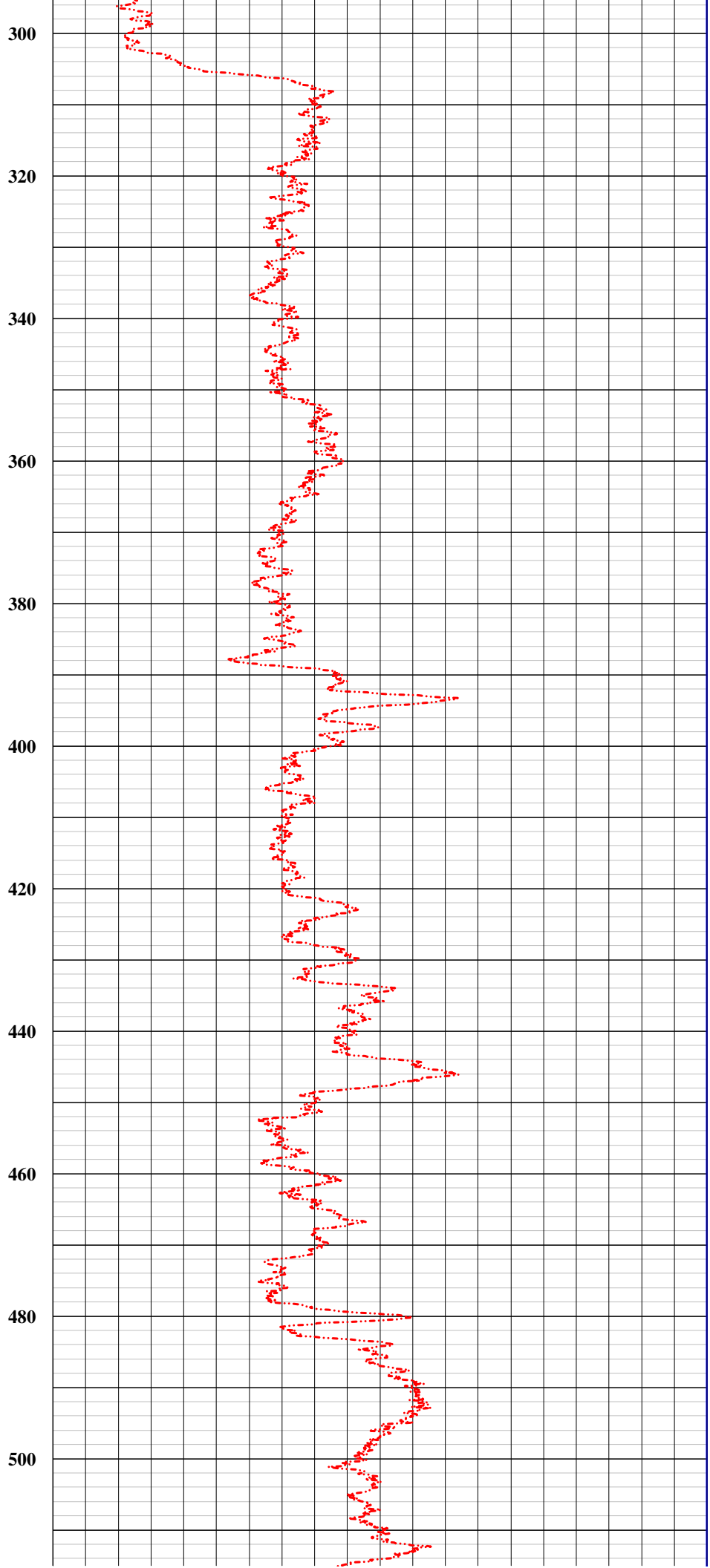
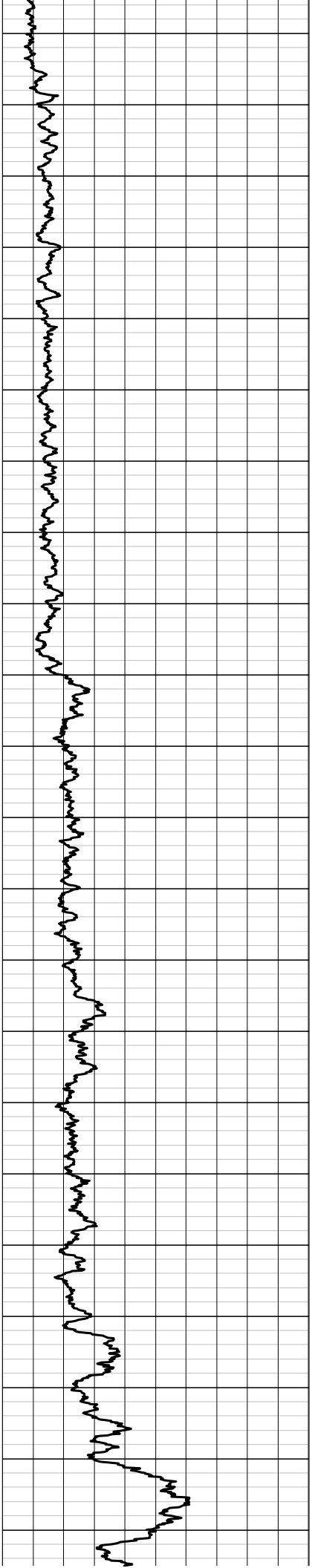
## GEOPHYSICAL SERVICES, LLC.

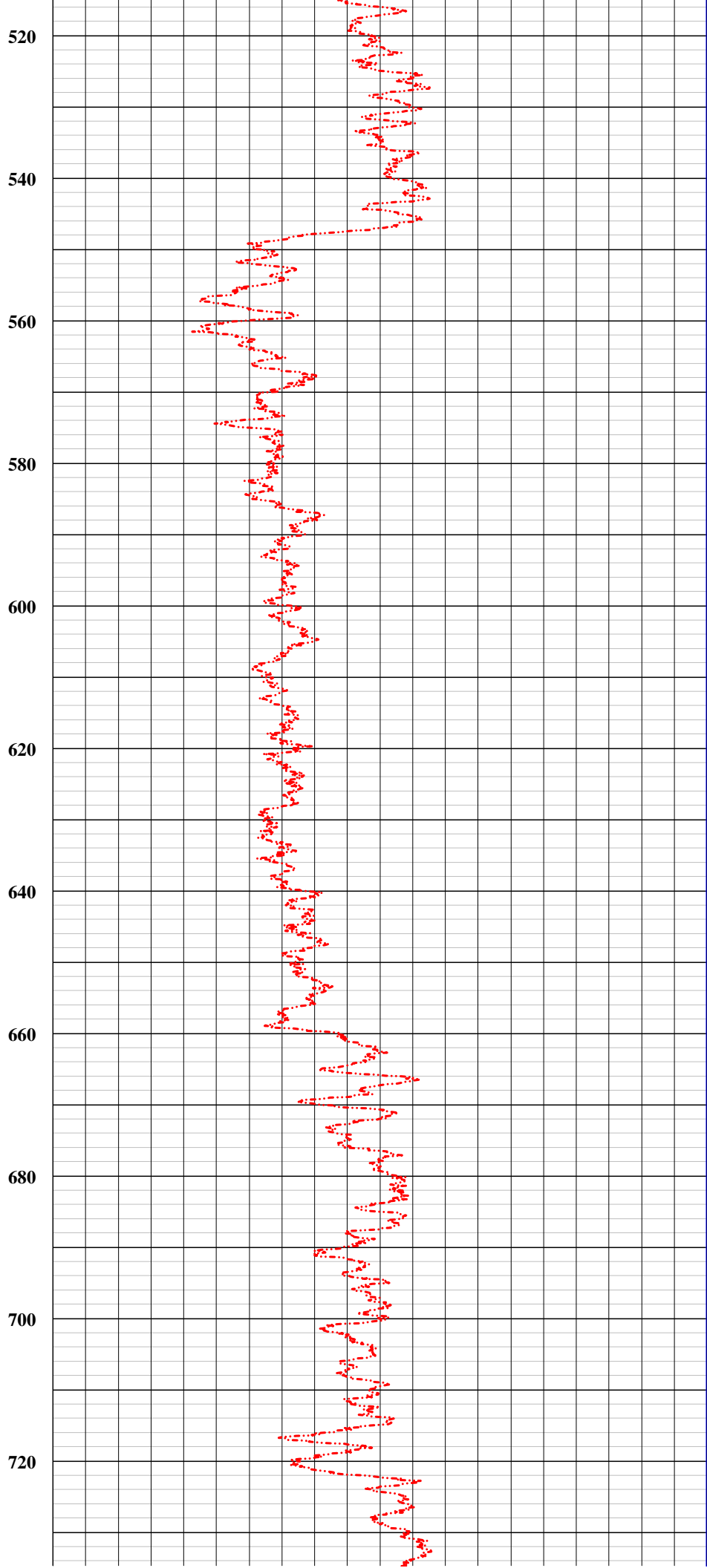
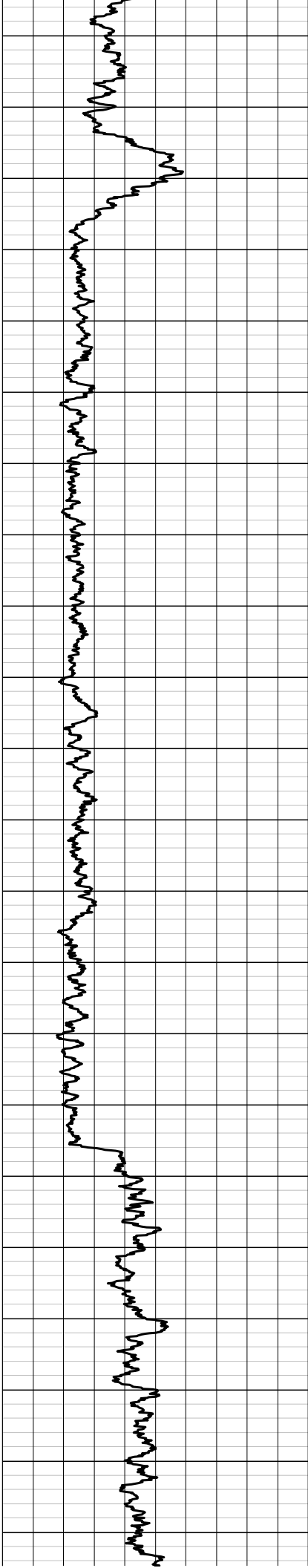
State Plane 1927		COMPANY		Las Alamos National Labs			
Northing:		WELL ID		Cin No.1			
Easting:		FIELD		LANL (Los Alamos National Labs)			
		COUNTY		Los Alamos			
		STATE		New Mexico			
		<b>TYPE OF LOG: Gamma Ray, Neutron Log</b>					
LOCATION		OTHER SERVICES		None			
SEC	TWP	RGE	API No.				
PERMANENT DATUM		Ground Level		ELEVATION			
LOG MEAS. FROM		Ground Level		ABOVE PERM. DATUM			
DRILLING MEAS. FROM		Ground Level		G.L.			
DATE	06-20-2016	TYPE FLUID IN HOLE		Air/water			
RUN No.	one	SALINITY					
TYPE LOG	QL-NB730	DENSITY					
DEPTH-DRILLER	1015 ft.	LEVEL		884 ft.			
DEPTH-LOGGER	1012 ft.	MAX. REG. TEMP					
BTM LOGGED INTERVAL	1011 ft.	DIGITIZE INTERVAL		0.1 ft.			
TOP LOGGED INTERVAL	Surface						
OPERATING RIG TIME							
RECORDED BY	A.Henderson						
WITNESSED BY	Yellowjacket Dtg.						
BOREHOLE RECORD		CASING RECORD					
RUN NO.	BIT	FROM	TO	SIZE	WGT.	FROM	TO
1				20 inch	steel	0 ft.	42 ft.
2				18 inch	steel	0 ft.	307 ft.
3				14 inch	steel	0 ft.	1040 ft.
REMARKS:							

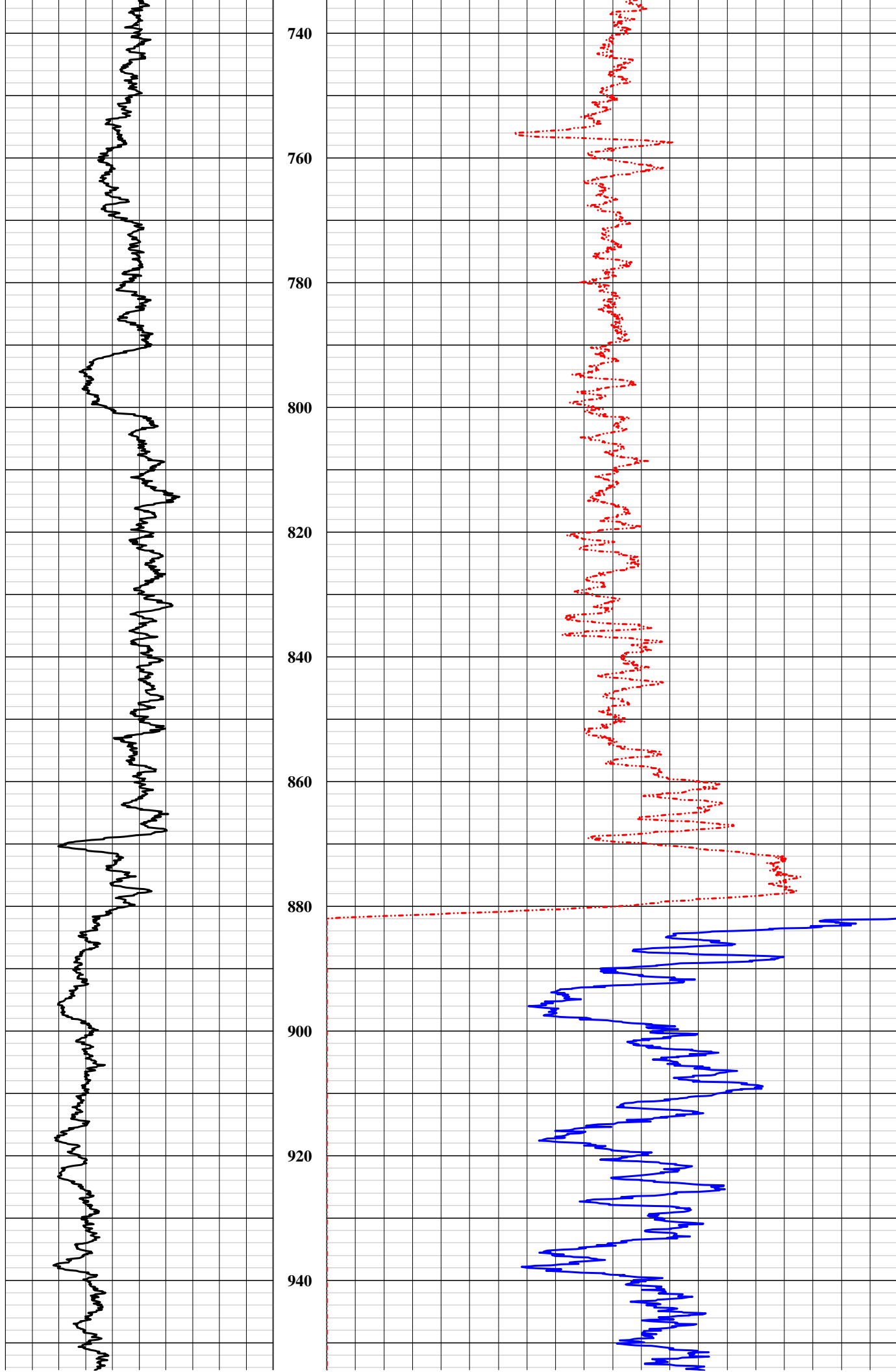


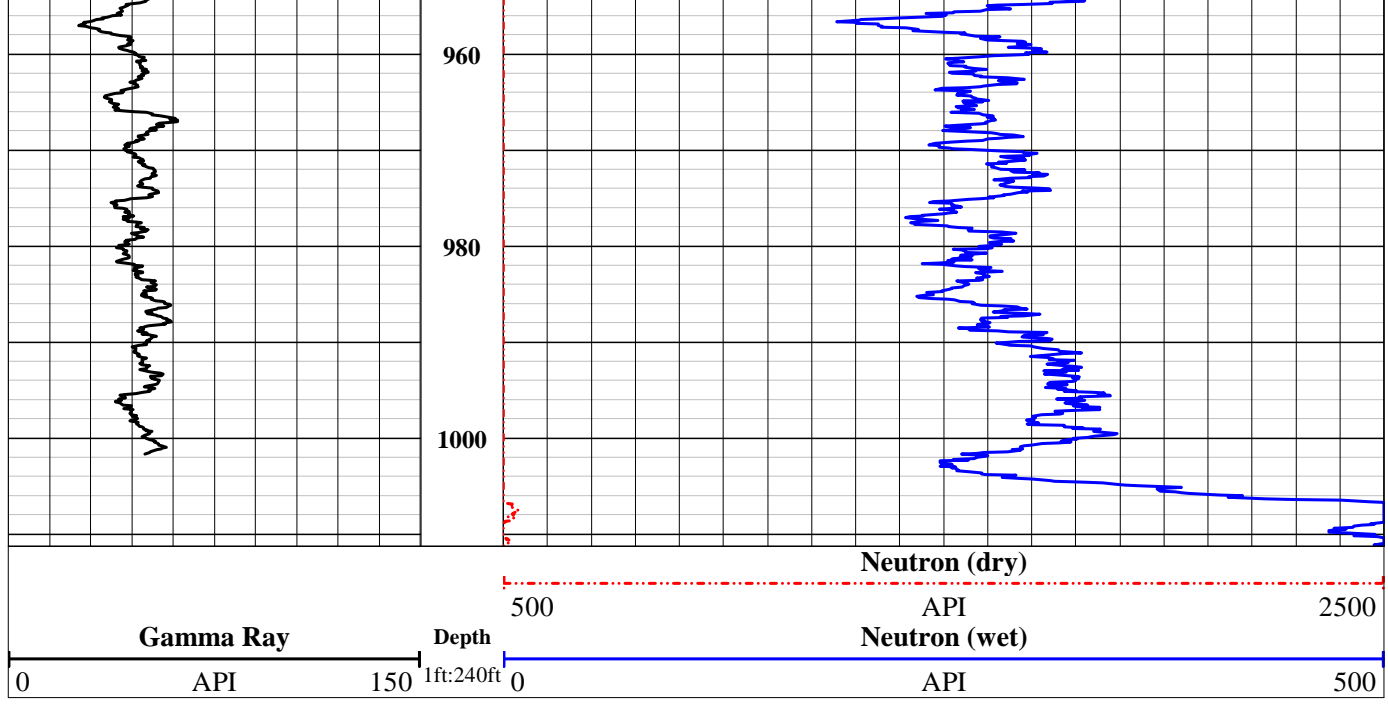












# JET WEST

## GEOPHYSICAL SERVICES, LLC.

State Plane 1927  
 Northing:  
 Easting:

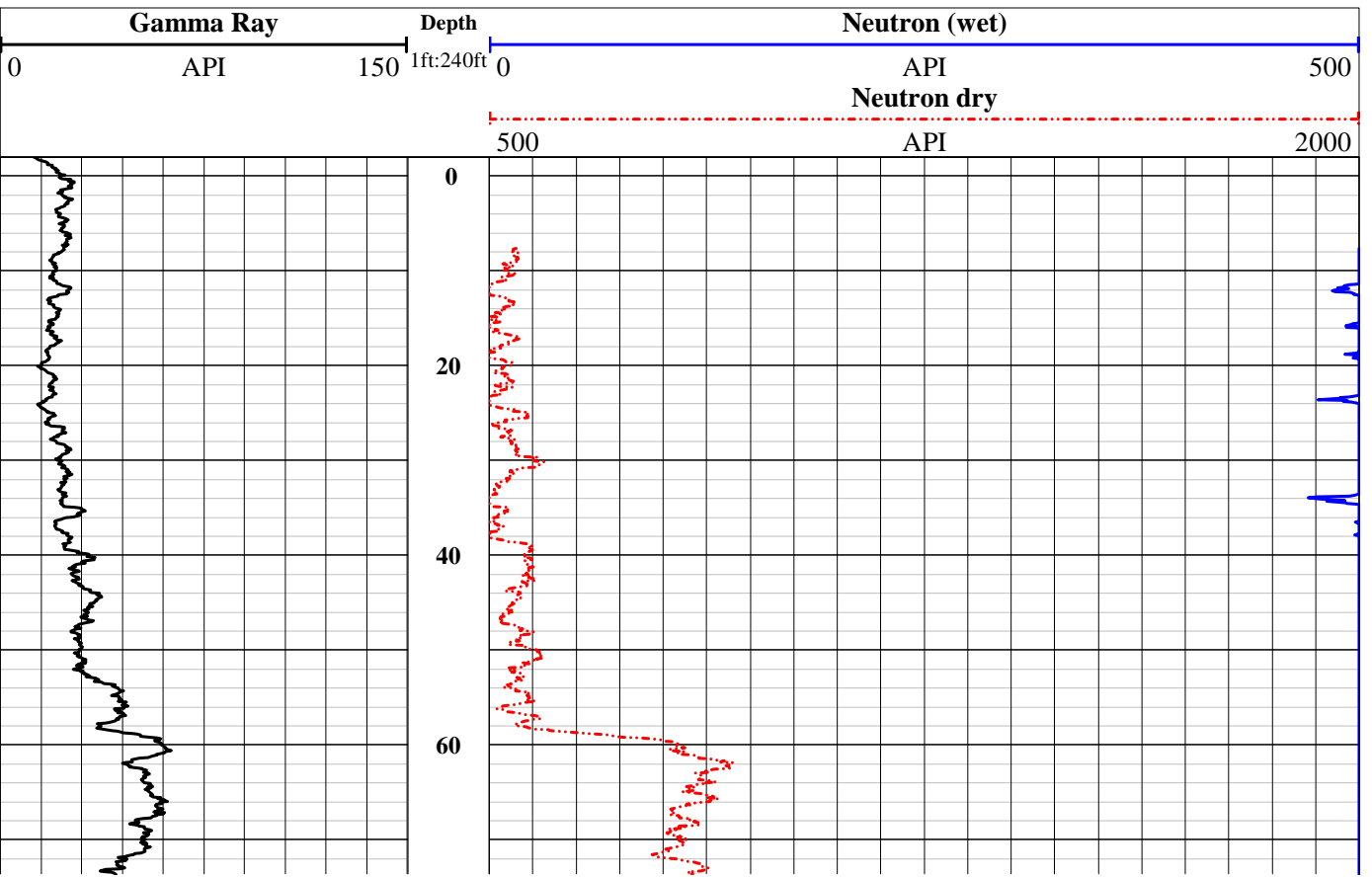
COMPANY Las Alamos National Labs  
 WELL ID Cin No.2  
 FIELD LANL (Los Alamos National Labs)  
 COUNTY Los Alamos STATE New Mexico  
**TYPE OF LOG: Gamma Ray, Neutron Log**  
 LOCATION  
 SEC TWP RGE  
 ELEVATION  
 PERMANENT DATUM Ground Level ABOVE PERM. DATUM  
 LOG MEAS. FROM Ground Level  
 DRILLING MEAS. FROM Ground Level

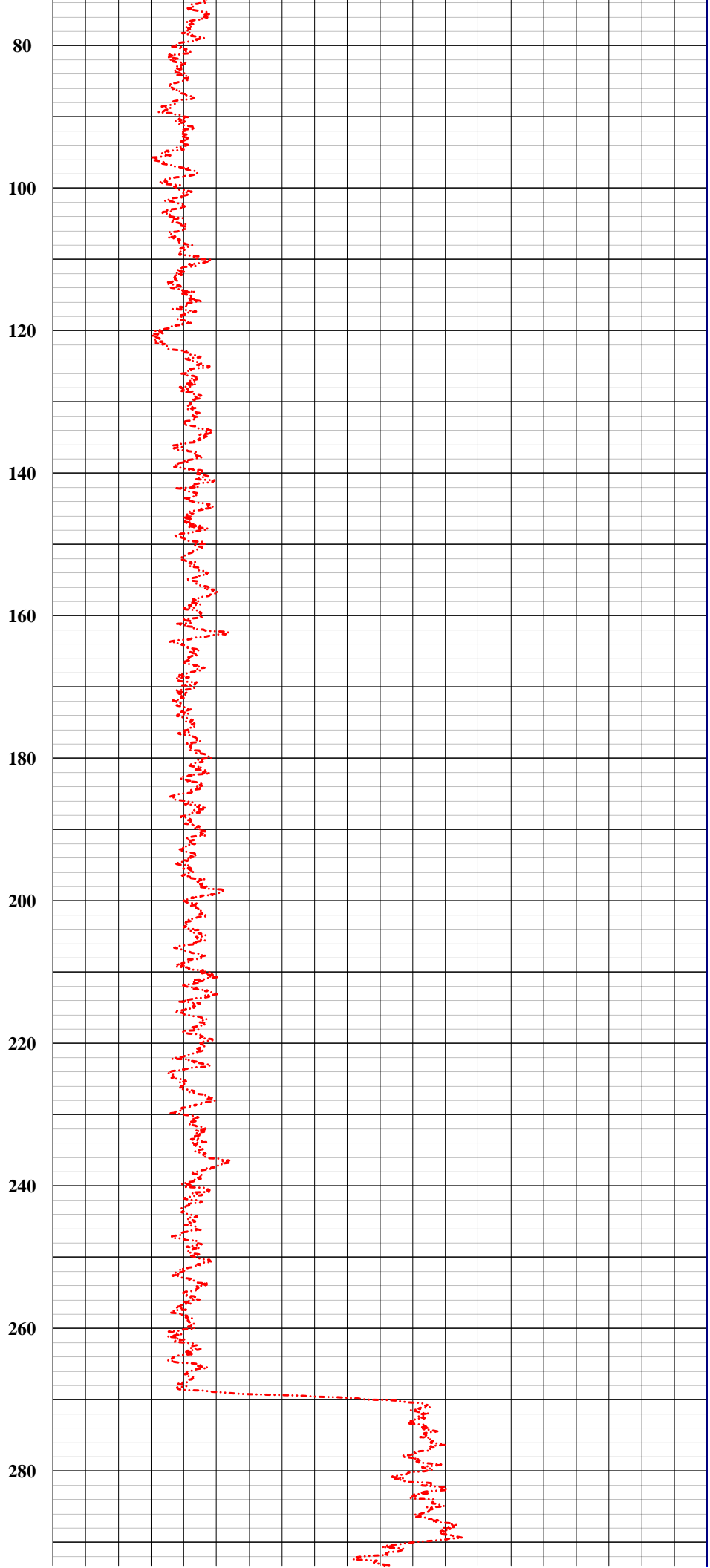
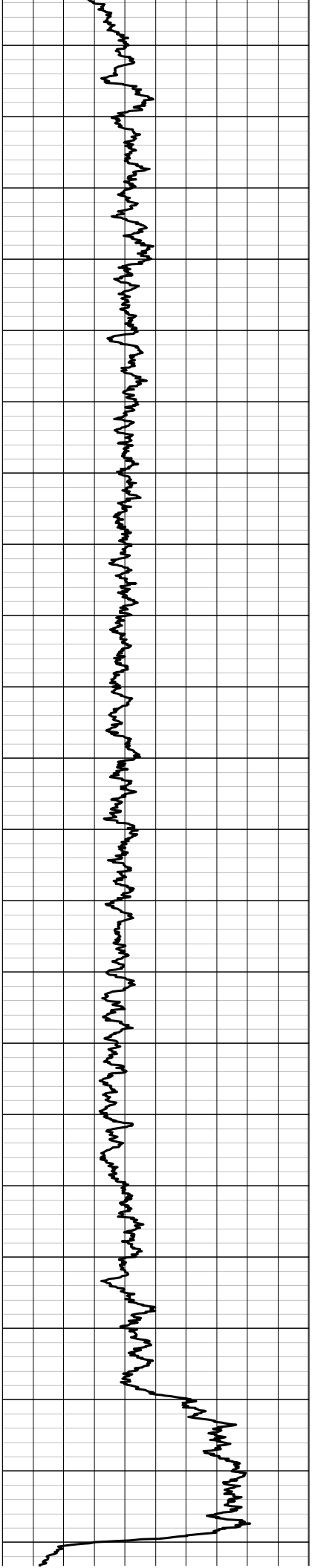
OTHER SERVICES  
 Density  
 Gamma Ray

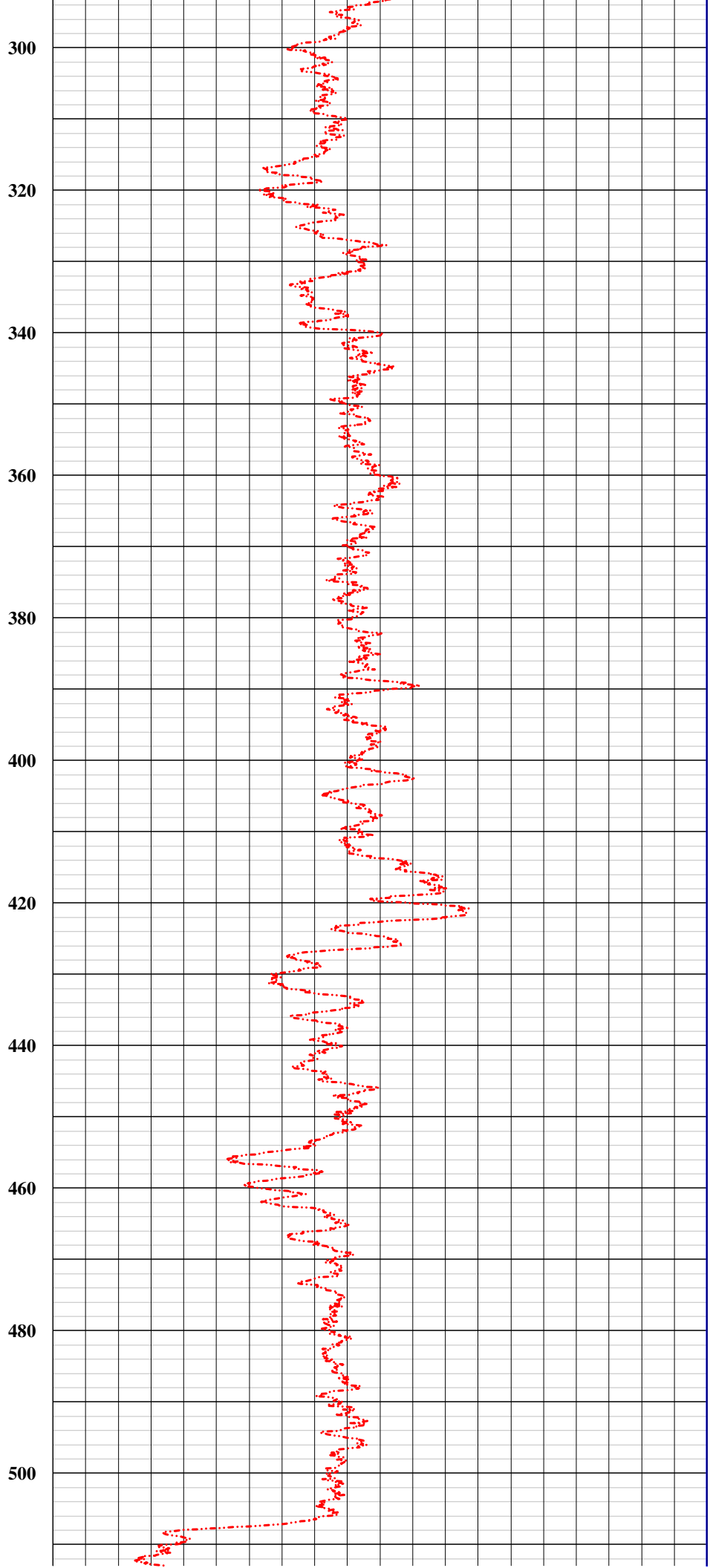
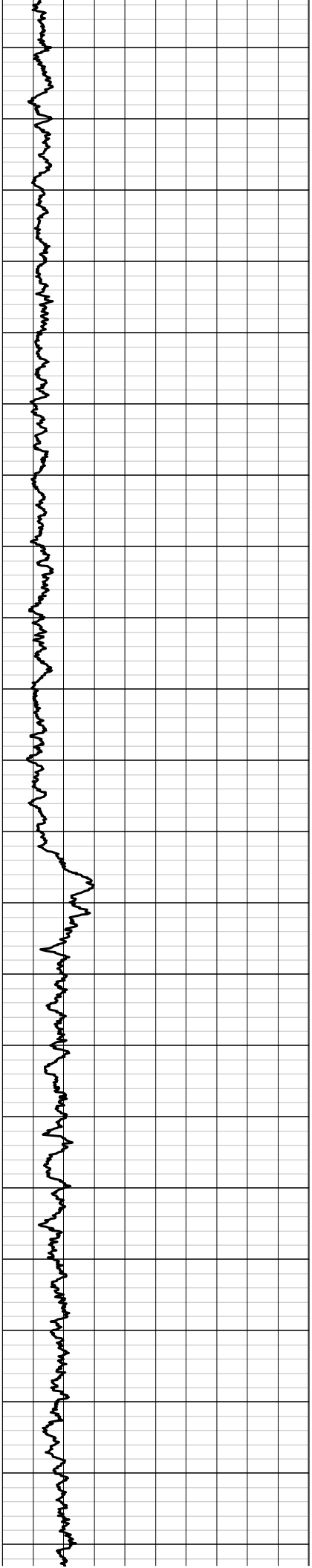
DATE 05-09-2016 TYPE FLUID IN HOLE Air/water  
 RUN No. one SALINITY  
 TYPE LOG QL-NB696 DENSITY  
 DEPTH-DRILLER 1062 ft. LEVEL 896 ft.  
 DEPTH-LOGGER 1052 ft. MAX. REG. TEMP  
 BTM LOGGED INTERVAL 1051 ft. DIGITIZE INTERVAL 0.1 ft.  
 TOP LOGGED INTERVAL Surface  
 OPERATING RIG TIME  
 RECORDED BY A.Henderson  
 WITNESSED BY Yellowjacket Drlg.

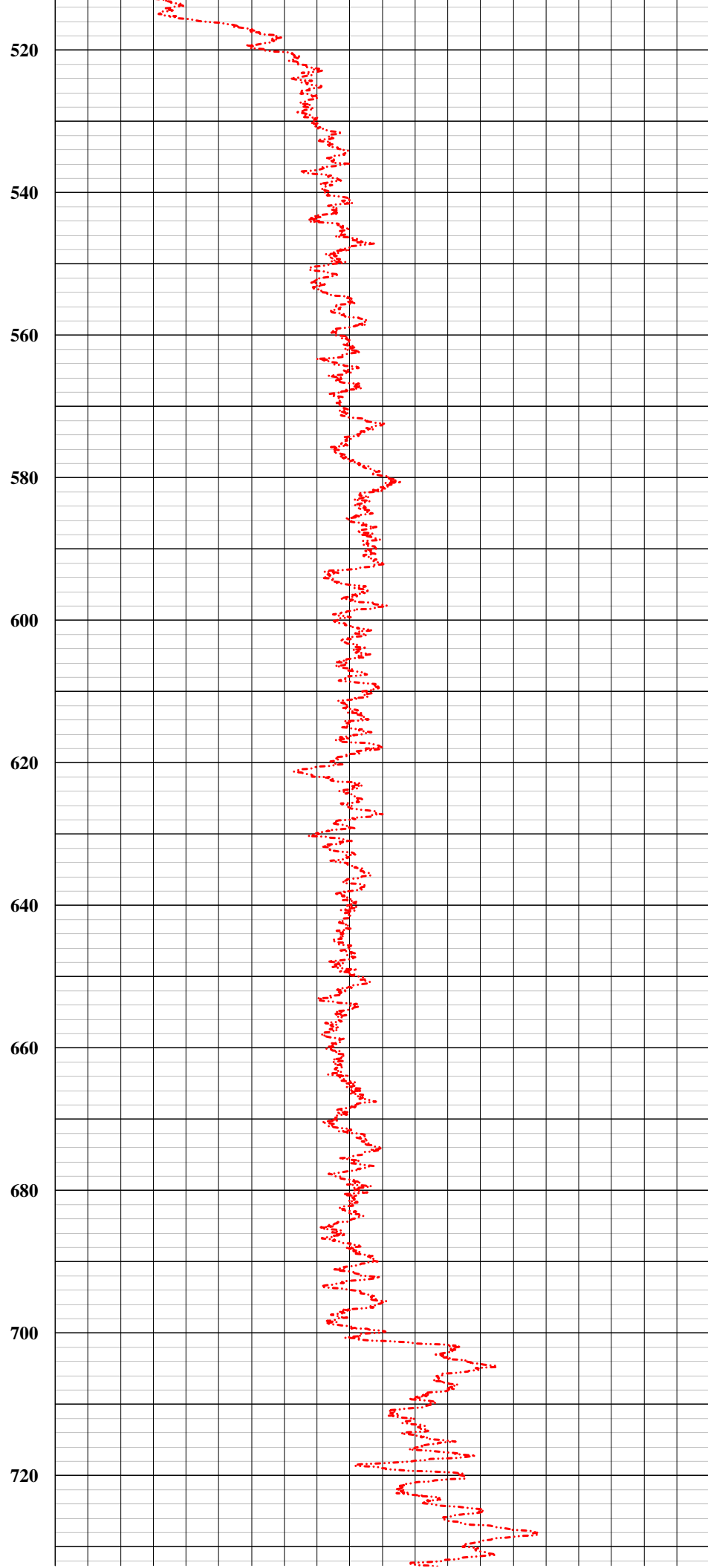
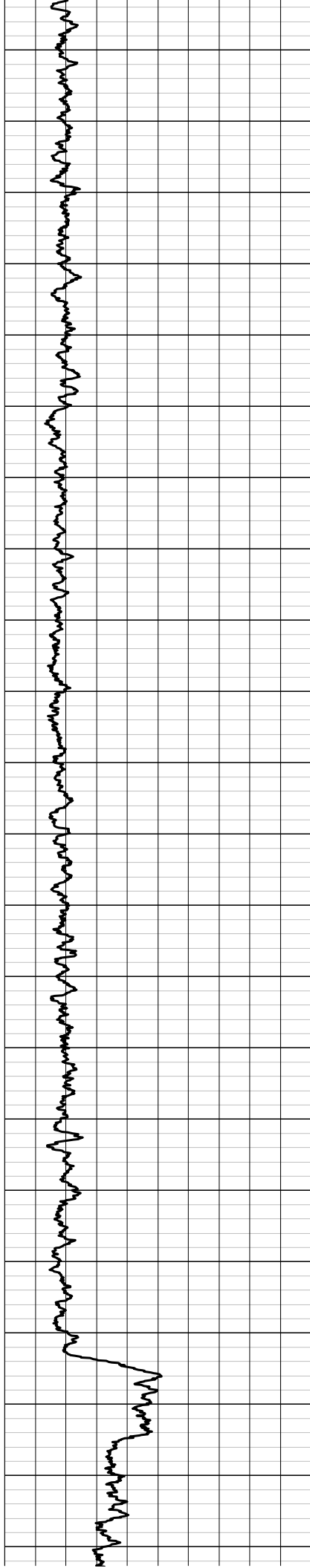
BOREHOLE RECORD			CASING RECORD			
RUN NO.	BIT FROM	TO	SIZE	WGT.	FROM	TO
1			20 inch	steel	0 ft.	60 ft.
2			18 inch	steel	0 ft.	273 ft.
3			14 inch	steel	0 ft.	1062 ft.

REMARKS:

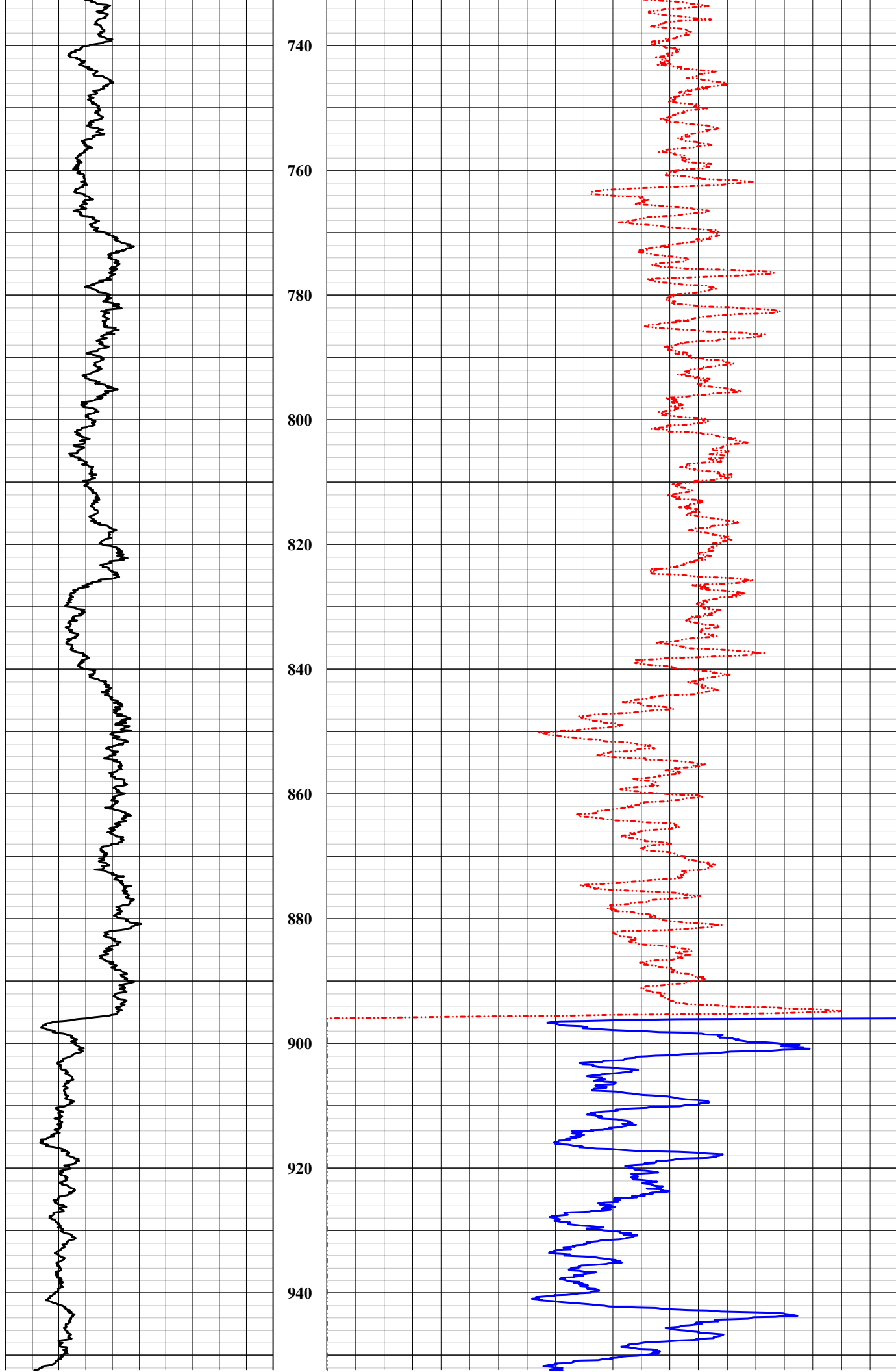


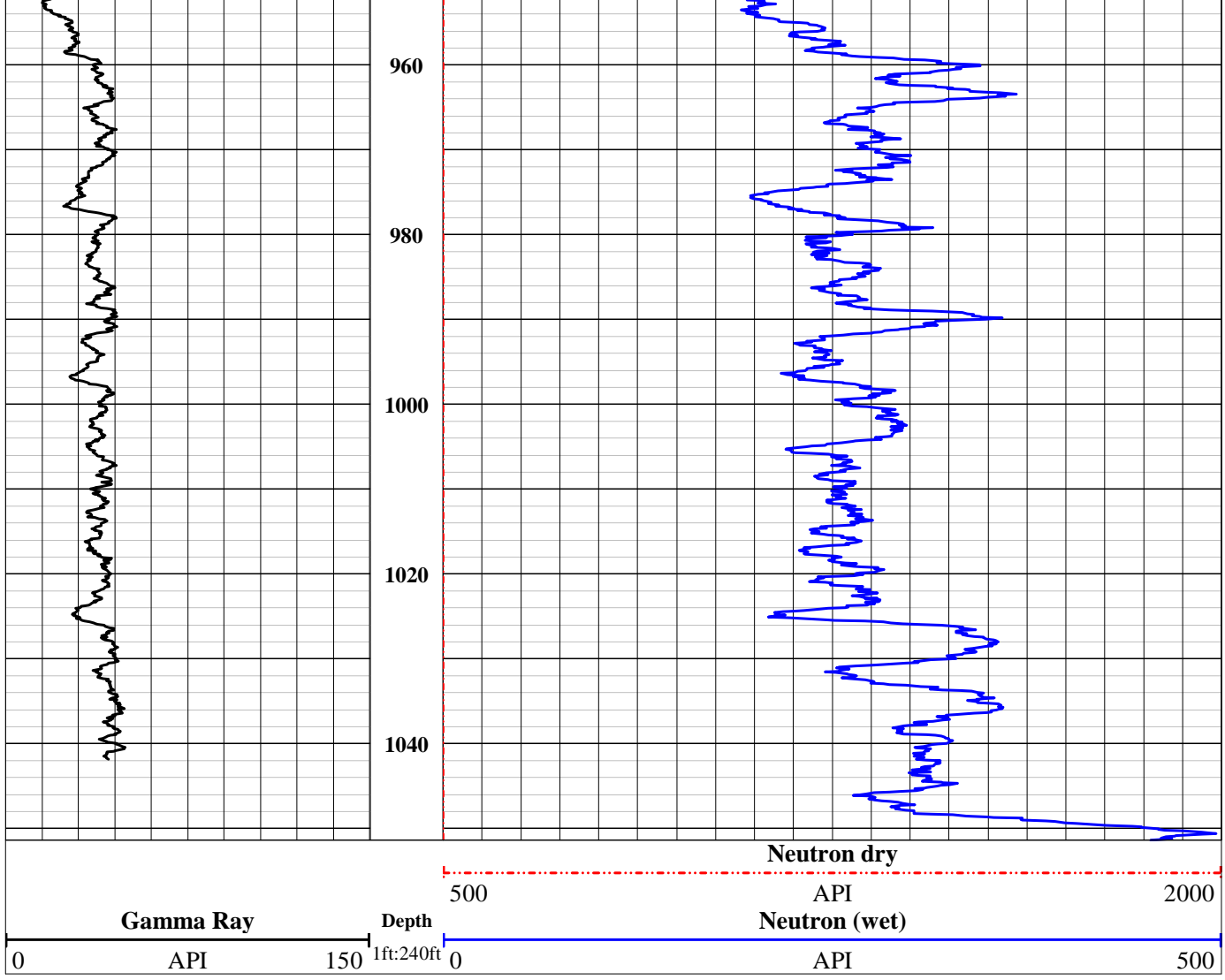














State Plane 1927

Northing:

Easting:

COMPANY Las Alamos National Labs

WELL ID Cin No.3

FIELD LANL (Los Alamos National Labs)

COUNTY Los Alamos STATE New Mexico

**TYPE OF LOG: Gamma Ray, Neutron Log**

OTHER SERVICES  
None

LOCATION

SEC TWP RGE

API No.

PERMANENT DATUM Ground Level ELEVATION K.B.

LOG MEAS. FROM Ground Level ABOVE PERM. DATUM T.O.C

DRILLING MEAS. FROM Ground Level G.L.

DATE 08-15-2016 TYPE FLUID IN HOLE Air/water

RUN No. one SALINITY

TYPE LOG QL-NB696 DENSITY

DEPTH-DRILLER 1025.08 ft. LEVEL 954 ft.

DEPTH-LOGGER 1003.67 ft. MAX. REG. TEMP

BTM LOGGED INTERVAL 1003.00 ft. DIGITIZE INTERVAL 0.1 ft.

TOP LOGGED INTERVAL Surface

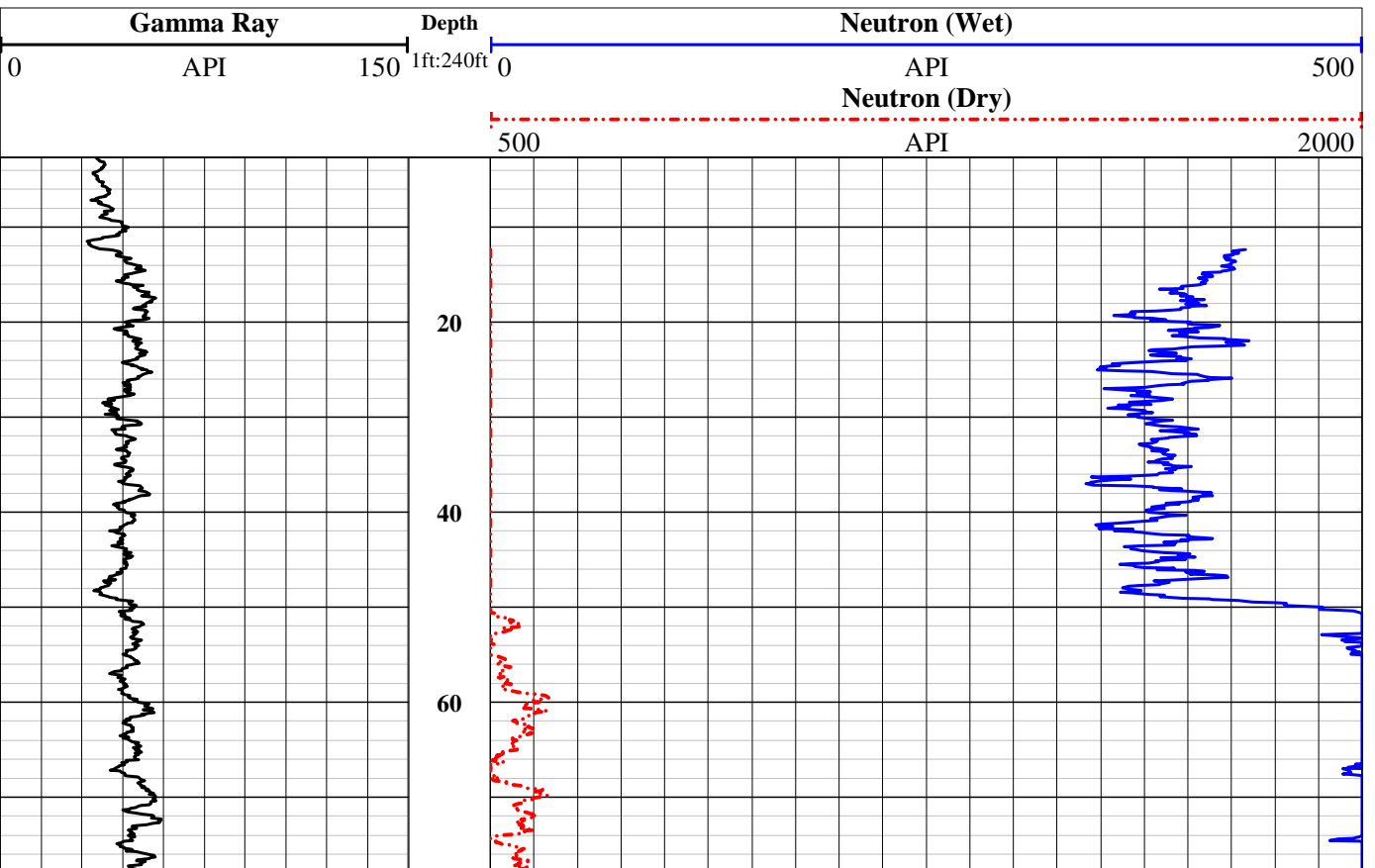
OPERATING RIG TIME

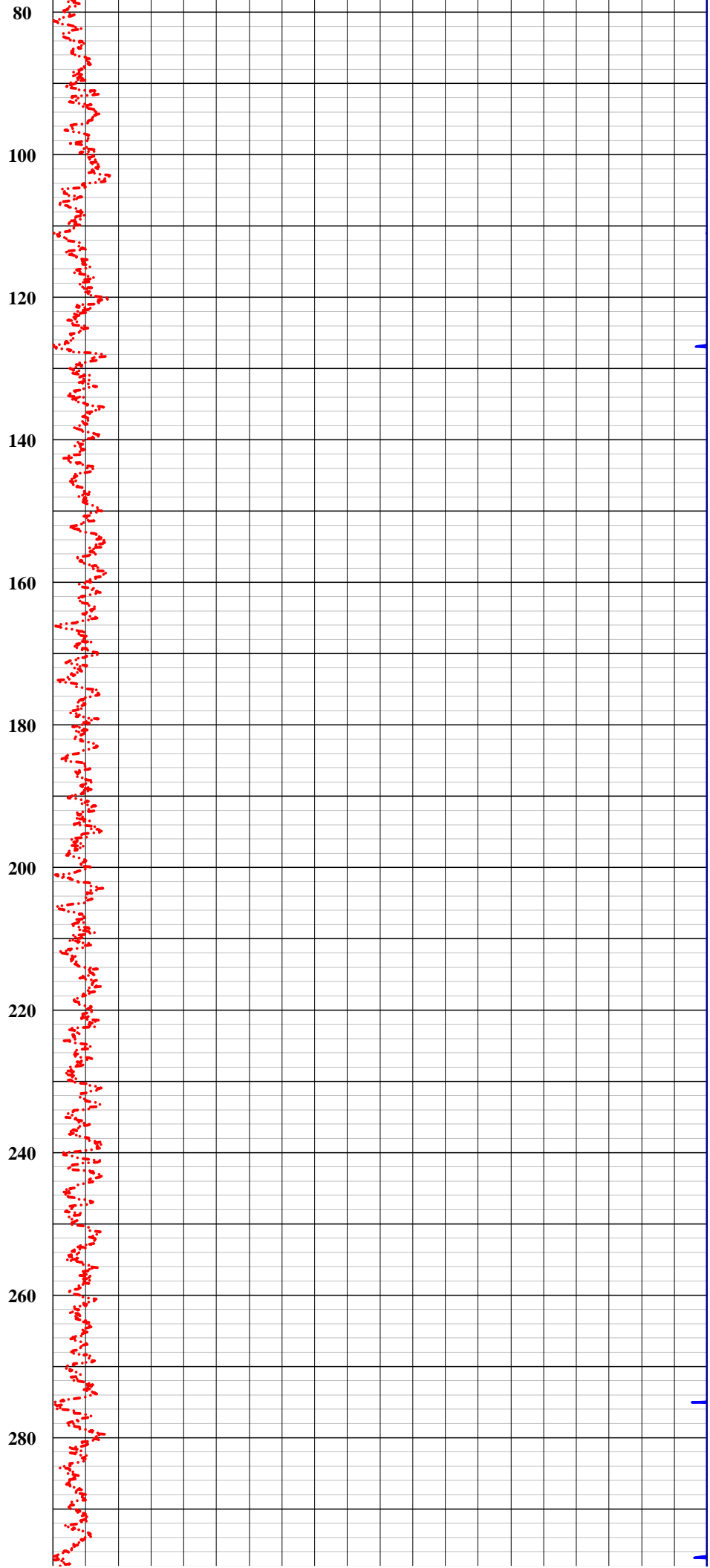
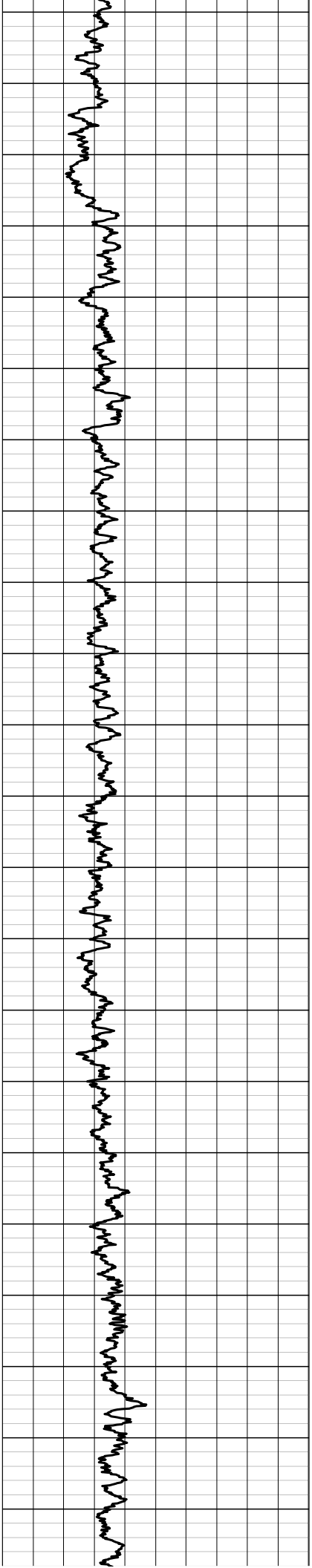
RECORDED BY A.Henderson

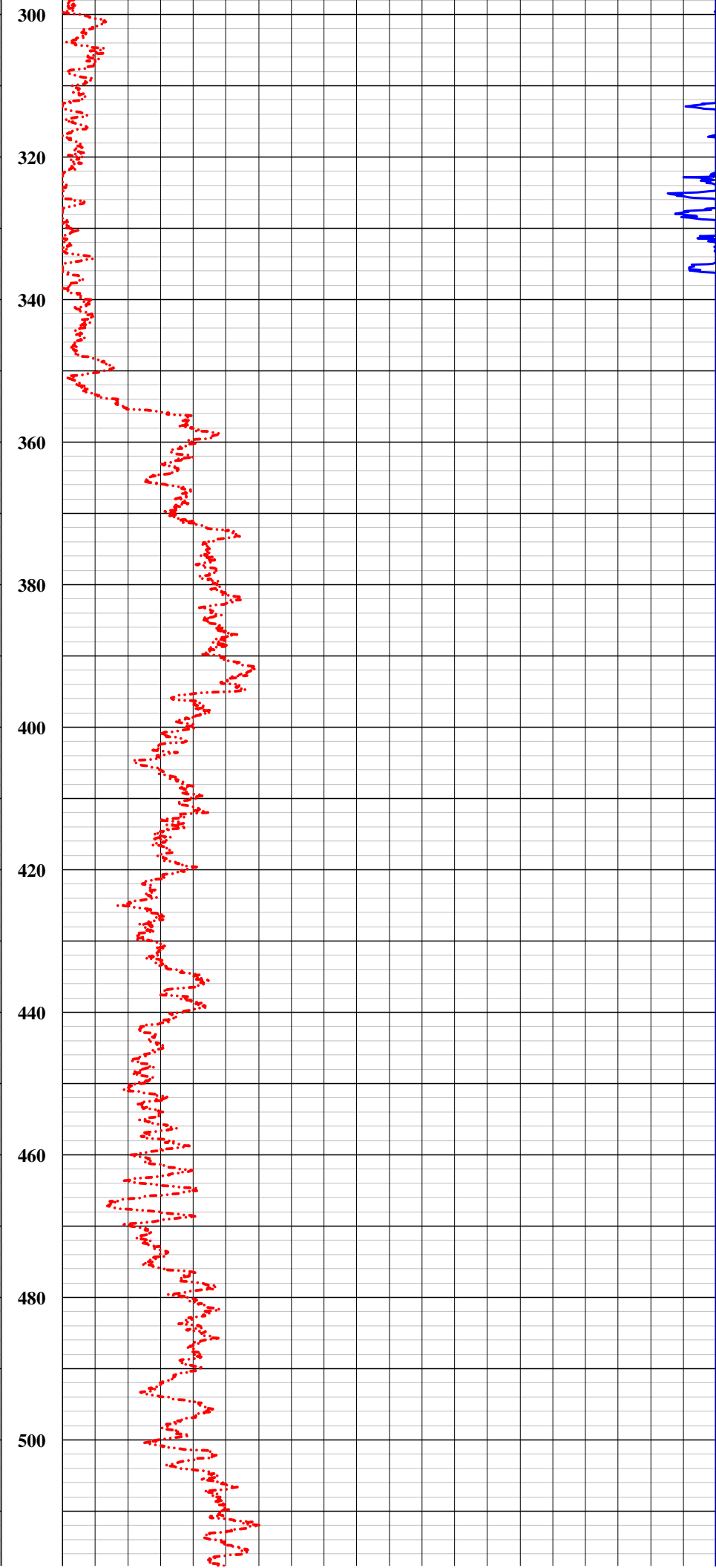
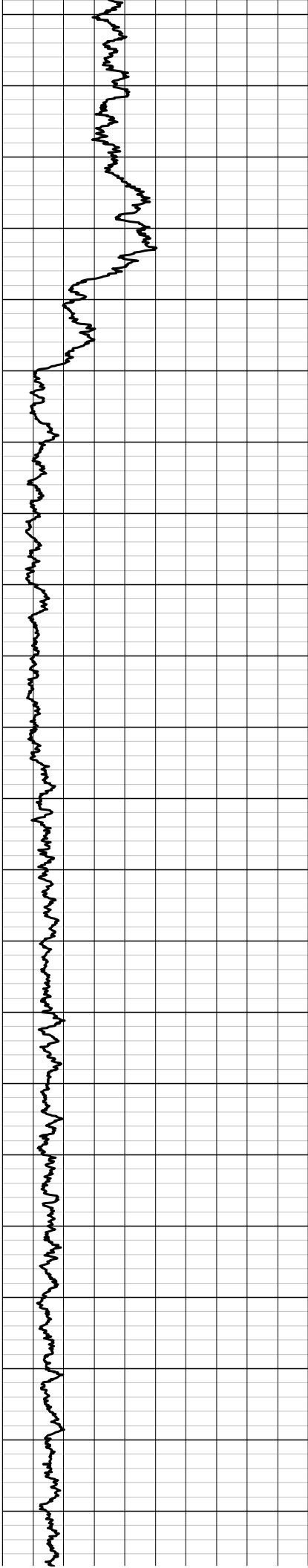
WITNESSED BY Holt Services

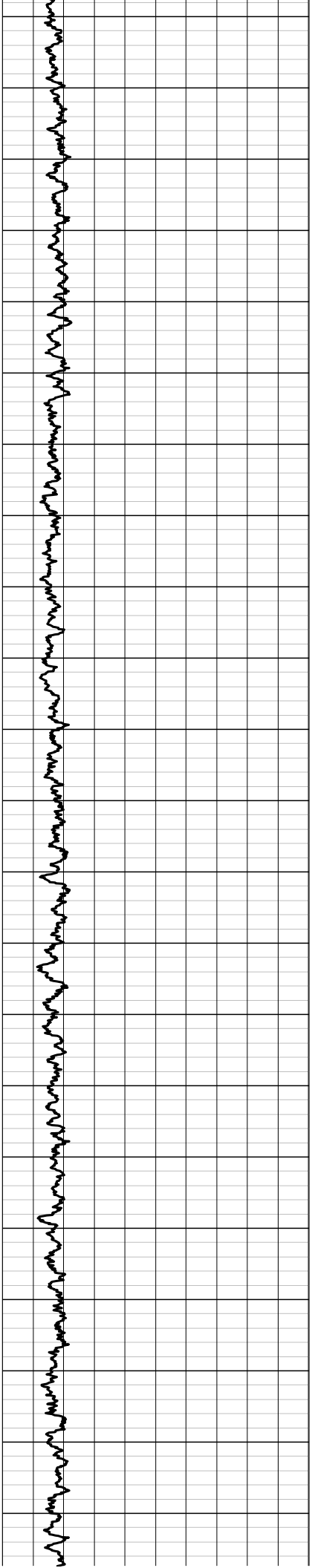
BOREHOLE RECORD			CASING RECORD			
RUN NO.	BIT FROM	TO	SIZE	WGT.	FROM	TO
1			20 inch	steel	0 ft.	49.45 ft.
2			18 inch	steel	0 ft.	359.76 ft.
3			16 inch	steel	0 ft.	763.52 ft.

REMARKS: Well is 17° angle from vertical.

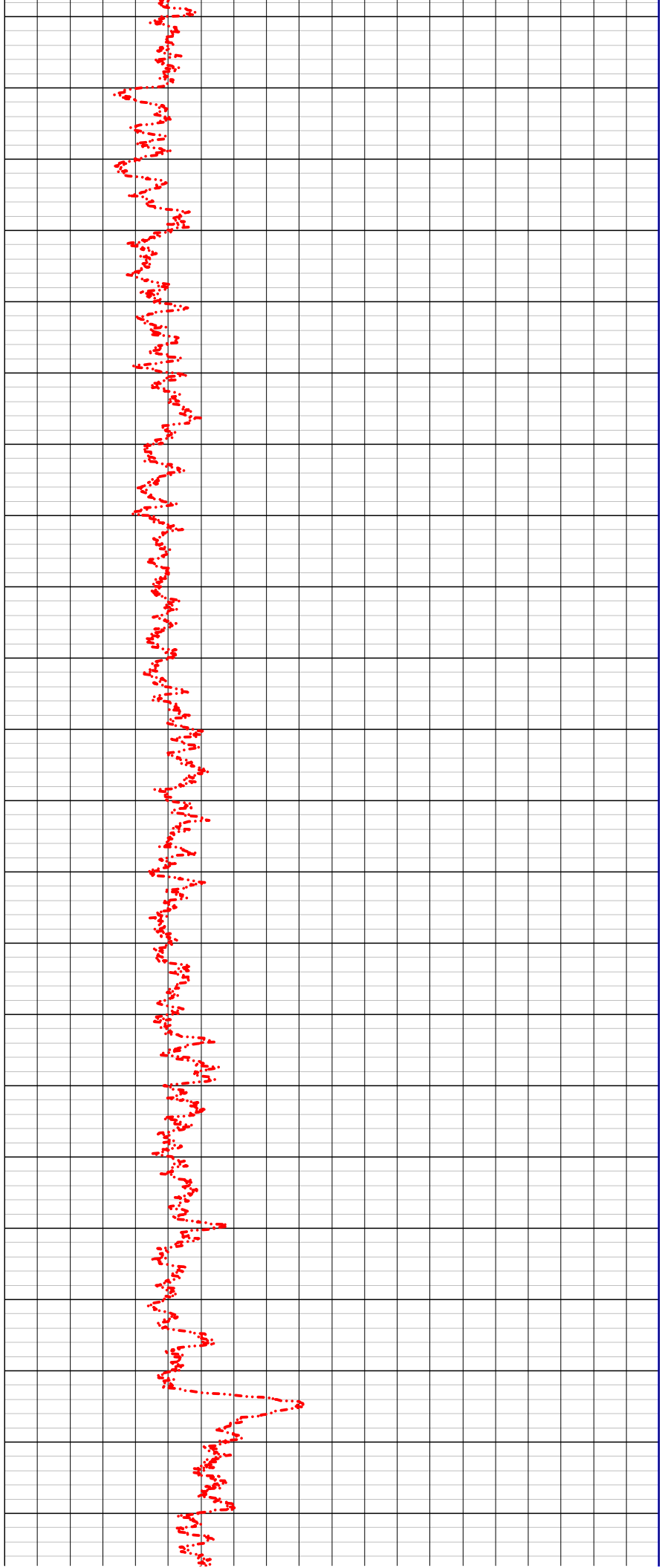


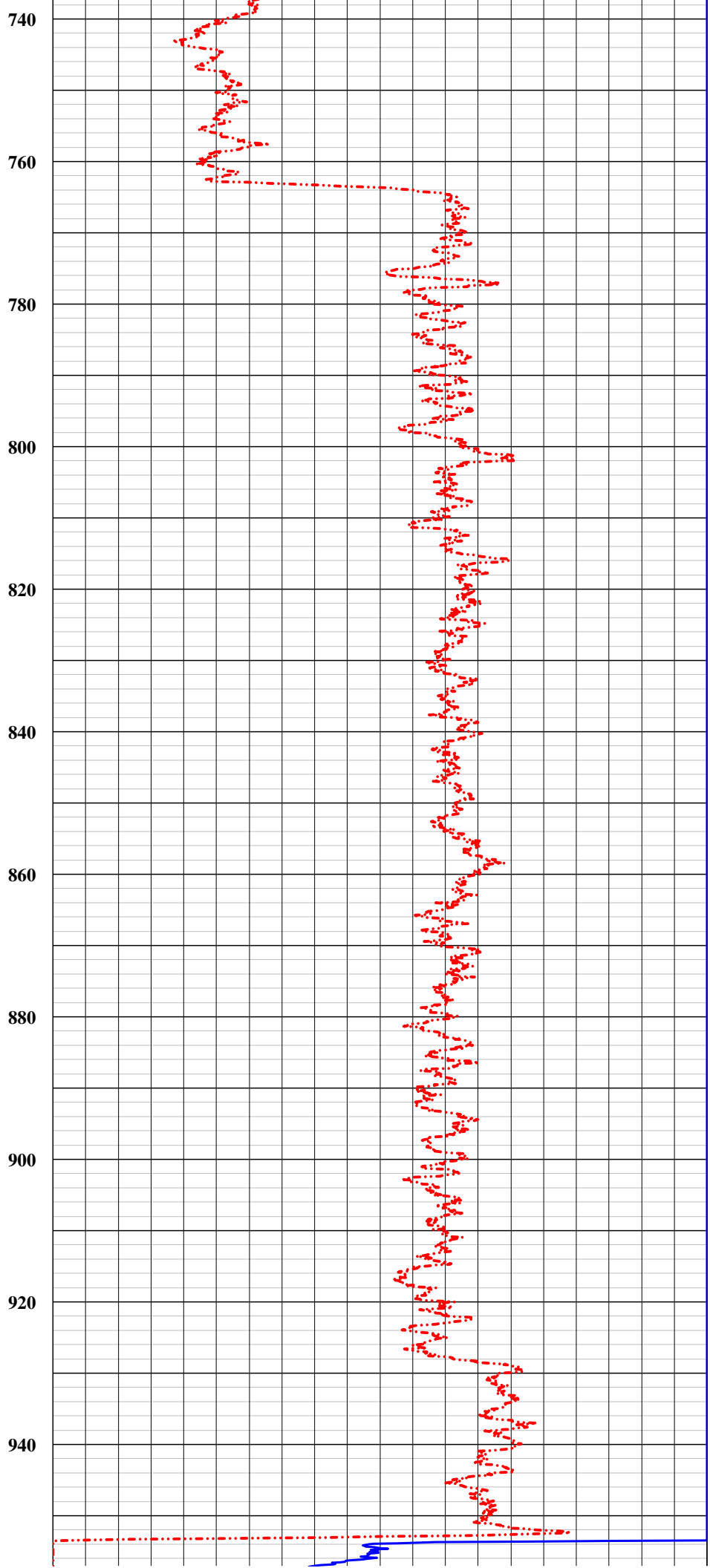
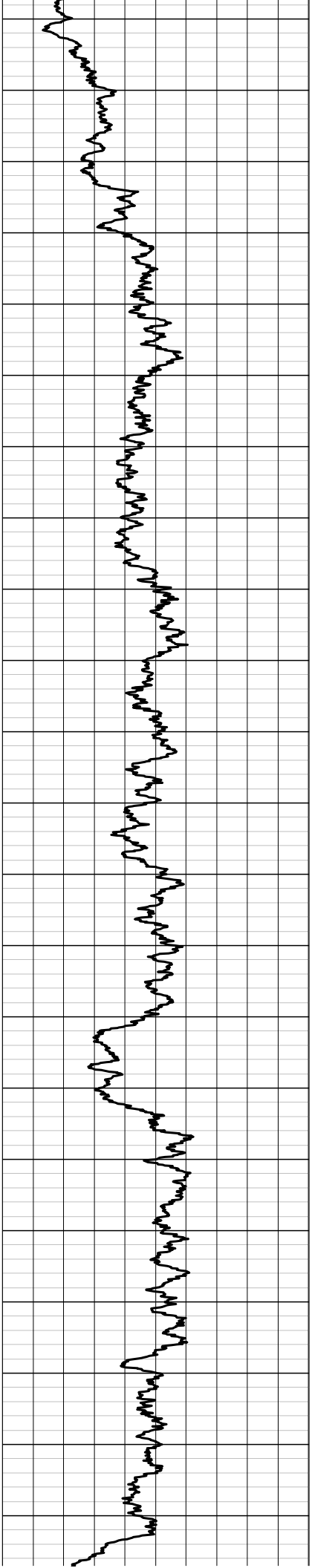


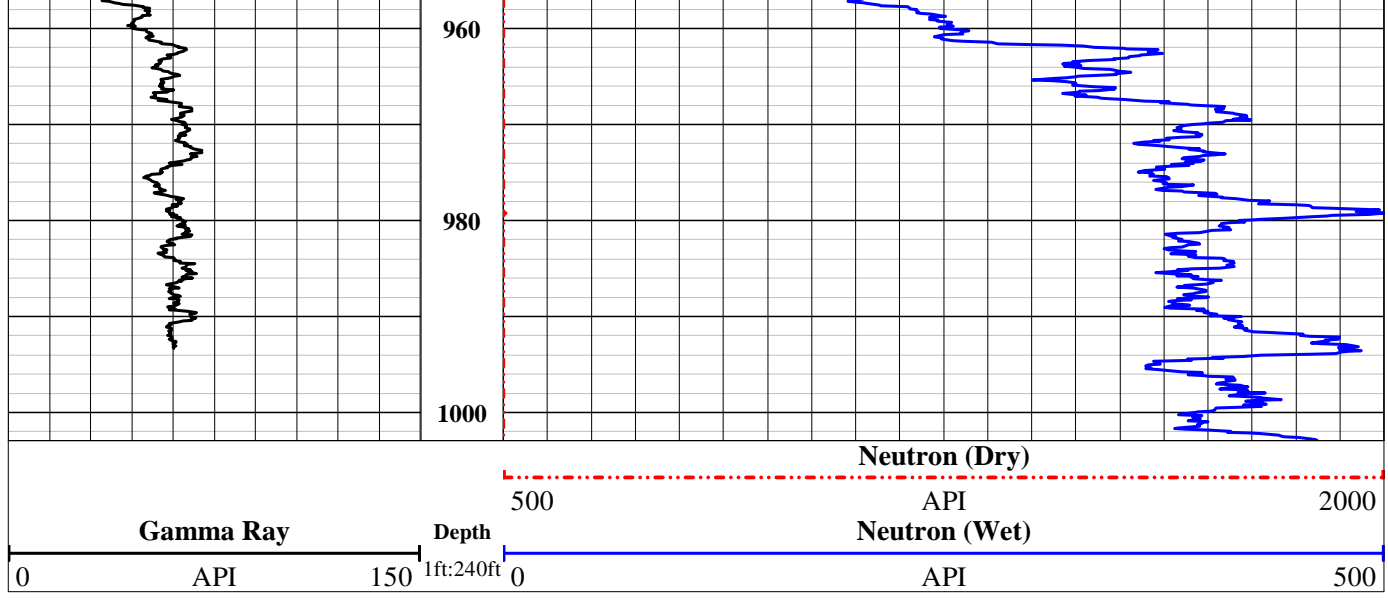




520  
540  
560  
580  
600  
620  
640  
660  
680  
700  
720









# JET WEST

## GEOPHYSICAL SERVICES, LLC.

State Plane 1927		COMPANY		Las Alamos National Labs			
Northing:		WELL ID		Cin No.4			
Easting:		FIELD		LANL (Los Alamos National Labs)			
LOCATION		COUNTY		Los Alamos			
SEC		TWP		RGE			
PERMANENT DATUM		Ground Level		ELEVATION			
LOG MEAS. FROM		Ground Level		ABOVE PERM. DATUM			
DRILLING MEAS. FROM		Ground Level		TYPE FLUID IN HOLE			
DATE		05-11-2016		SALINITY			
RUN No.		one		DENSITY			
TYPE LOG		QL-NB696		LEVEL			
DEPTH-DRILLER		1202 ft.		MAX. REG. TEMP			
DEPTH-LOGGER		1193.6 ft.		DIGITIZE INTERVAL			
BTM LOGGED INTERVAL		1193 ft.		0.1 ft.			
TOP LOGGED INTERVAL		Surface					
OPERATING RIG TIME							
RECORDED BY		A.Henderson					
WITNESSED BY		Holt Services					
RUN		BOREHOLE RECORD		CASING RECORD			
NO.	BIT	FROM	TO	SIZE	WGT.	FROM	TO
1				20 inch	steel	0 ft.	61.25 ft.
2				18 inch	steel	0 ft.	595.28 ft.
3				16 inch	steel	0 ft.	821.76 ft.

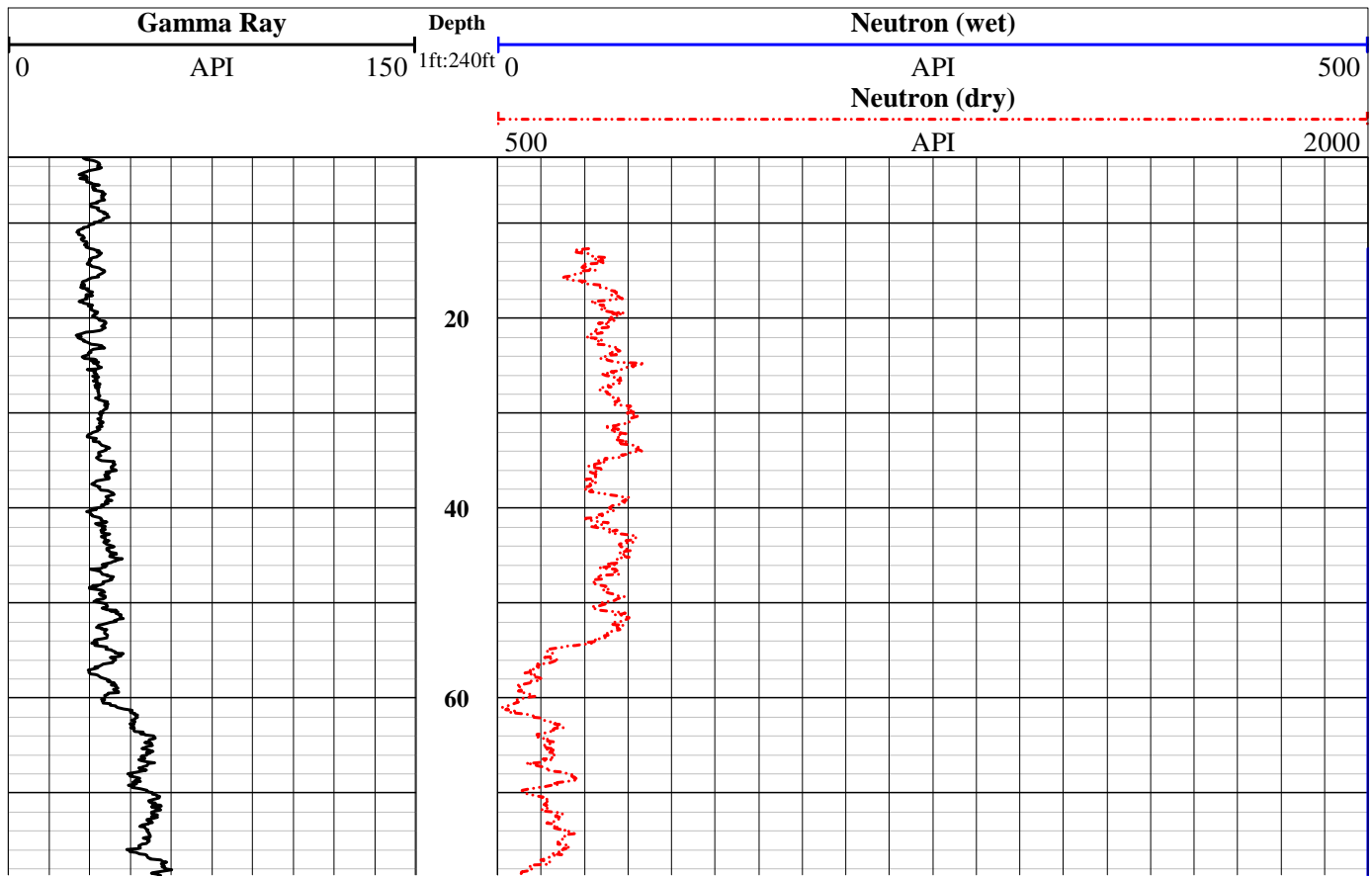
REMARKS: Well is 11° angle from vertical.

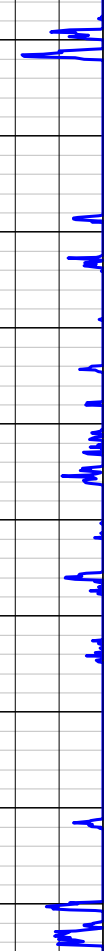
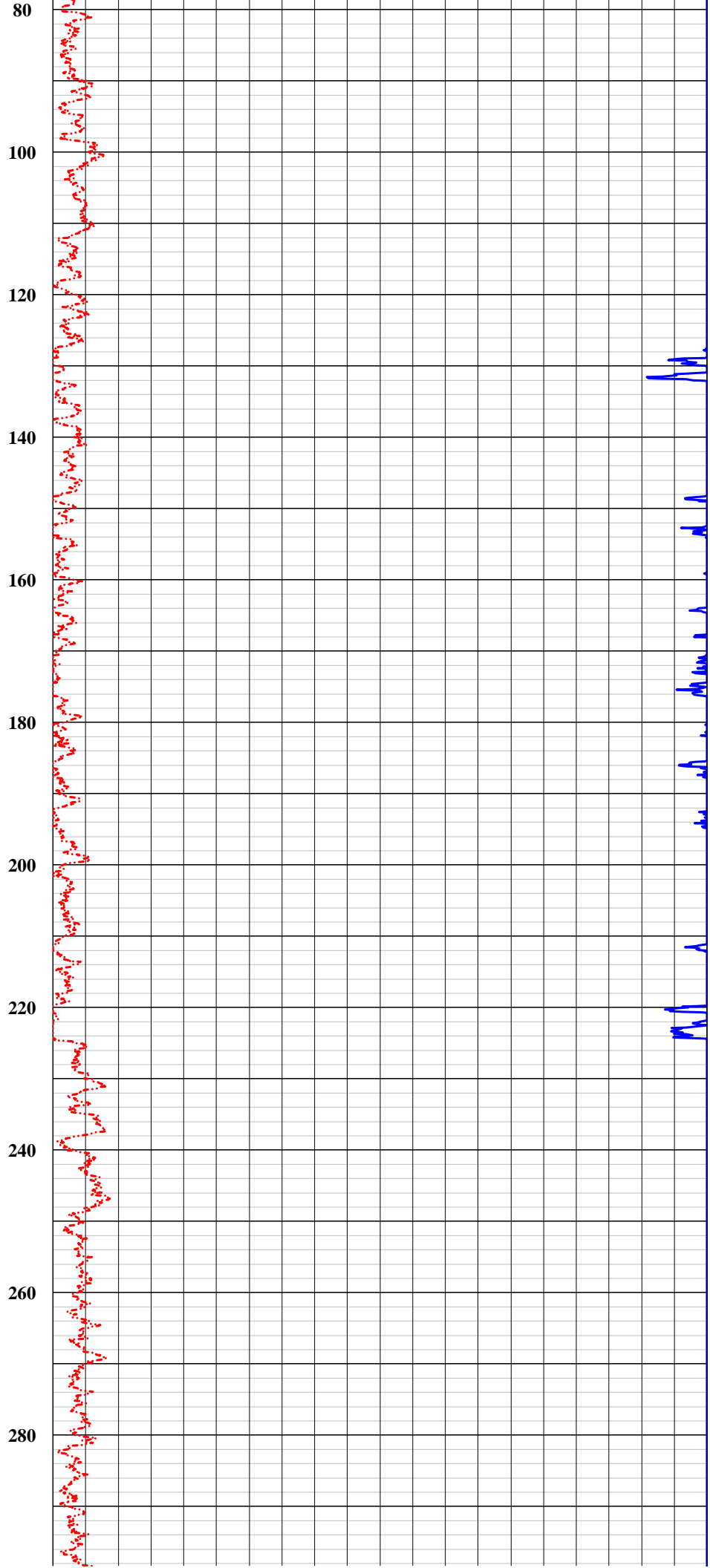
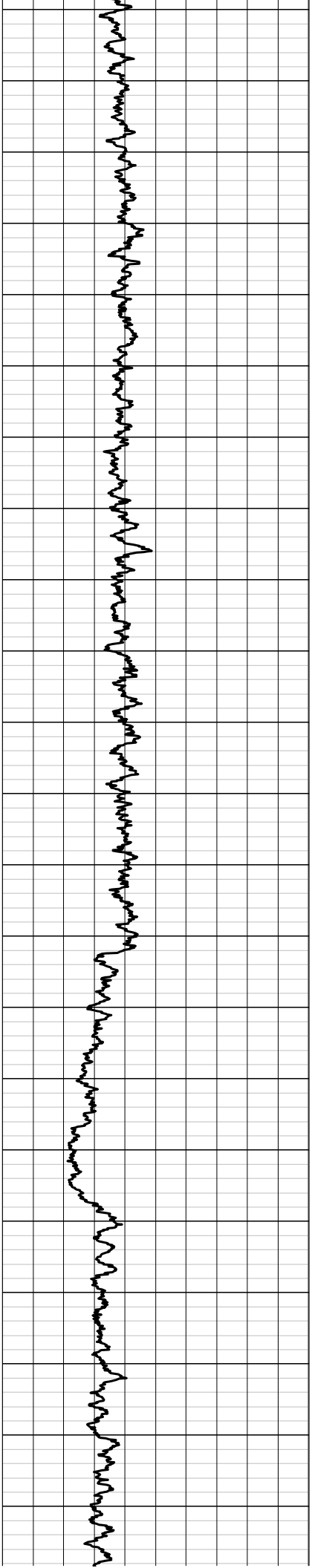
14 inch

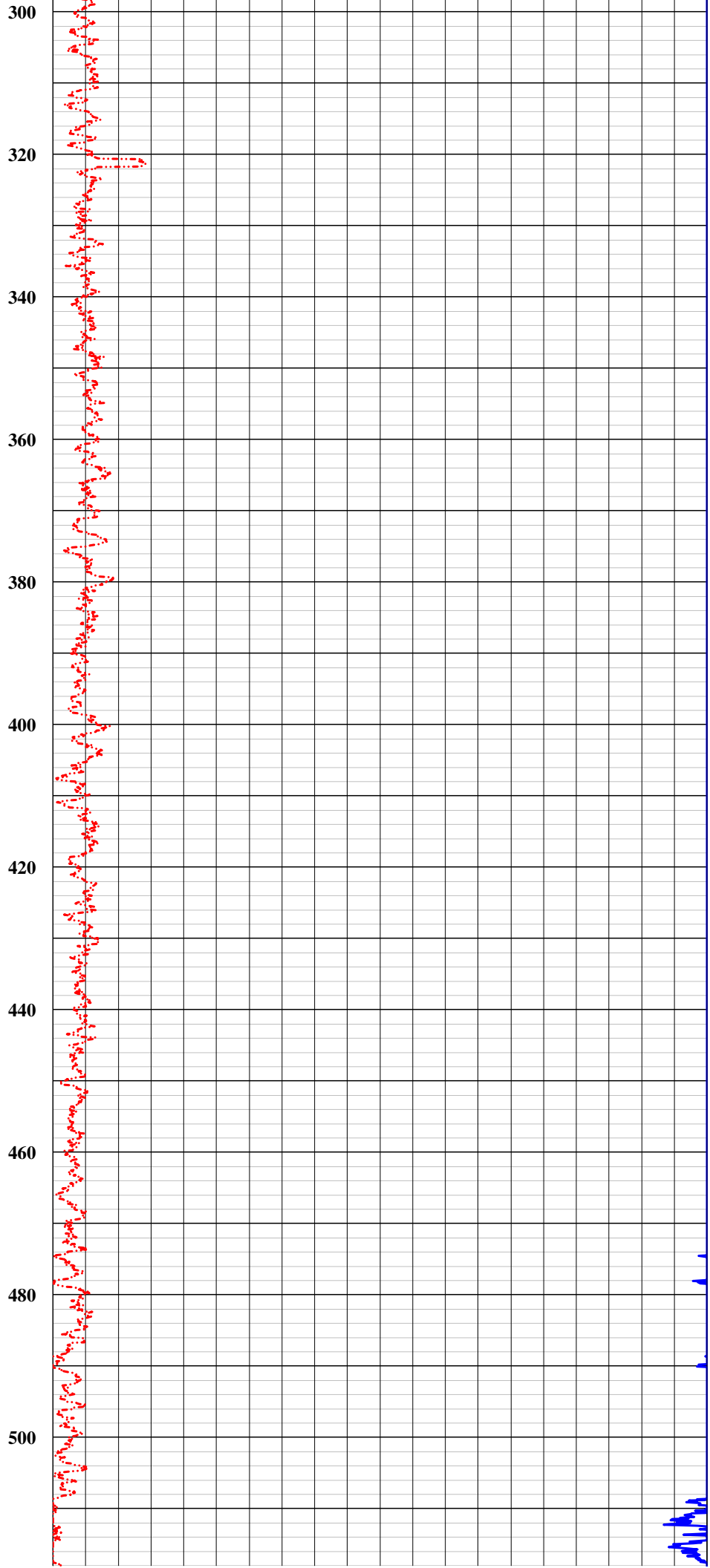
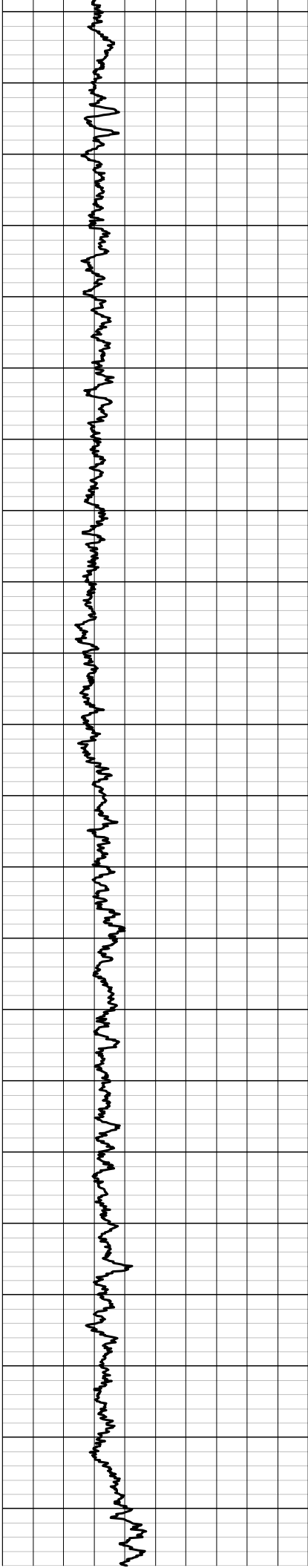
steel

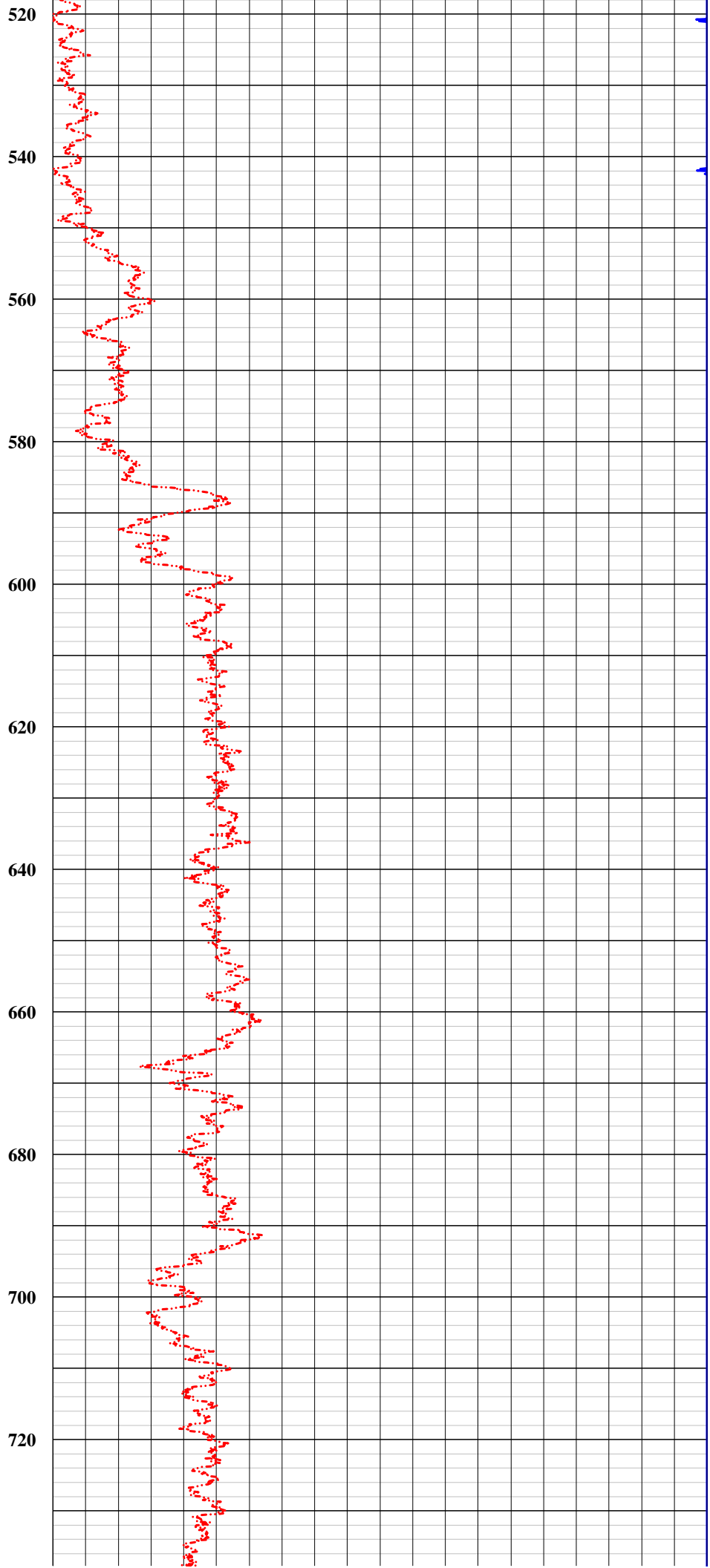
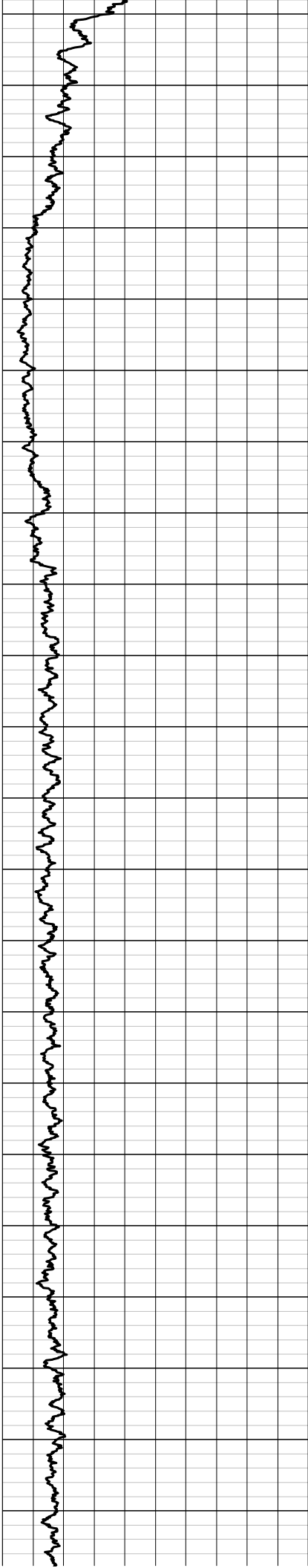
0 ft.

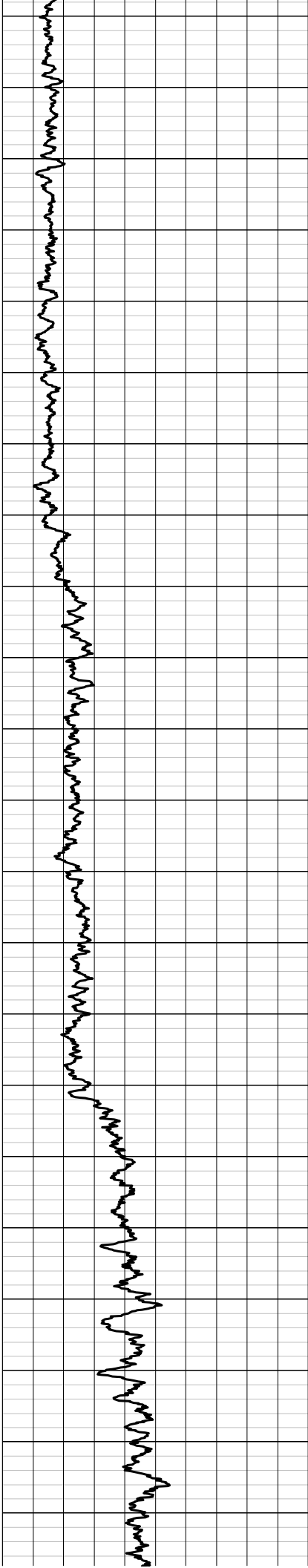
1202 ft.



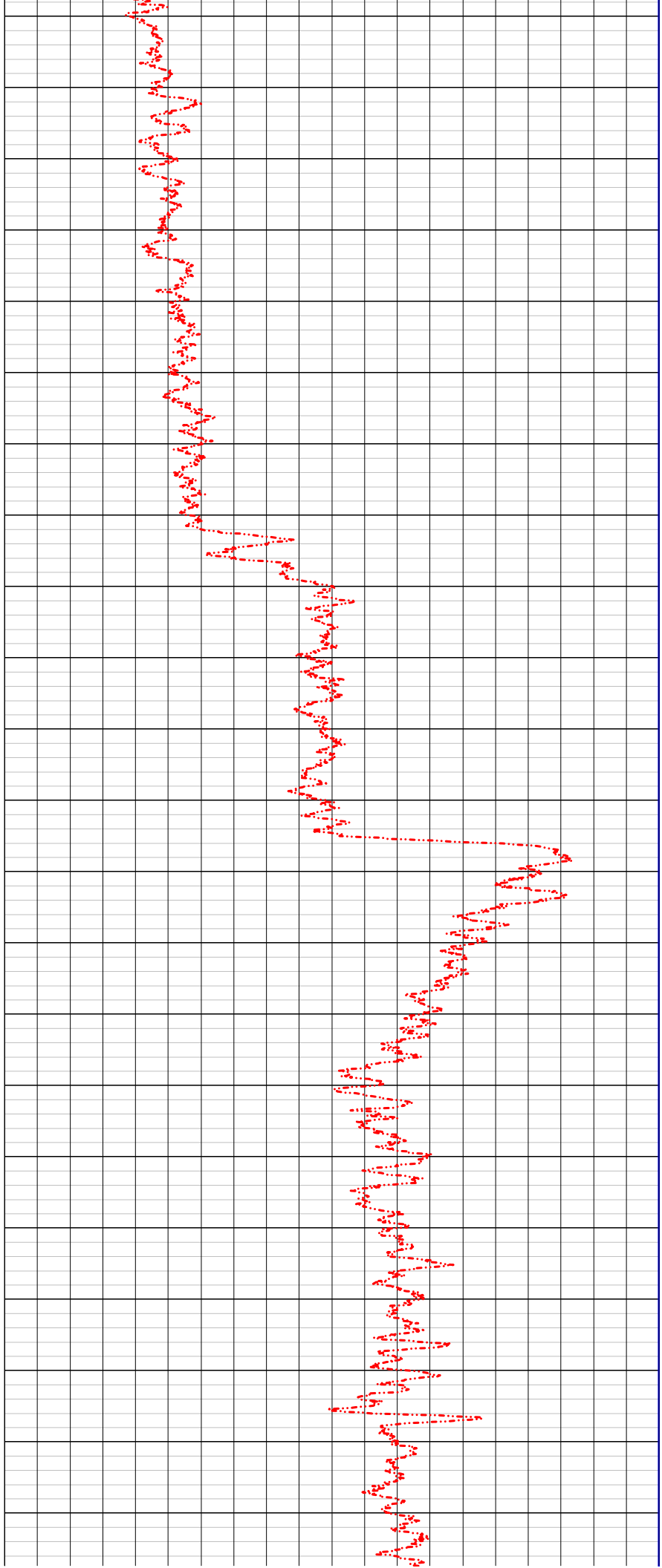


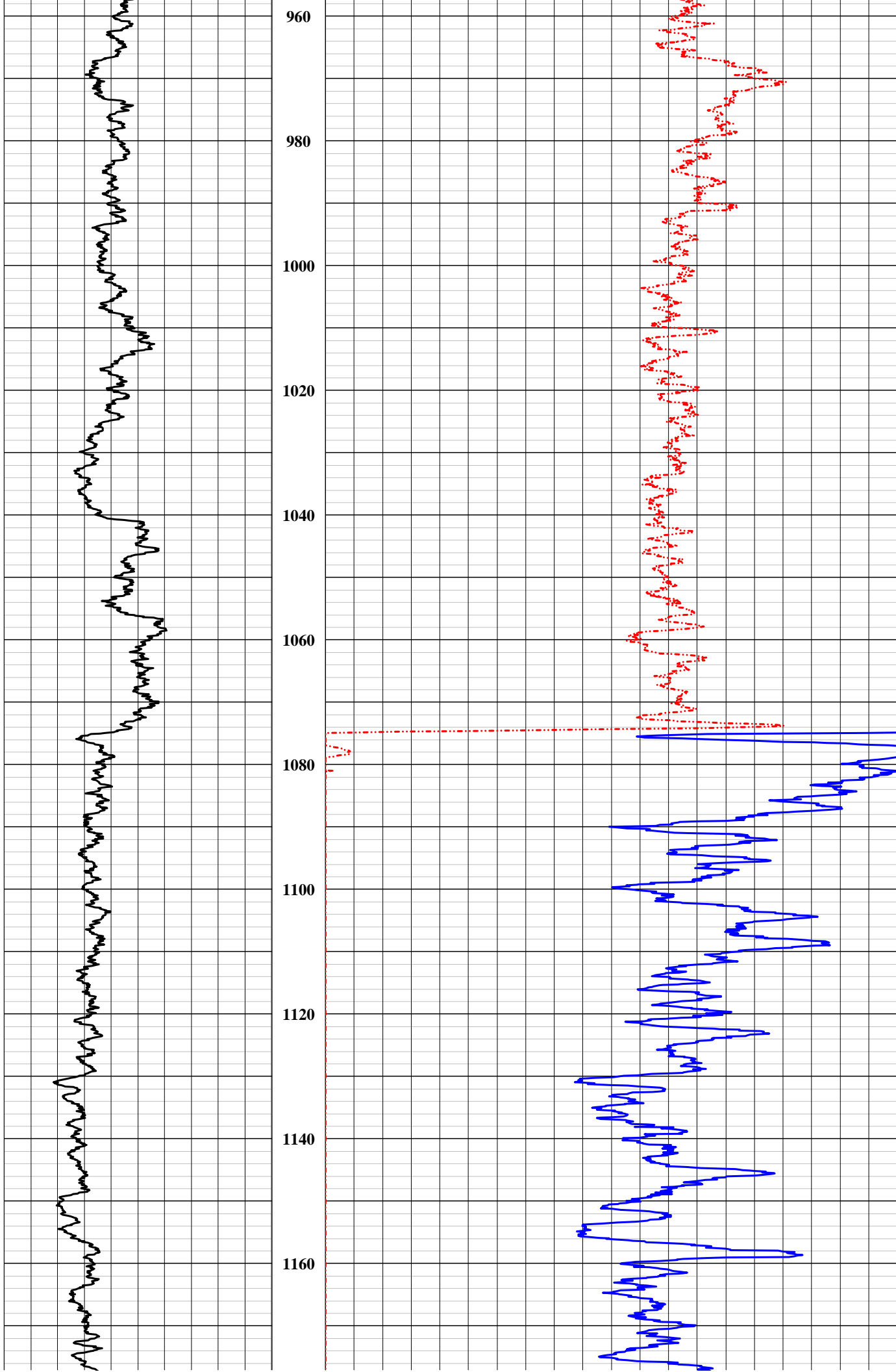


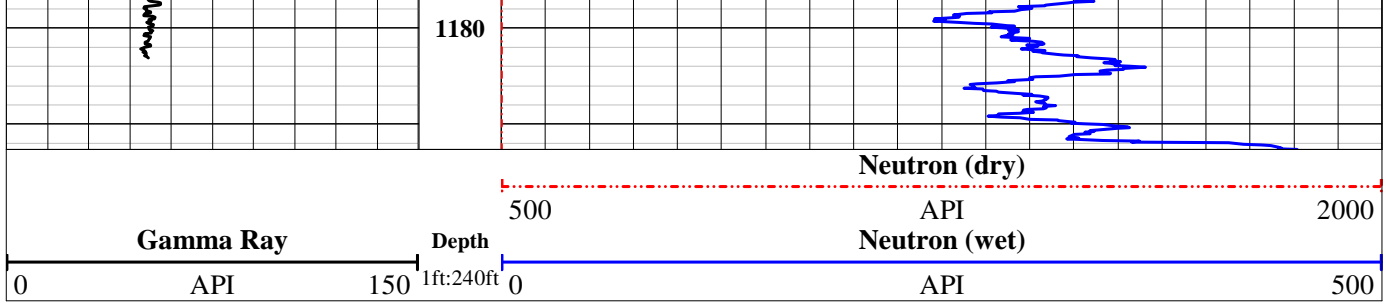




740  
760  
780  
800  
820  
840  
860  
880  
900  
920  
940







**Gamma Ray**

**Depth**

**Neutron (dry)**

**Neutron (wet)**

0 API 150

1ft:240ft

500

API

2000

API

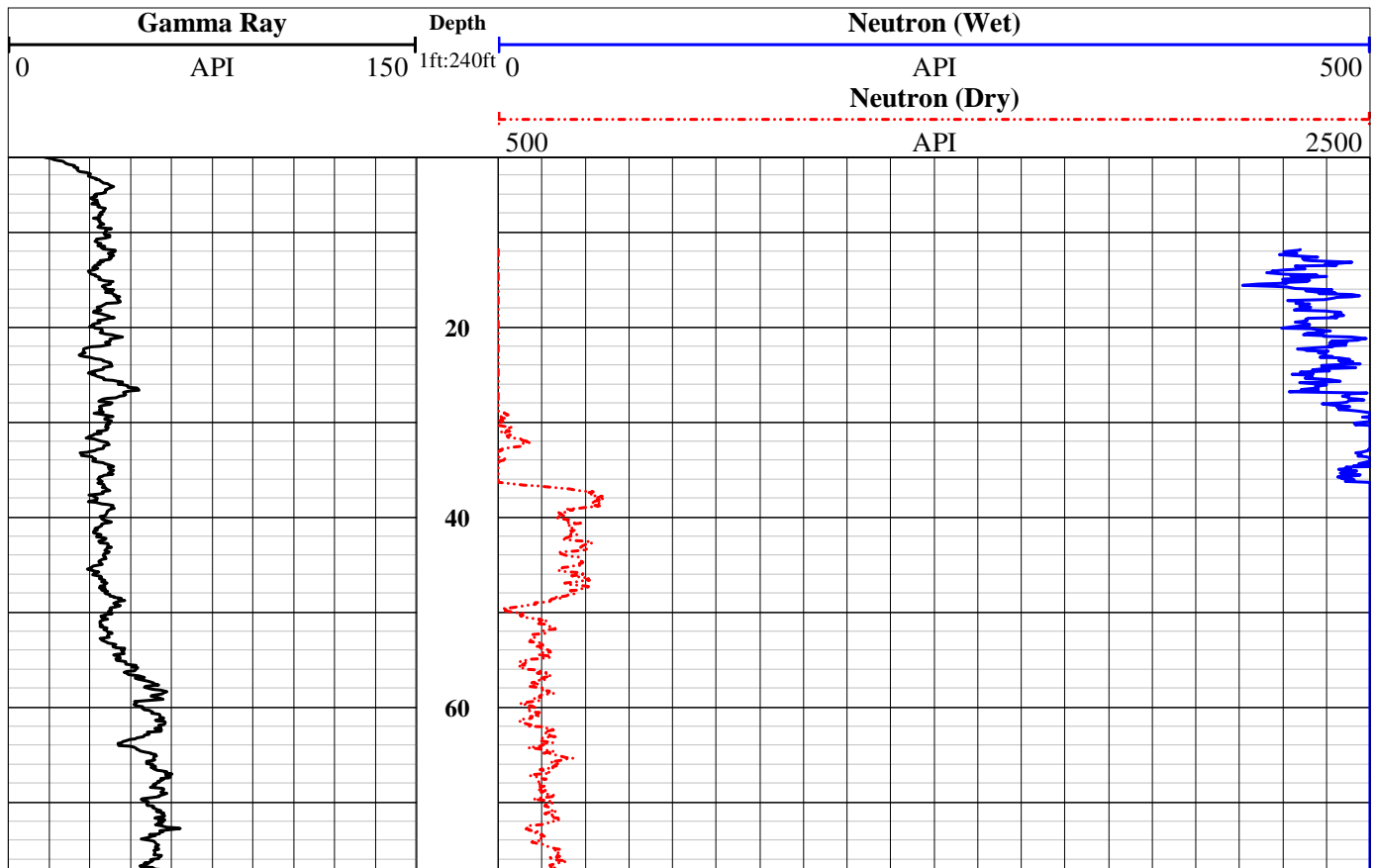
500

# JET WEST

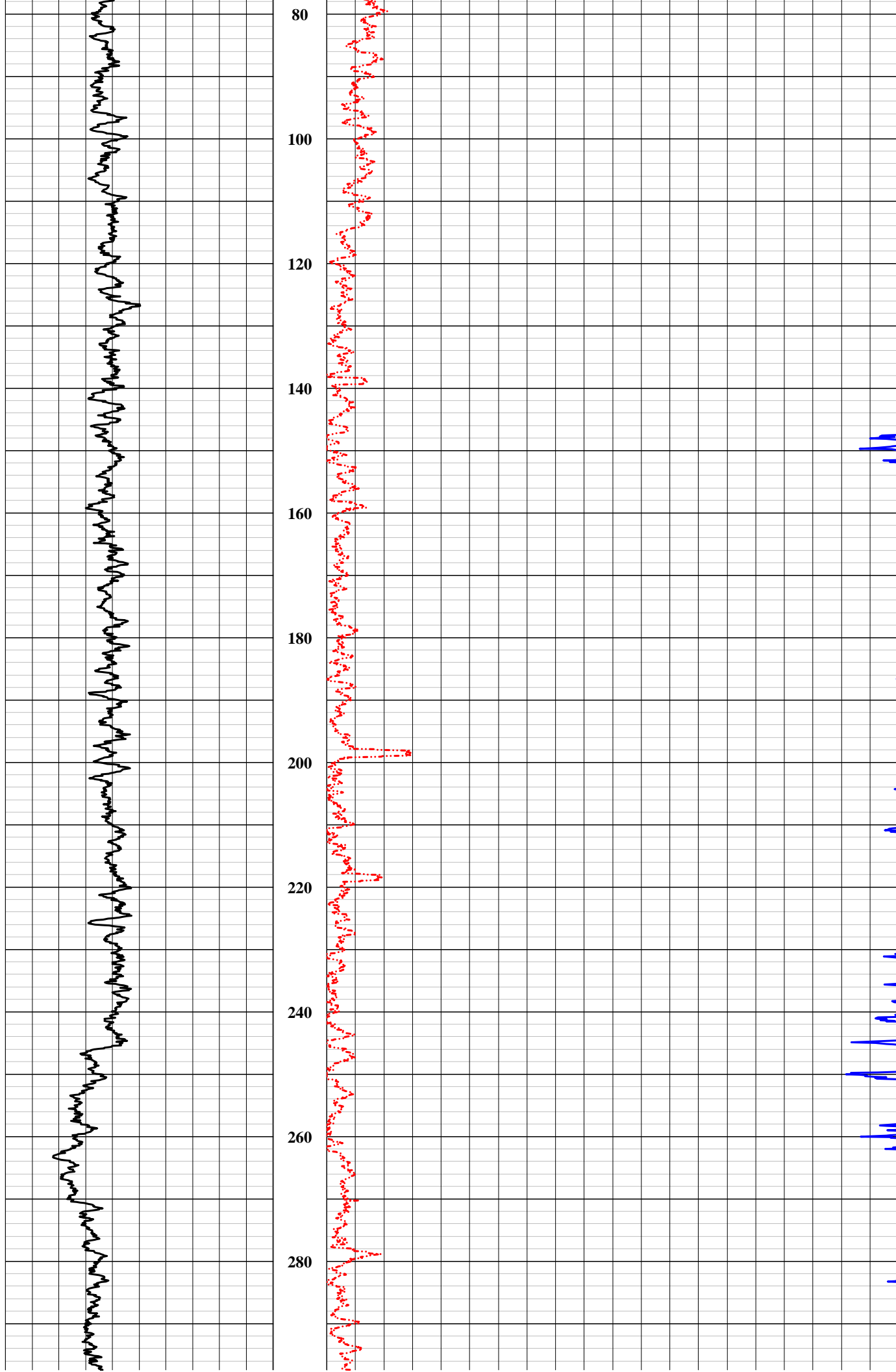
## GEOPHYSICAL SERVICES, LLC.

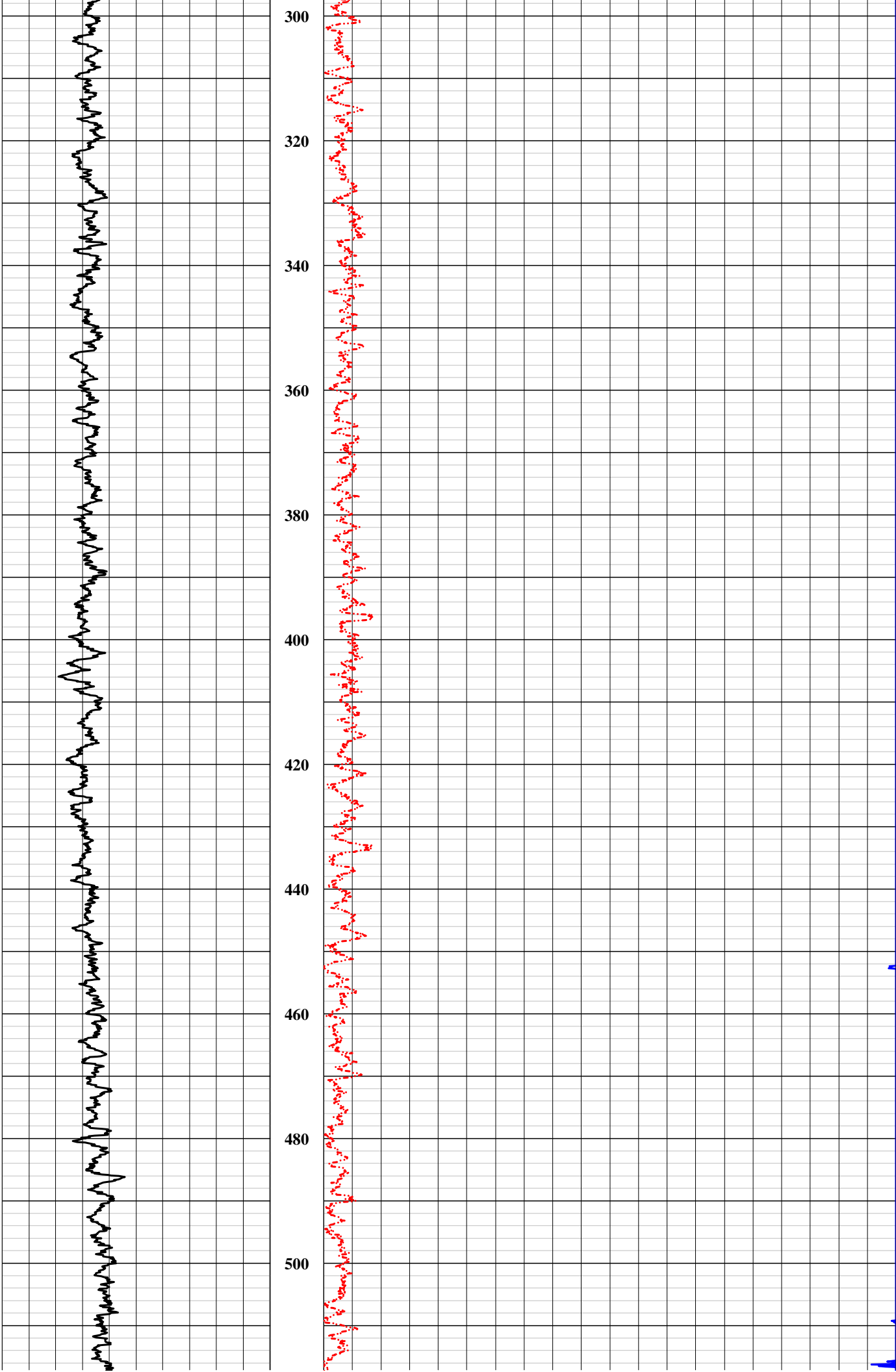
State Plane 1927		COMPANY		Las Alamos National Labs			
Northing:		WELL ID		Cin No.5			
Easting:		FIELD		LANL (Los Alamos National Labs)			
LOCATION		COUNTY		Los Alamos			
SEC		TWP		RGE			
PERMANENT DATUM		Ground Level		ELEVATION			
LOG MEAS. FROM		Ground Level		ABOVE PERM. DATUM			
DRILLING MEAS. FROM		Ground Level		G.L.			
DATE		07-01-2016		TYPE FLUID IN HOLE			
RUN No.		one		SALINITY			
TYPE LOG		QL-NB696		DENSITY			
DEPTH-DRILLER		1290 ft.		LEVEL			
DEPTH-LOGGER		1282 ft.		MAX. REG. TEMP			
BTM LOGGED INTERVAL		1281 ft.		DIGITIZE INTERVAL			
TOP LOGGED INTERVAL		Surface					
OPERATING RIG TIME							
RECORDED BY		A.Henderson					
WITNESSED BY		Holt Services					
RUN		BOREHOLE RECORD		CASING RECORD			
NO.	BIT	FROM	TO	SIZE	WGT.	FROM	TO
1				20 inch	steel	0 ft.	55.77 ft.
2				18 inch	steel	0 ft.	594.41 ft.
3				16 inch	steel	0 ft.	914.11 ft.

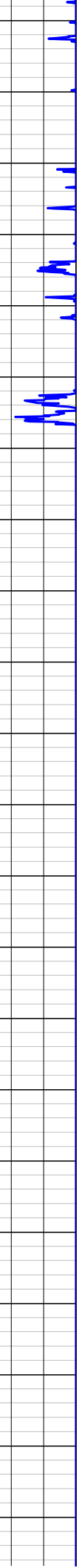
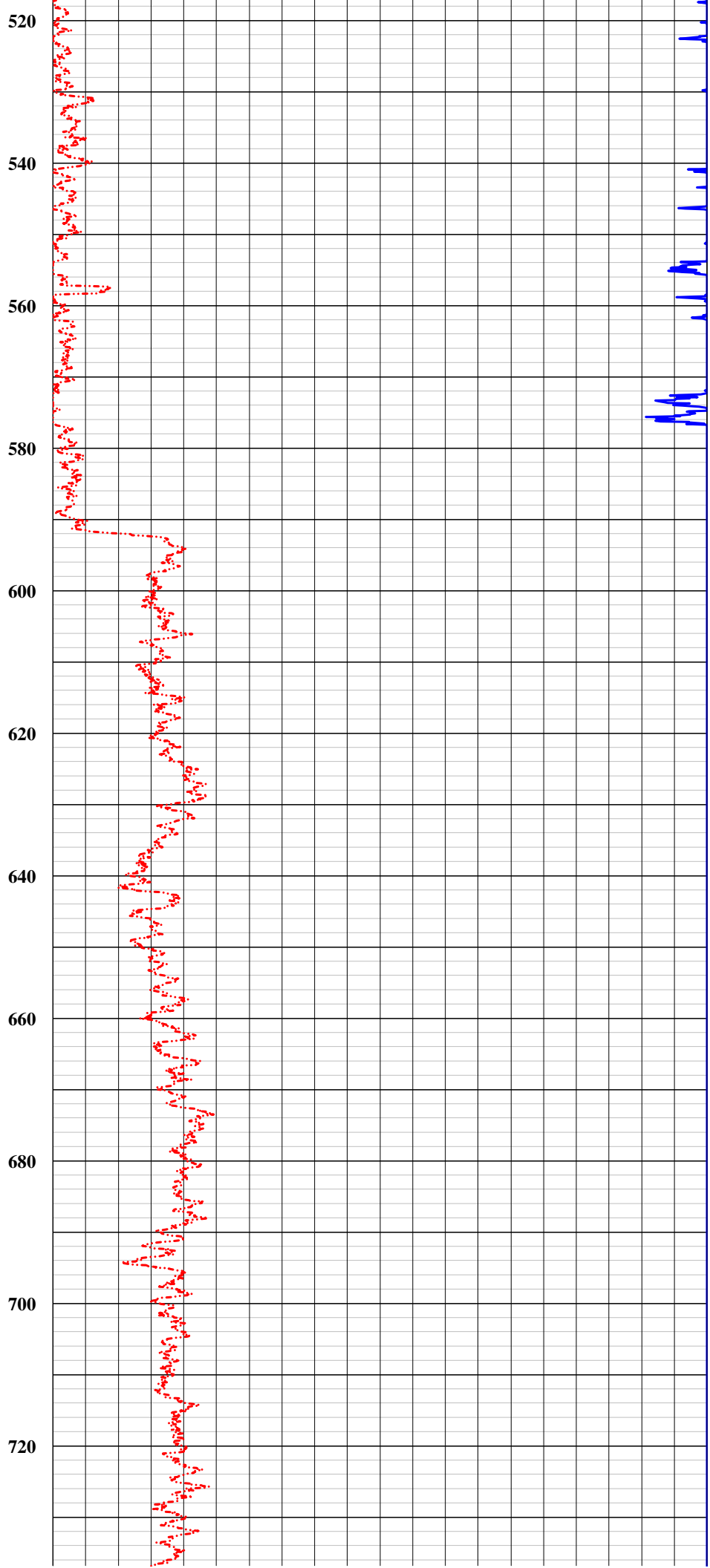
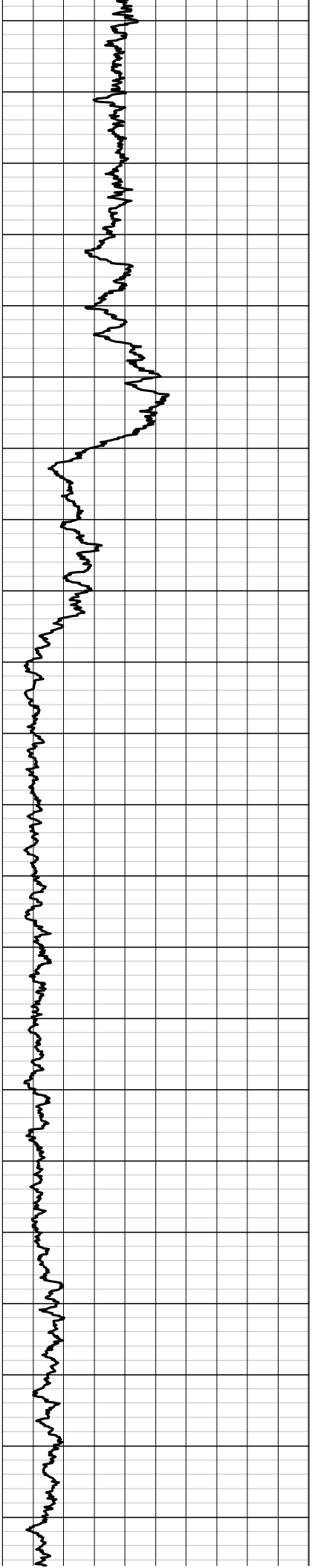
REMARKS: Well is 26° angle from vertical.  
14 inch steel casing 0 ft. to 1290.00 ft.

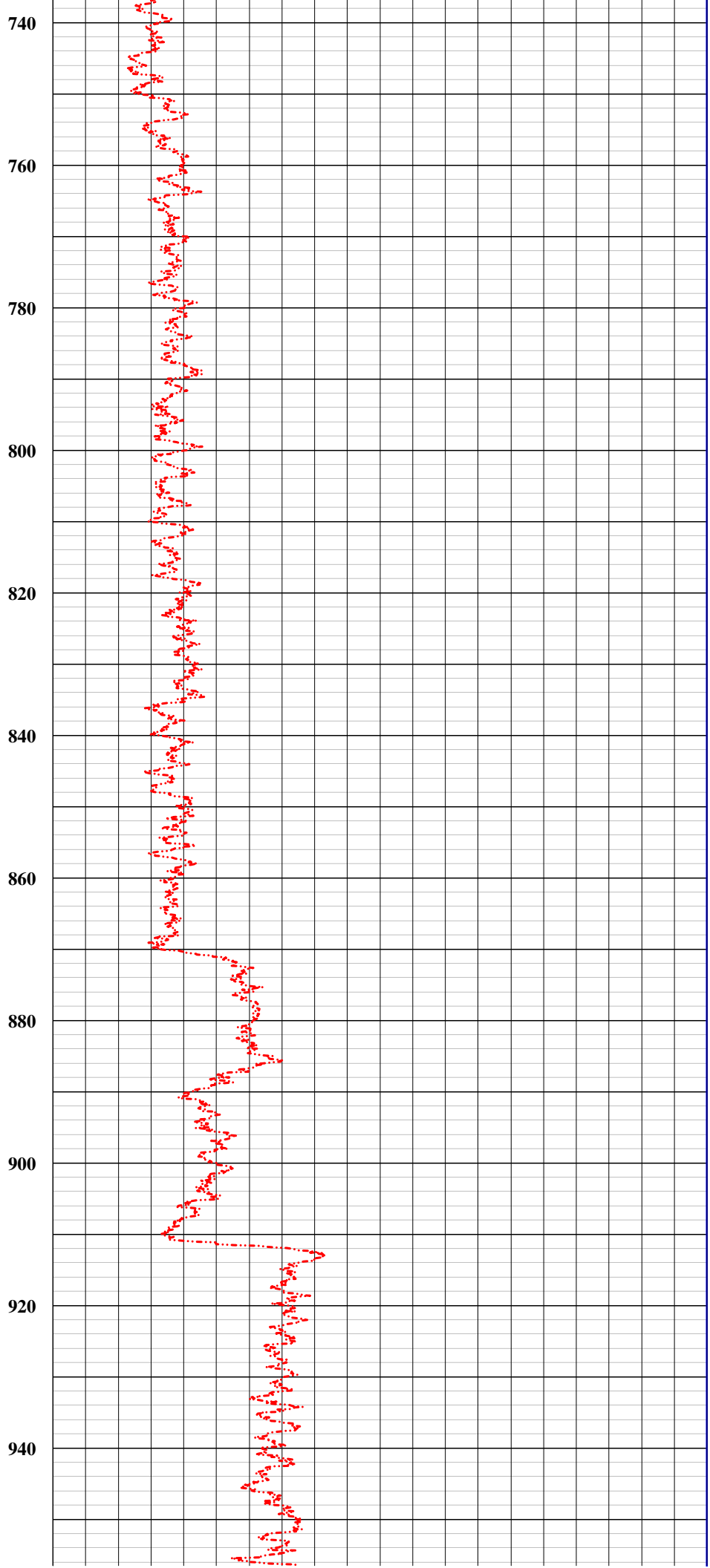
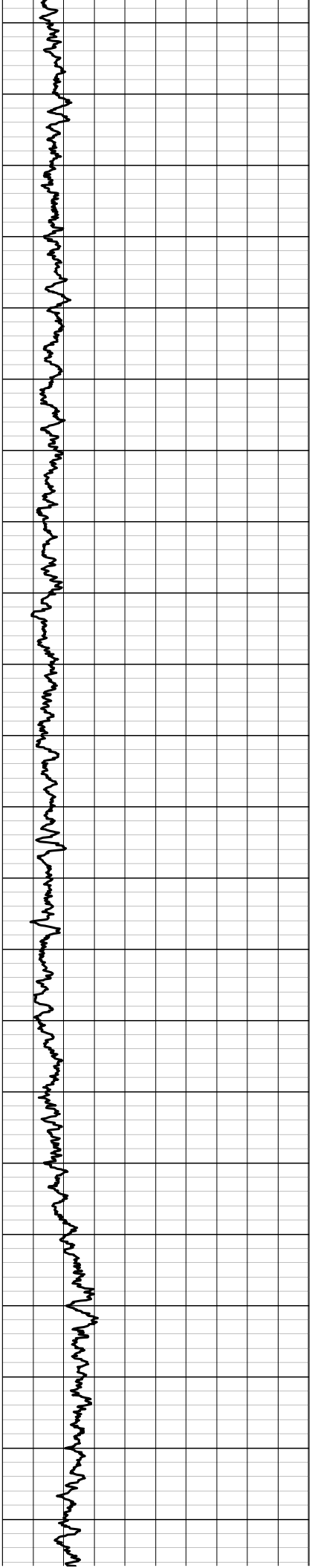


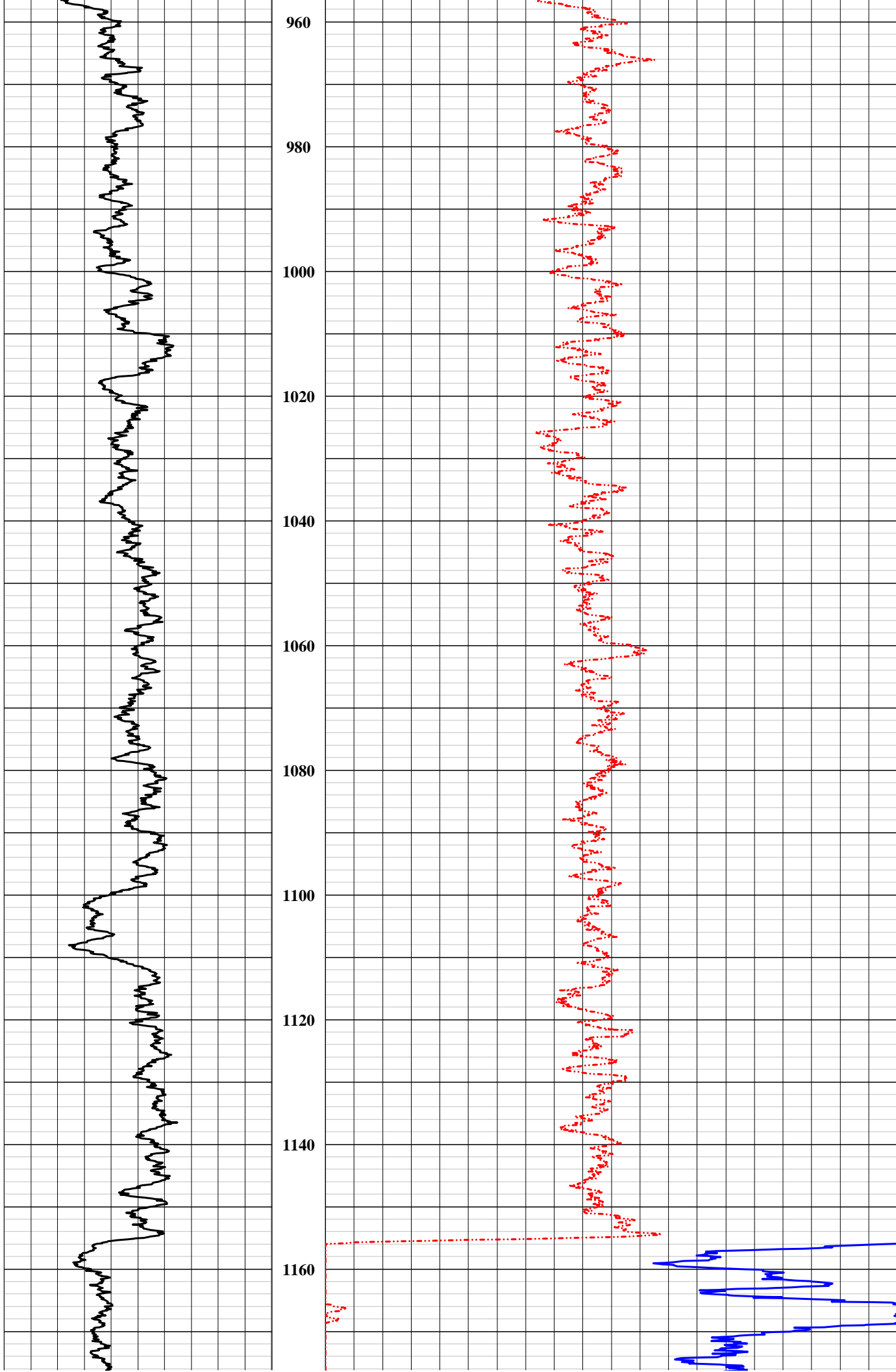


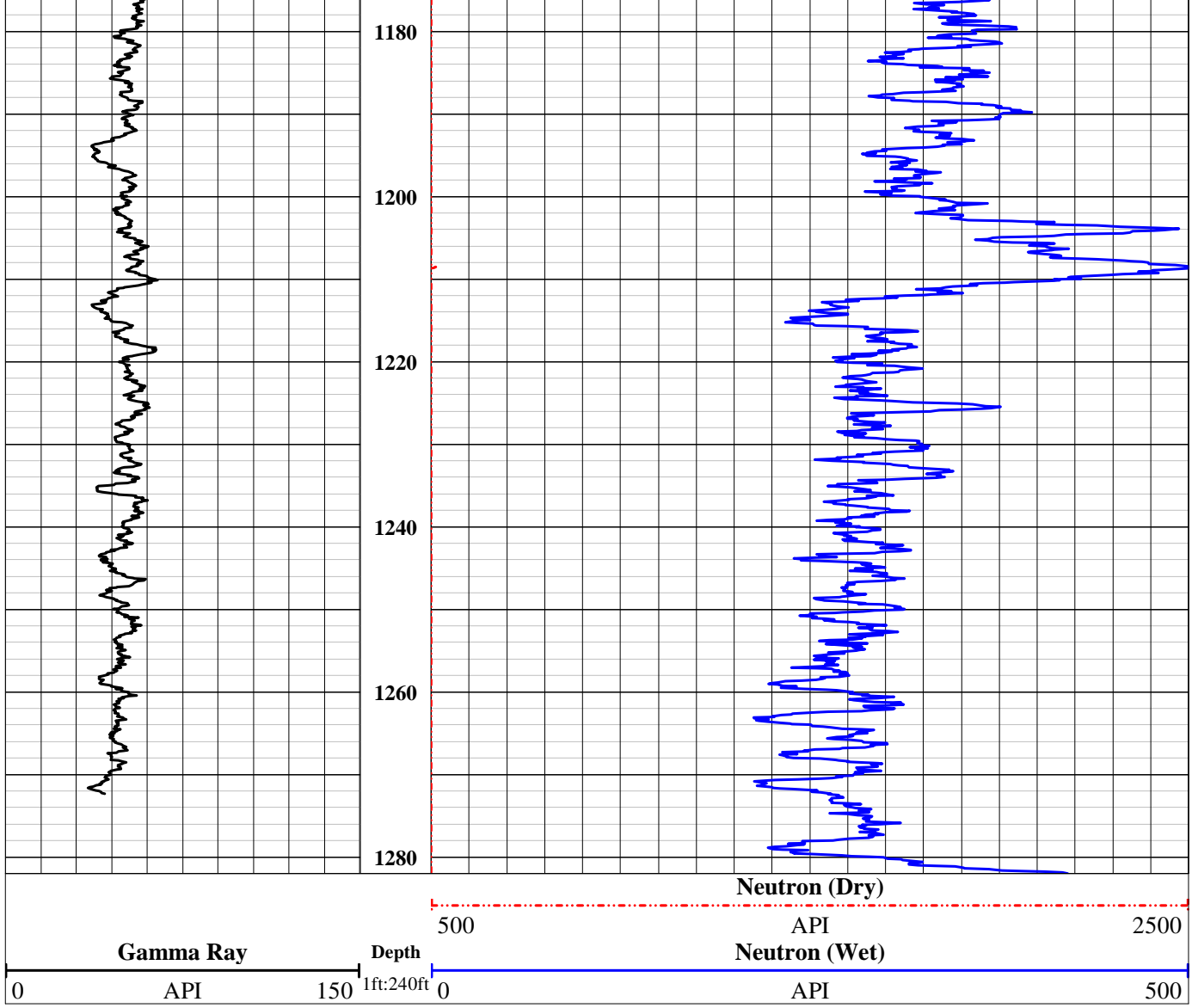












# **Appendix C**

---

*Final Well Design and  
New Mexico Environment Department Approval*





**From:** [Dale, Michael, NMENV](#)  
**To:** [White, Stephen Spalding](#)  
**Cc:** [Wear, Benjamin, NMENV](#); [Dhawan, Neelam, NMENV](#); [Cobrain, Dave, NMENV](#); [Swickley, Stephani Fuller](#); [Ball, Ted](#); [Katzman, Danny](#); [Longmire, Patrick](#); [Granzow, Kim P](#); [Yanicak, Stephen M](#)  
**Subject:** Re: CrIN-1 well design  
**Date:** Wednesday, June 22, 2016 11:09:18 AM

---

Steve,

New Mexico Environment Department (NMED) has reviewed the proposed well design plan (Plan) for injection well CrIN-1 that was received through e-mail correspondence on June 21, 2016 at 5:05 pm as shown below, and hereby issues this approval. Note that this approval is based on the information available to NMED at time of the approval. LANL must provide the results of groundwater sampling, any modifications to the well design as proposed in the above-mentioned e-mail, and any additional information relevant to the installation of the well as soon as such data or information become available. In addition, please provide NMED reasonable-time (e.g., 1 -2 days) notification prior to the initiation of well development, the step-drawdown test, and constant-rate aquifer testing at CrIN-1. Please call if you have any questions concerning this approval.

Thank you,

Michael R. Dale  
New Mexico Environment Department  
1183 Diamond Drive, Suite B  
Los Alamos, NM 87544  
LANL MS M894  
Cell Phone: (505) 231-5423  
Office Phone (505) 476-3078

---

**From:** White, Stephen Spalding <ssw@lanl.gov>  
**Sent:** Tuesday, June 21, 2016 5:05 PM  
**To:** Dale, Michael, NMENV; Katzman, Danny  
**Cc:** Wear, Benjamin, NMENV; Dhawan, Neelam, NMENV; Cobrain, Dave, NMENV; Swickley, Stephani Fuller; Ball, Ted  
**Subject:** RE: CrIN-1 well design

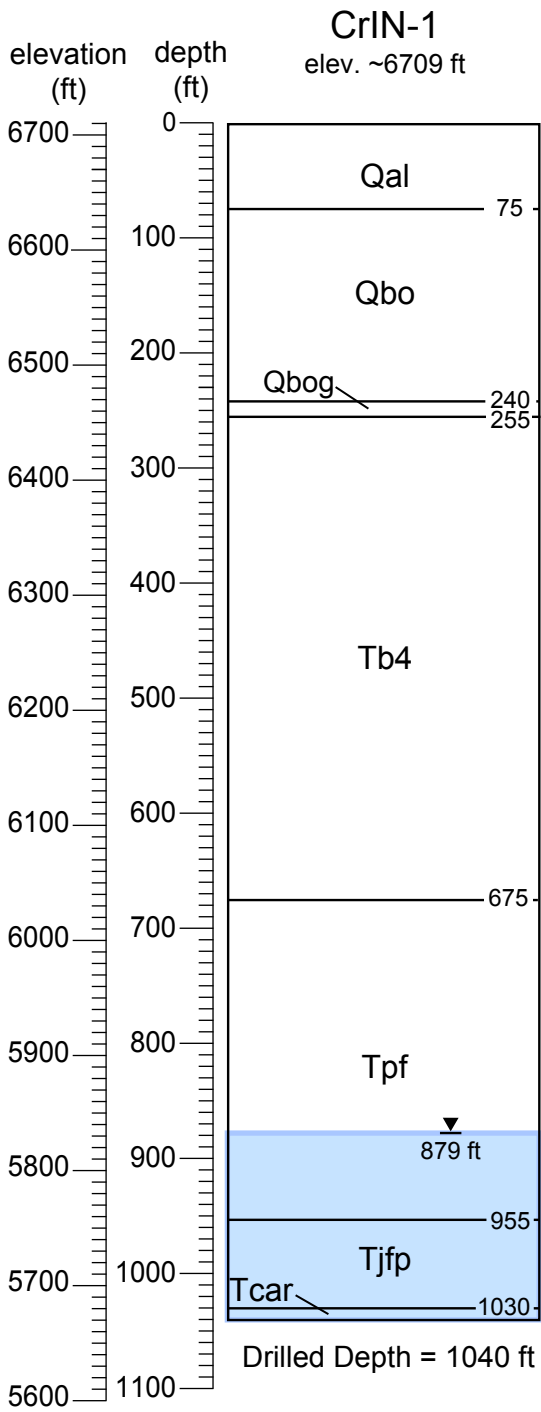
Michael,

Please find attached our well design proposal for CrIN-1.

Thanks,

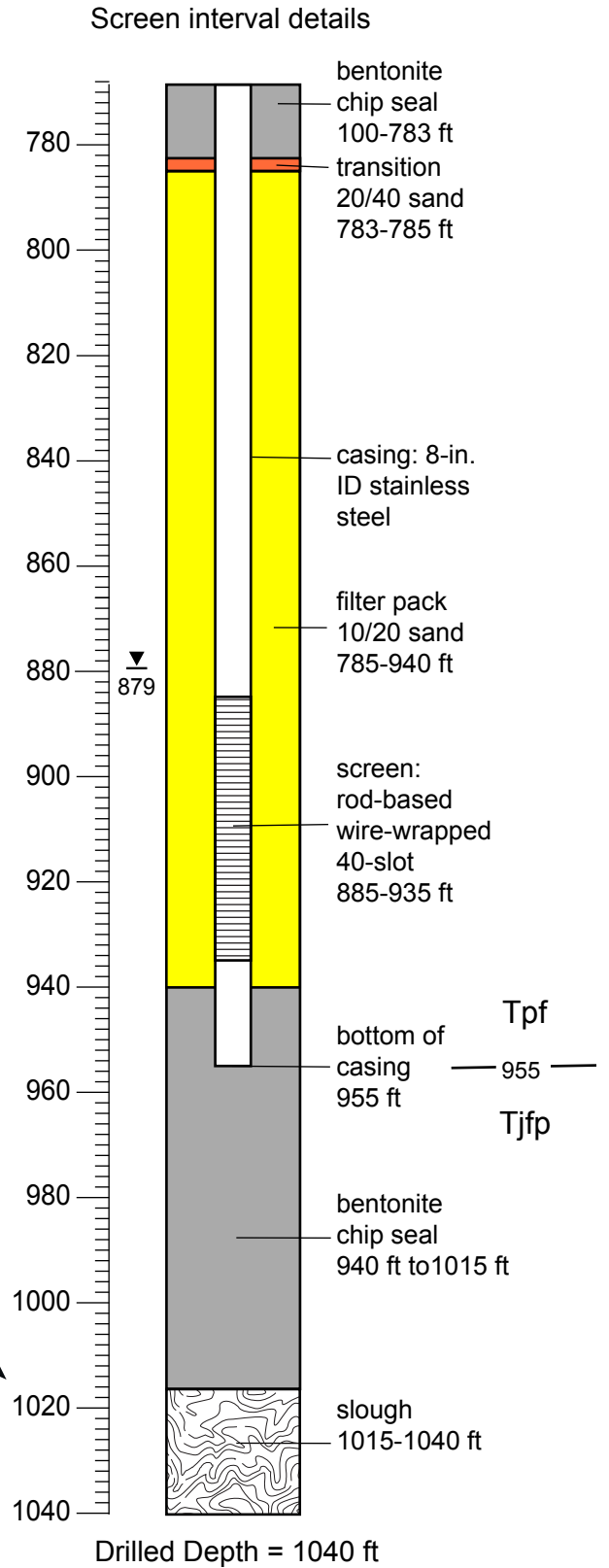
SW

Steve White  
LANL ER-ES  
505-257-8299 (cell)  
505-667-9005 (desk)



Approximate NM State Plane Coordinates:  
 x = 1640096 E y = 17668289 N

Note: Geologic contacts are preliminary



**From:** [Dale, Michael, NMENV](#)  
**To:** [Katzman, Danny](#)  
**Cc:** [Swickley, Stephani Fuller](#); [White, Stephen Spalding](#); [Everett, Mark Capen](#); [Rodriguez, Cheryl L](#); [Wear, Benjamin, NMENV](#); [Cobrain, Dave, NMENV](#); [Kulis, Jerzy, NMENV](#); [Fellenz, David Richard](#); [Green, Megan, NMENV](#); [Longmire, Patrick](#); [Granzow, Kim P](#); [mayer.richard@epa.gov](mailto:mayer.richard@epa.gov)  
**Subject:** RE: CrIN-2 Well Design Plan  
**Date:** Wednesday, May 11, 2016 9:46:26 AM

---

Danny,

New Mexico Environment Department (NMED) has reviewed the proposed well design plan (Plan) for injection well CrIN-2 that was received through e-mail correspondence on May 10, 2016 at 1:37 pm as shown below, and hereby issues this approval. As a result of the review, NMED recommends that LANL evaluate the potential use of larger filter-pack grain size(s) along the screened interval and above the regional water table within the vadose zone. An overall larger grain size and/or grading of grain sizes may optimize injection rates and long-term efficiency of the well with respect to reducing biofouling and formation of inorganic scale. Note that this approval is based on the information available to NMED at time of the approval. LANL must provide the results of groundwater sampling, any modifications to the well design as proposed in the above-mentioned e-mail, and any additional information relevant to the installation of the well as soon as such data or information become available. In addition, please provide NMED reasonable-time (e.g., 1 -2 days) notification prior to the initiation of well development, the step-drawdown test, and constant-rate aquifer testing at CrIN-2. Please call if you have any questions concerning this approval.

Thank you,

Michael R. Dale  
New Mexico Environment Department  
1183 Diamond Drive, Suite B  
Los Alamos, NM 87544  
LANL MS M894  
Cell Phone: (505) 231-5423  
Office Phone (505) 476-3078

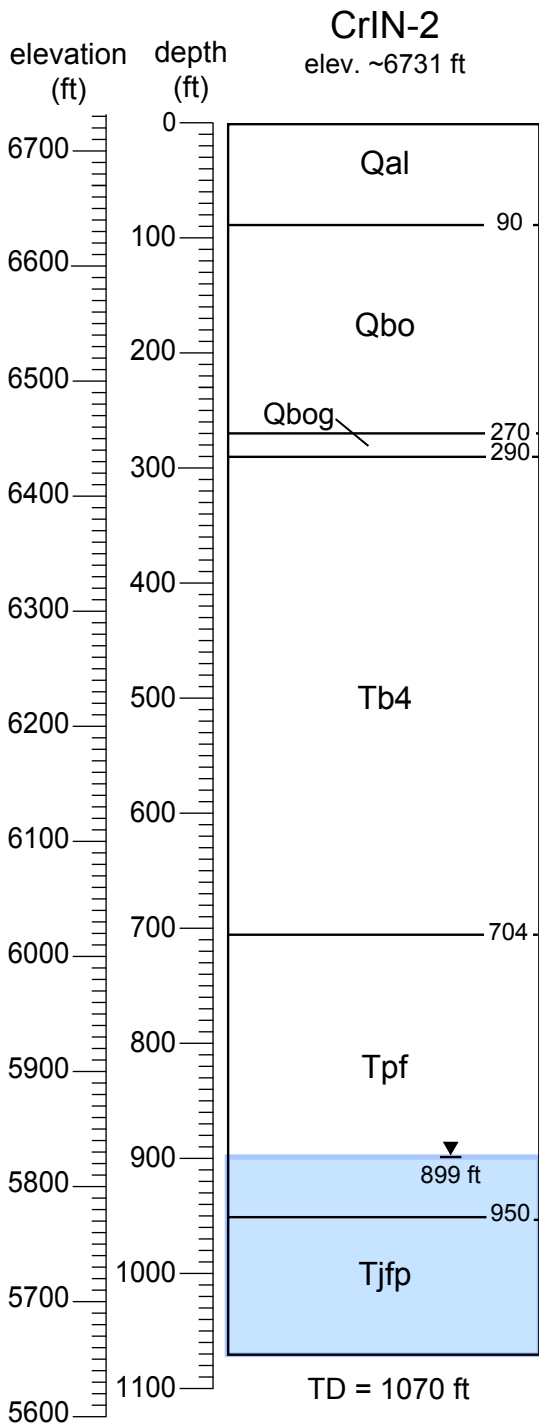
---

**From:** Katzman, Danny [mailto:katzman@lanl.gov]  
**Sent:** Tuesday, May 10, 2016 1:37 PM  
**To:** Dale, Michael, NMENV  
**Cc:** Swickley, Stephani Fuller; White, Stephen Spalding; Everett, Mark Capen; Rodriguez, Cheryl L  
**Subject:** CrIN-2 Well Design Plan

Michael- attached is our proposal for the CrIN-2 well design. Please review at your earliest convenience. We are hoping to begin construction on Wed.

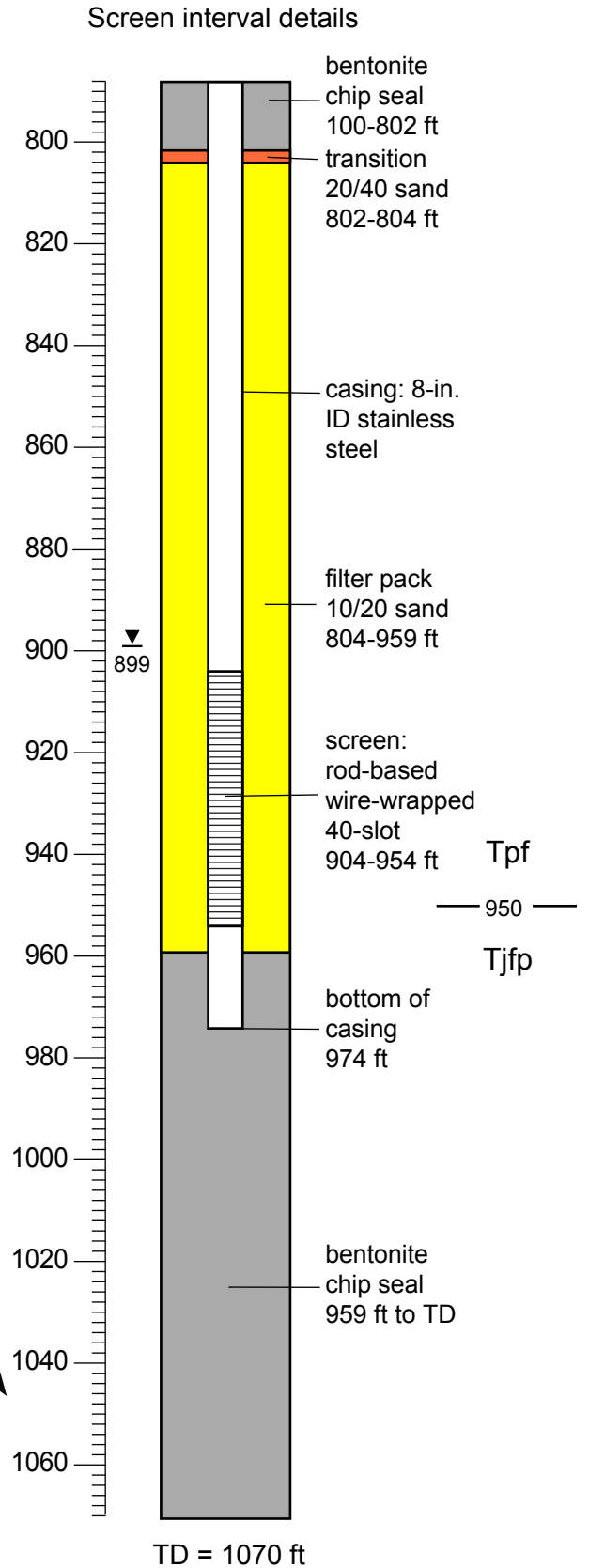
Thanks.

Danny



Approximate NM State Plane Coordinates:  
 x = 1639775 E y = 1767837 N

Note: Geologic contacts are preliminary



**From:** [Dale, Michael, NMENV](#)  
**To:** [White, Stephen Spalding](#)  
**Cc:** [Katzman, Danny](#); [Swickley, Stephani Fuller](#); [Ball, Ted](#); [Rodriguez, Cheryl L](#); [Shen, Hai](#); [Wear, Benjamin, NMENV](#); [Cobrain, Dave, NMENV](#); [Dhawan, Neelam, NMENV](#); [Huddleson, Steven, NMENV](#); [Longmire, Patrick](#); [Fellenz, David Richard](#); [Granzow, Kim P](#); [Green, Megan](#); [Yanicak, Stephen M](#)  
**Subject:** RE: CrIN3 sell design proposal  
**Date:** Wednesday, August 17, 2016 2:15:07 PM

---

Steve,

New Mexico Environment Department (NMED) has reviewed the proposed well design plan (Plan) for injection well CrIN-3 that was received today, August 17, 2016 at 11:24 am, and hereby issues this approval. Note that this approval is based on the information available to NMED at time of the approval. LANL must provide the results of groundwater sampling, any modifications to the well design as proposed in the above-mentioned e-mail, and any additional information relevant to the installation of the well as soon as such data or information become available. In addition, please provide NMED reasonable-time (e.g., 1 -2 days) notification prior to the initiation of well development, the step-drawdown test, and constant-rate aquifer testing at CrIN-3. Please call if you have any questions concerning this approval.

Thank you,

Michael R. Dale  
New Mexico Environment Department  
1183 Diamond Drive, Suite B  
Los Alamos, NM 87544  
LANL MS M894  
Cell Phone: (505) 231-5423  
Office Phone (505) 476-3078

---

**From:** White, Stephen Spalding [mailto:[ssw@lanl.gov](mailto:ssw@lanl.gov)]  
**Sent:** Wednesday, August 17, 2016 11:24 AM  
**To:** Dale, Michael, NMENV  
**Cc:** Katzman, Danny; Swickley, Stephani Fuller; Ball, Ted; Rodriguez, Cheryl L; Shen, Hai  
**Subject:** CrIN3 sell design proposal

Michael,

Please find attached our well design proposal for Chromium Injection Well #3 (CrIN-3).

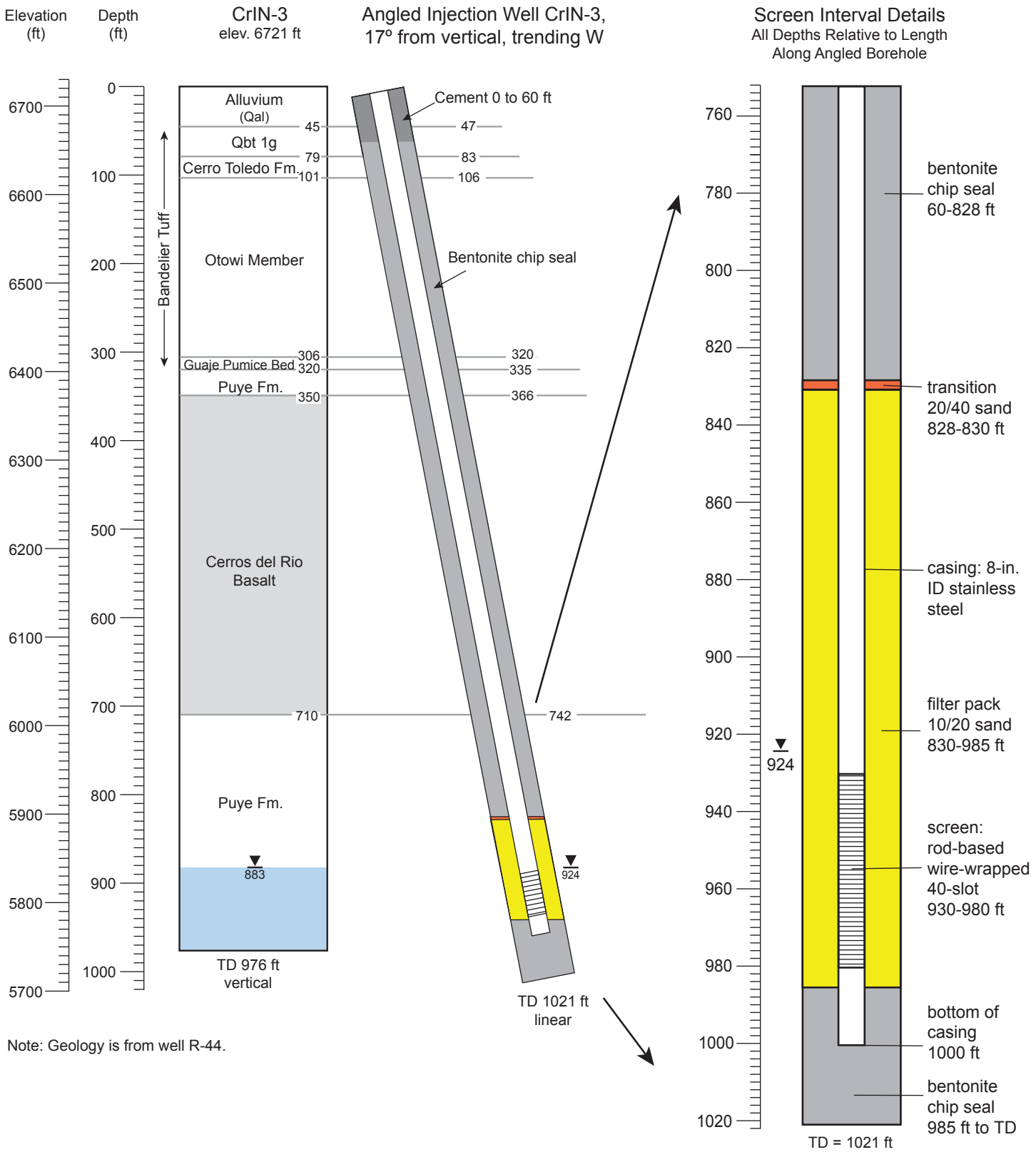
We had to coax some material out of the bottom of the drill casing and wait a bit for the water level to find static, but we're in good shape now; nothing in the drill casing and a SWL at 924 ft.

Let us know what you think.

Thanks,

SW

Steve White  
LANL ER-ES  
505-257-8299 (cell)  
505-667-9005 (desk)



**From:** [Dale, Michael, NMENV](#)  
**To:** [White, Stephen Spalding](#)  
**Cc:** [Wear, Benjamin, NMENV](#); [Kulis, Jerzy, NMENV](#); [Katzman, Danny](#); [Rodriguez, Cheryl L](#); [Everett, Mark Capen](#); [Fellenz, David Richard](#); [Green, Megan](#); [Granzow, Kim P](#); [Yanicak, Stephen M](#)  
**Subject:** RE: Email Policy Violation  
**Date:** Thursday, May 12, 2016 4:53:48 PM

---

Steve,

New Mexico Environment Department (NMED) has reviewed the proposed well design plan for injection well CrIN-4 that was received today, May 12, 2016 at 1:28 pm as attached in your e-mail below, and hereby issues this approval. Note that this approval is based on the information available to NMED at time of the approval. LANL must provide the results of groundwater sampling, any modifications to the well design as proposed in the above-mentioned e-mail, and any additional information relevant to the installation of the well as soon as such data or information become available. In addition, please provide NMED reasonable-time (e.g., 1 -2 days) notification prior to the initiation of well development, the step-drawdown test, and constant-rate aquifer testing at CrIN-4. Please call if you have any questions concerning this approval.

Michael R. Dale  
New Mexico Environment Department  
1183 Diamond Drive, Suite B  
Los Alamos, NM 87544  
LANL MS M894  
Cell Phone: (505) 231-5423  
Office Phone (505) 476-3078

---

From: White, Stephen Spalding [ssw@lanl.gov]  
Sent: Thursday, May 12, 2016 1:28 PM  
To: Dale, Michael, NMENV  
Cc: Katzman, Danny; Wear, Benjamin, NMENV  
Subject: RE: Email Policy Violation

No problem. It's a site map that's causing the trouble.

SW

Steve White  
LANL ER-ES  
505-257-8299 (cell)  
505-667-9005 (desk)

-----Original Message-----

From: Dale, Michael, NMENV [<mailto:Michael.Dale@state.nm.us>]  
Sent: Thursday, May 12, 2016 1:04 PM  
To: White, Stephen Spalding <ssw@lanl.gov>  
Cc: Katzman, Danny <katzman@lanl.gov>; Wear, Benjamin, NMENV <Benjamin.Wear@state.nm.us>  
Subject: FW: Email Policy Violation

Steve,

The e-mail, the CrIN-4 proposed well design, I suspect, that you tried sending was too large for the State system. Maybe try reducing the file size?

Thanks,

Michael



-----Original Message-----

From: enterpriseemailadministrators@state.nm.us [<mailto:enterpriseemailadministrators@state.nm.us>]

Sent: Thursday, May 12, 2016 12:25 PM

Subject: Email Policy Violation

Email Security service has detected content matching a policy in place for your organization, in the following email that was sent to you:

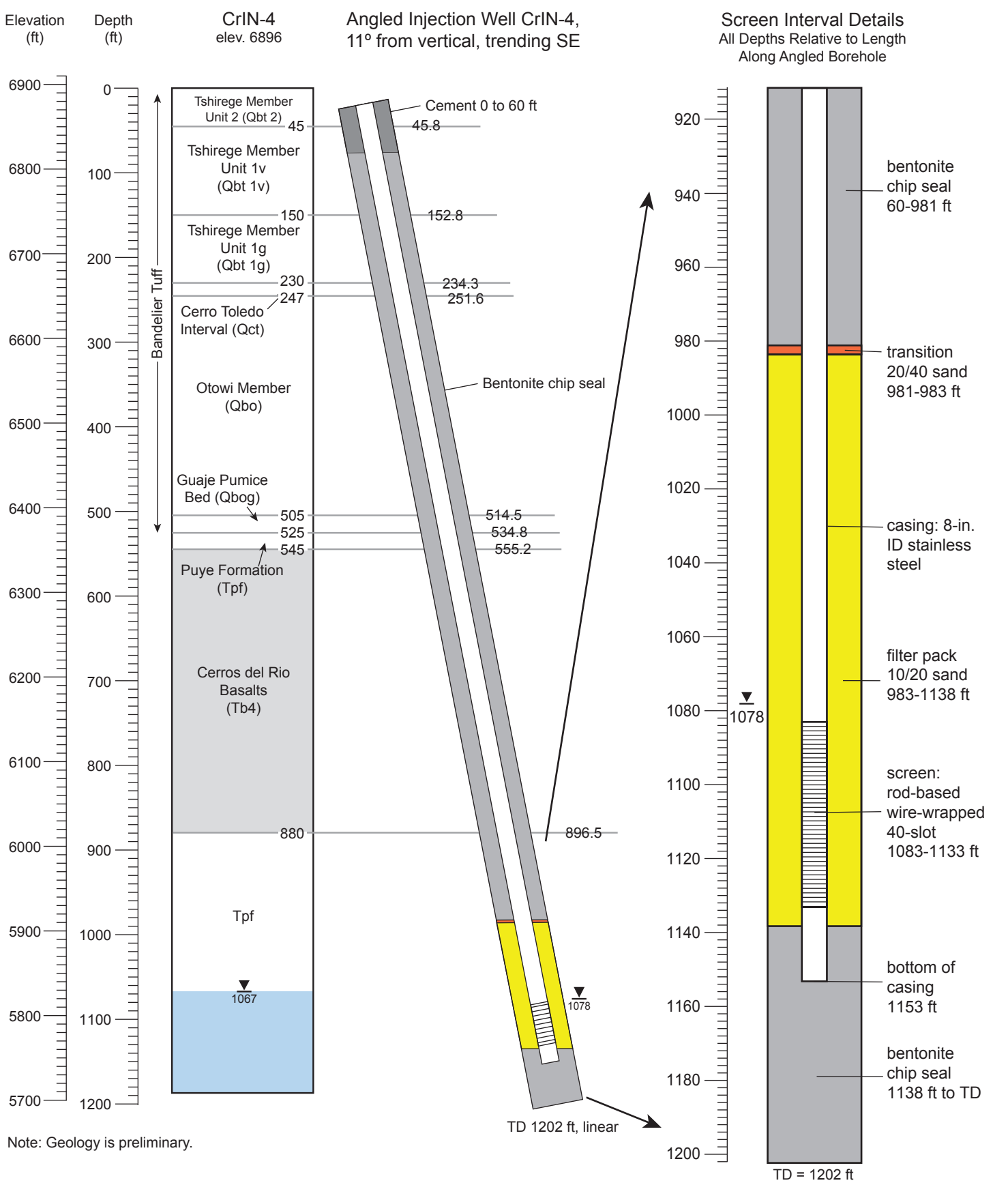
Sender: ssw@lanl.gov

Date: Thu, 12 May 2016 18:23:26 +0000

Subject: CrIN-4 well design

Please contact your IT Helpdesk or System Administrator for further assistance.

Matching Policy: Message Exceeds the Maximum Allowed Size



**From:** [Dale, Michael, NMENV](#)  
**To:** [White, Stephen Spalding](#)  
**Cc:** [Katzman, Danny](#); [Swickley, Stephani Fuller](#); [Rodriguez, Cheryl L](#); [Shen, Hai](#); [Wear, Benjamin, NMENV](#); [Cobrain, Dave, NMENV](#); [Fellenz, David Richard](#); [Green, Megan](#); [Granzow, Kim P](#); [Yanicak, Stephen M](#); [LucasKamat, Susan, NMENV](#); [Trujillo, Antonio Geronimo](#); [longmire@cybermesa.com](mailto:longmire@cybermesa.com)  
**Subject:** RE: CrIN5 well design proposal  
**Date:** Saturday, July 02, 2016 10:28:31 AM

---

Steve,

New Mexico Environment Department (NMED) has reviewed the proposed well design plan (Plan) for injection well CrIN-5 that was received through e-mail correspondence today, July 2, 2016 at 9:14 am as shown below, and hereby issues this approval. Note that this approval is based on the information available to NMED at time of the approval. LANL must provide the results of groundwater sampling, any modifications to the well design as proposed in the above-mentioned e-mail, and any additional information relevant to the installation of CrIN-5 as soon as such data or information become available. In addition, please provide NMED reasonable-time (e.g., 1 -2 days) notification prior to the initiation of well development, the step-drawdown test, and constant-rate aquifer testing at CrIN-5. Please call if you have any questions concerning this approval.

Thank you,

Michael R. Dale  
New Mexico Environment Department  
1183 Diamond Drive, Suite B  
Los Alamos, NM 87544  
LANL MS M894  
Cell Phone: (505) 231-5423  
Office Phone (505) 476-3078

---

**From:** White, Stephen Spalding [mailto:[ssw@lanl.gov](mailto:ssw@lanl.gov)]  
**Sent:** Saturday, July 02, 2016 9:14 AM  
**To:** Dale, Michael, NMENV  
**Cc:** Katzman, Danny; Swickley, Stephani Fuller; Rodriguez, Cheryl L; Shen, Hai  
**Subject:** CrIN5 well design proposal

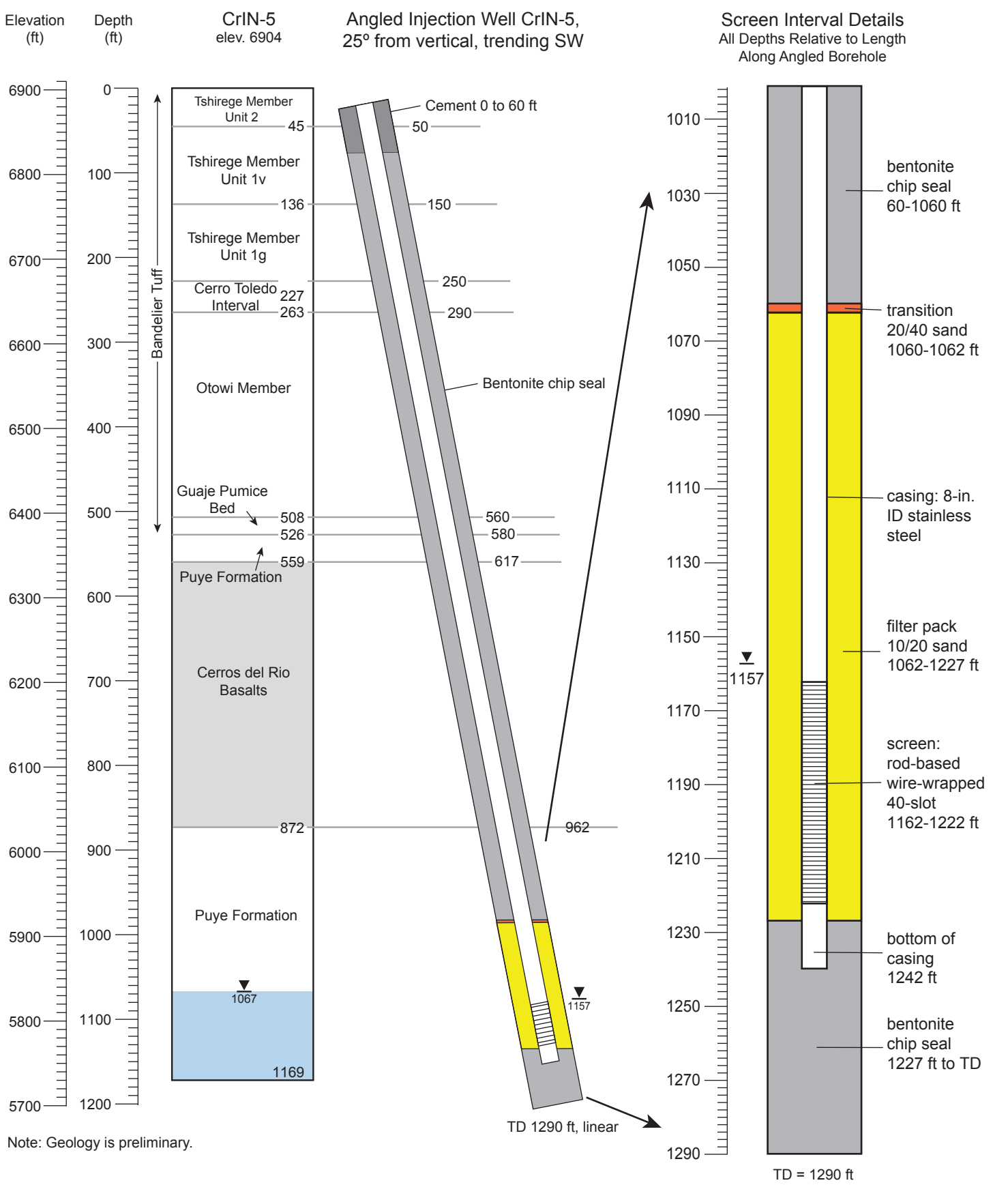
Hi Michael,

Please find attached our well design proposal for CrIN-5. Let me know if you have any questions.

Thanks,

SW

Steve White  
LANL ER-ES  
505-257-8299 (cell)  
505-667-9005 (desk)



# **Appendix D**

---

*Analysis of CrIN Pumping Test Data*



## D-1.0 INTRODUCTION

This appendix describes the hydraulic analysis of the five pumping tests conducted from May 31 to September 11, 2016, at chromium injection (CrIN) wells CrIN-1, CrIN-2, CrIN-3, CrIN-4, and CrIN-5 to characterize the regional aquifer at the Los Alamos National Laboratory (LANL or the Laboratory). The wells are screened in the Puye Formation. The test data are applied to estimate aquifer (hydraulic) parameters. It is assumed that the pumping tests are conducted in a partially penetrated aquifer with limited thickness, which is homogeneous and anisotropic. The aquifer is assumed to have a uniform thickness (without boundary effects). The software AQTESOLV (Duffield 2007, 601723) is used to interpret the pumping test data. Two theoretical models built in the software AQTESOLV, Theis (1934-1935, 098241), and Neuman (1974, 085421) are applied for estimate aquifer parameters. The Theis model is representative for confined aquifer conditions; however, the Theis model was applied with a correction for unconfined effects. The Neuman model is representative of unconfined aquifer conditions. The analyses allow transmissivity, hydraulic conductivity, storage coefficient, specific yield, and anisotropic factor to be estimated.

It is important to note that in the Theis analyses presented below, the storage coefficient estimates are not expected to be realistic. Typically, single-well pumping tests do not provide reasonable storage coefficient estimates. Good estimates for storage coefficient are typically obtained using cross-well pumping tests.

Determining hydraulic conductivity of the aquifer materials based on the estimated aquifer transmissivity is challenging because the effective aquifer thickness is impacted during the pumping tests and it is unknown. The total aquifer thickness of the regional aquifer extends more than 1000 ft. However, during the pumping tests conducted near the regional water table, only a small vertical portion of the regional aquifer is affected by the pumping tests. The effective aquifer thickness depends on the length of the well screen (and filter pack) and the hydraulic properties of the aquifer (especially the vertical anisotropy). The saturated thickness is also impacted by pumping because it causes a decline in the regional water table. Based on previous analyses, aquifer thickness of 30 m (100 ft) is assumed and is considered to be representative for the chromium site wells at the Laboratory.

**Theis model:** Theis model (Theis 1934-1935, 098241) was derived for simulating the transient flow to a fully penetrating well in a confined aquifer with uniform thickness and hydraulic properties. The solution assumes a line source for the pumped well and neglects wellbore storage:

$$s = \frac{Q}{4\pi T} \int_u^\infty \frac{e^{-y}}{y} dy = \frac{Q}{4\pi T} W(u) \quad \text{Equation D-1}$$

$$u = \frac{r^2 \mu}{4Tt} \quad \text{Equation D-2}$$

where,  $s$  is drawdown (L);  $Q$  is pumping rate [ $L^3/T$ ];  $T$  is transmissivity [ $L^2/T$ ];  $r$  is radial distance [L];  $\mu$  is storativity [dimensionless]; and  $t$  is time [T]; and  $W(u)$  is the Theis well function. The Theis solution is derived for confined aquifers. However, Jacob's correction for partial dewatering of water-table (unconfined) aquifers allows the use of the Theis solution for unconfined aquifers as well. Jacob's correction was applied as implemented in the software AQTESOLV (Duffield 2007, 601723) in the Theis analyses presented below.

Hantush (Hantush 1961, 098237; Hantush 1961, 106003) modified the Theis model for simulating the effects of partial penetration in an aquifer with uniform thickness. For a piezometer, the partial penetration correction is computed as follows:

$$s = \frac{Q}{4\pi T} \left\{ W(u) + \frac{2b}{\pi(l-d)} \sum_{n=1}^{\infty} \frac{1}{n} \left[ \sin\left(\frac{n\pi l}{b}\right) - \sin\left(\frac{n\pi d}{b}\right) \right] \cos\left(\frac{n\pi z}{b}\right) W\left(u, \sqrt{\frac{K_z}{K_r} \frac{n\pi r}{b}}\right) \right\} \quad \text{Equation D-3}$$

where,  $b$  is aquifer thickness [L];  $d$  is depth to top of pumping well screen [L];  $l$  is depth to bottom of pumping well screen [L];  $K_z/K_r$  is vertical to horizontal hydraulic conductivity anisotropy [dimensionless];  $W(u,\beta)$  is the Hantush-Jacob well function; and  $z$  is depth to piezometer opening [L].

**Neuman model:** The Neuman model was developed to address the delayed gravity response of the unconfined aquifer (Neuman 1974, 085421). The “delayed yield” represents the gravitational drainage (infiltration) from the vadose zone into aquifer from pumping. Therefore, the pumping test analyses using Neuman model also provide information about the properties of the vadose zone in addition to the regional aquifer properties. An analytical solution was derived for simulating the transient flow to a fully or partially penetrating well in a homogeneous, anisotropic unconfined aquifer with delayed gravity response. The Neuman model assumes instantaneous drainage at the water table. The solution also assumes a line source for the pumped well and neglects wellbore storage.

$$s = \frac{Q}{4\pi T} \int_0^{\infty} 4y J_0(y\sqrt{\beta}) \{u_0(y) + \sum_{n=1}^{\infty} u_n(y)\} dy \quad \text{Equation D-4}$$

$$\beta = \frac{r^2 K_z}{b^2 K_r} \quad \text{Equation D-5}$$

where,  $J_0$  is Bessel function of first kind and zero order;  $u_0$  and  $u_n$  are functions for computing drawdowns in a piezometer or in a partially penetrating observation well (Neuman 1974, 085421). The drawdown in a piezometer is calculated using the following two equations:

$$u_0(y) = \frac{[1 - \exp(-t_s \beta (y^2 - \gamma_0^2))] \cosh(\gamma_0 Z_D)}{[y^2 + (1 + \sigma) \gamma_0^2 - \frac{(y^2 - \gamma_0^2)^2}{\sigma}] \cosh(\gamma_0)} \cdot \frac{\sinh(\gamma_0(1 - d_D)) - \sinh(\gamma_0(1 - l_D))}{(l_D - d_D) \sinh(\gamma_0)} \quad \text{Equation D-6}$$

$$u_n(y) = \frac{[1 - \exp(-t_s \beta (y^2 - \gamma_0^2))] \cos(\gamma_0 Z_D)}{[y^2 + (1 + \sigma) \gamma_0^2 - \frac{(y^2 - \gamma_0^2)^2}{\sigma}] \cos(\gamma_0)} \cdot \frac{\sin(\gamma_0(1 - d_D)) - \sin(\gamma_0(1 - l_D))}{(l_D - d_D) \sin(\gamma_0)} \quad \text{Equation D-7}$$

where  $d_D$  is dimensionless depth to top of pumping well screen ( $d/b$ );  $l_D$  is dimensionless depth to bottom of pumping well screen ( $l/b$ );  $Z_D$  is dimensionless elevation of piezometer opening above the base of aquifer ( $z/b$ ); and the gamma terms are computed numerically. Neuman model is built in the software AQTESOLV for simulating water flow in unconfined aquifers. By using the principle of superposition in time, AQTESOLV also accounts for transient pumping rates.

The analyses presented below are performed using the Theis and Neuman solutions coded into the software AQTESOLV (Duffield 2007, 601723). AQTESOLV uses the principle of superposition to account for the transient in the pumping rate. The solutions are applied to account for unconfined aquifer conditions.

The following sections will discuss the interpretations of the pumping test data collected from wells CrIN-1, CrIN-2, CrIN-3, CrIN-4, and CrIN-5.



## D-2.0 CRIN-1

The pumping test at CrIN-1 was conducted from July 18 to July 21, 2016, and the pump was run at multiple steps with various constant pumping rates (Figure D-1). The observation of the well pressure transients started from 13:01 on July 18. At 13:58, a constant pumping rate of 30 gallons per minute (gpm) was initiated for about 1 h, then increased to 50 gpm for about another hour, and then increased to 70 gpm for an additional 1 h. After 3 h and three-step pumping, the pump was stopped for a 16-h recovery, and the water levels were monitored until 8:58 on July 19. At 8:58, the pump was restarted with a constant rate of 70 gpm for 24 h, after which the pump was stopped for another 16-h recovery period (see Figure D-1).

The observed water depths were converted to corrected displacements or drawdowns (in feet) by using the mean water depth before the pumping as the initial water depth (Figure D-2). First, the Theis model was used to fit the drawdown data of multistep pumping test and recovery data. The well structure and pumping test parameters are shown in Tables D-1 and D-2. The estimated hydraulic conductivity is 5.64 m/d, and the storage coefficient is very small ( $10^{-6}$ ). The computed drawdowns from the Theis model cannot fit the observations, especially during the 1-d constant pumping period (Figure D-3). Although the weighting coefficients of the drawdown observations were adjusted to be very small for the late-time data during this 1-d pumping period, the data points could not be made to fit well. The drawdowns during this period decreased with time, which may be the result of some additional recharge resources from boundaries and caused by the pumping test. The Theis model used no-flow boundaries for the top and bottom boundaries and could not simulate any additional recharge sources.

The Neuman model was also used to fit the observed drawdown and recovery data. A new parameter, "specific yield," was added to address the delayed gravity response of the unconfined aquifer, the computed drawdowns from the Neuman model can fit the data better than the Theis model. The estimated parameters are listed in Table D-3: conductivity is 2.27 m/d, storage coefficient is 0.000799, and specific yield is 0.32, which is close to the expected total (water-filled) porosity of the Puye Formation. The parameter  $\beta$  is a coefficient to describe the hydraulic conductivity anisotropic ratio ( $\frac{r^2 K_z}{b^2 K_r}$ ), where  $r$  is radial distance,  $b$  is aquifer thickness,  $K_z$  is vertical conductivity, and  $K_r$  is horizontal conductivity. In this case, the parameter  $\beta$  is 0.001488, and the anisotropic ratio of  $\frac{K_z}{K_r}$  is equal to 0.23. The curve fitting is shown in Figure D-4. The objective function (sum of squares) was reduced to 29.4 from 366.3 obtained from the Theis model. However, the computed drawdowns from the Neuman model still do fit the late-time observations during the 1-d constant-pumping period very well.

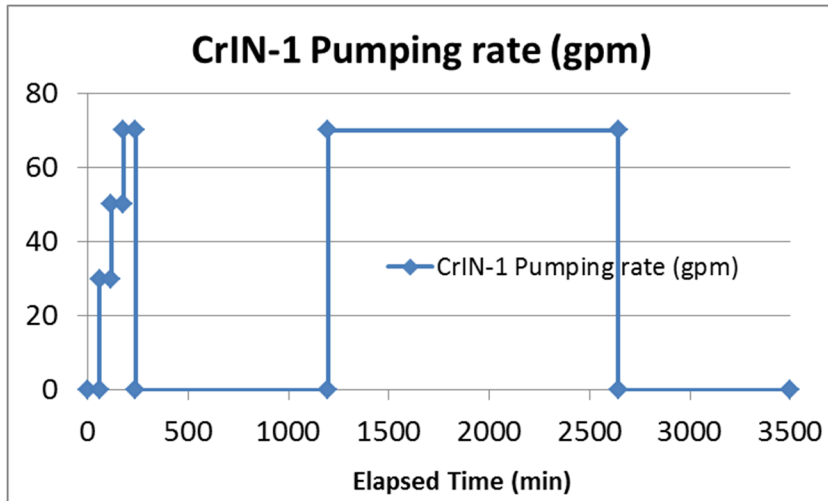


Figure D-1 Variable pumping rates for the test at well CrIN-1

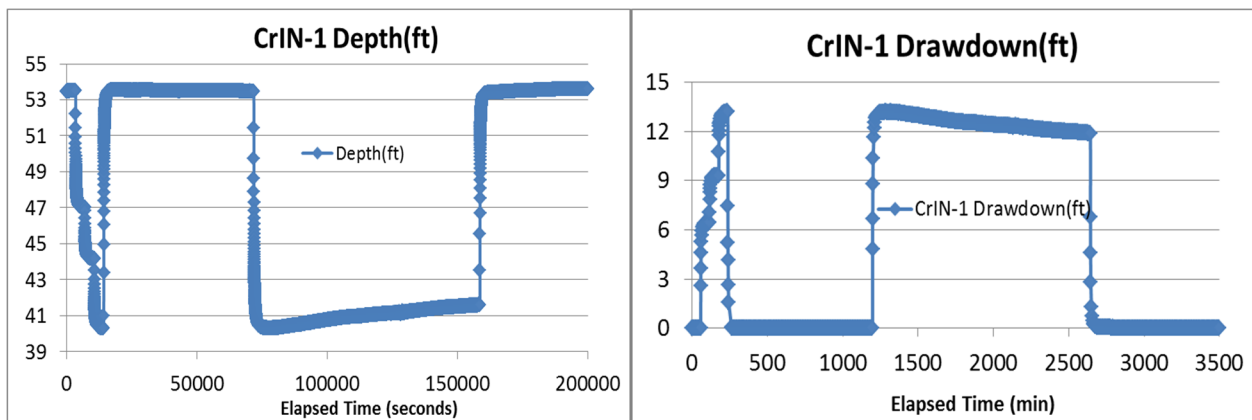


Figure D-2 Measured water depth (left) and drawdown (right) from the pumping test of well CrIN-1

**Table D-1  
CrIN-1 Well Structure and Pumping Test Data Applied in the Pumping Test Analyses**

Data Set: E:\EP2016\AquiferTest\CrIN\CrIN-1-Theis2.aqt Title: CrIN-1 pumping test Date: 09/23/16 Time: 16:29:51					
<u>PROJECT INFORMATION</u>					
Company: LANL Client: zd Project: ep Location: Puye Test Date: 2016 Test Well: CrIN-1					
<u>AQUIFER DATA</u>					
Saturated Thickness: 100. ft Anisotropy Ratio (Kz/Kr): 0.01					
<u>PUMPING WELL DATA</u>					
No. of pumping wells: 1					
Pumping Well No. 1: CrIN-1					
X Location: 0. ft					
Y Location: 0. ft					
Casing Radius: 8.625 ft					
Well Radius: 8. ft					
Partially Penetrating Well					
Depth to Top of Screen: 36. ft					
Depth to Bottom of Screen: 86. ft					
No. of pumping periods: 14					
<u>Pumping Period Data</u>					
<u>Time (min)</u>	<u>Rate (gal/min)</u>	<u>Time (min)</u>	<u>Rate (gal/min)</u>	<u>Time (min)</u>	<u>Rate (gal/min)</u>
0.	1.0E-6	177.3	50.	1197.3	70.
57.3	0.	177.3	70.	2643.1	70.
57.33	30.	237.1	70.	2643.2	0.
116.8	30.	237.2	0.	3500.	0.
116.9	50.	1197.3	0.		
<u>OBSERVATION WELL DATA</u>					
No. of observation wells: 1					
Observation Well No. 1: CrIN-1					
X Location: 0. ft					
Y Location: 0. ft					
Radial distance from CrIN-1: 0. ft					
Partially Penetrating Well					
Depth to Top of Screen: 36. ft					
Depth to Bottom of Screen: 86. ft					

**Table D-2  
Estimated Parameters Using the Theis Model for CrIN-1**

<u>SOLUTION</u>					
Pumping Test Aquifer Model: Unconfined Solution Method: Theis					
<u>VISUAL ESTIMATION RESULTS</u>					
<u>Estimated Parameters</u>					
<u>Parameter</u>	<u>Estimate</u>				
T	171.8	m <sup>2</sup> /day			
S	1.0E-6				
Kz/Kr	0.01				
b	100.	ft			
K = T/b = 5.637 m/day (0.006524 cm/sec) Ss = S/b = 1.0E-8 1/ft					
<u>AUTOMATIC ESTIMATION RESULTS</u>					
<u>Estimated Parameters</u>					
<u>Parameter</u>	<u>Estimate</u>	<u>Std. Error</u>	<u>Approx. C.I.</u>	<u>t-Ratio</u>	
T	171.8	7.664	+/- 15.05	22.42	m <sup>2</sup> /day
S	1.0E-6	2.176E-6	+/- 4.273E-6	0.4596	
Kz/Kr	0.01	0.02402	+/- 0.04718	0.4163	
b	100.	not estimated			ft
C.I. is approximate 95% confidence interval for parameter t-ratio = estimate/std. error No estimation window					
K = T/b = 5.637 m/day (0.006524 cm/sec) Ss = S/b = 1.0E-8 1/ft					
<u>Parameter Correlations</u>					
	<u>T</u>	<u>S</u>	<u>Kz/Kr</u>		
T	1.00	-0.03	-0.35		
S	-0.03	1.00	-0.93		
Kz/Kr	-0.35	-0.93	1.00		
<u>Residual Statistics</u>					
for weighted residuals					
Sum of Squares	....	366.3	ft <sup>2</sup>		
Variance	.....	0.6553	ft <sup>2</sup>		
Std. Deviation	.....	0.8095	ft		
Mean	.....	-0.4083	ft		
No. of Residuals	....	562			
No. of Estimates	....	3			

**Table D-3**  
**Estimated Parameters Using the Neuman Model for CrIN-1**

Estimated Parameters

<u>Parameter</u>	<u>Estimate</u>	
T	69.22	m <sup>2</sup> /day
S	0.0007993	
Sy	0.32	
β	0.001488	

K = T/b = 2.271 m/day (0.002629 cm/sec)

Ss = S/b = 7.993E-6 1/ft

AUTOMATIC ESTIMATION RESULTSEstimated Parameters

<u>Parameter</u>	<u>Estimate</u>	<u>Std. Error</u>	<u>Approx. C.I.</u>	<u>t-Ratio</u>	
T	69.22	2.438	+/- 4.789	28.39	m <sup>2</sup> /day
S	0.0007993	6.06E-5	+/- 0.000119	13.19	
Sy	0.32	0.06129	+/- 0.1204	5.221	
β	0.001488	0.0002617	+/- 0.0005139	5.687	

C.I. is approximate 95% confidence interval for parameter

t-ratio = estimate/std. error

No estimation window

K = T/b = 2.271 m/day (0.002629 cm/sec)

Ss = S/b = 7.993E-6 1/ft

Parameter Correlations

	<u>T</u>	<u>S</u>	<u>Sy</u>	<u>β</u>
T	1.00	-0.93	-0.86	-1.00
S	-0.93	1.00	0.83	0.93
Sy	-0.86	0.83	1.00	0.86
β	-1.00	0.93	0.86	1.00

Residual Statistics

for weighted residuals

Sum of Squares . . . . 29.39 ft<sup>2</sup>  
Variance . . . . . 0.04898 ft<sup>2</sup>  
Std. Deviation . . . . . 0.2213 ft  
Mean . . . . . -0.06275 ft  
No. of Residuals . . . . 604  
No. of Estimates . . . . 4

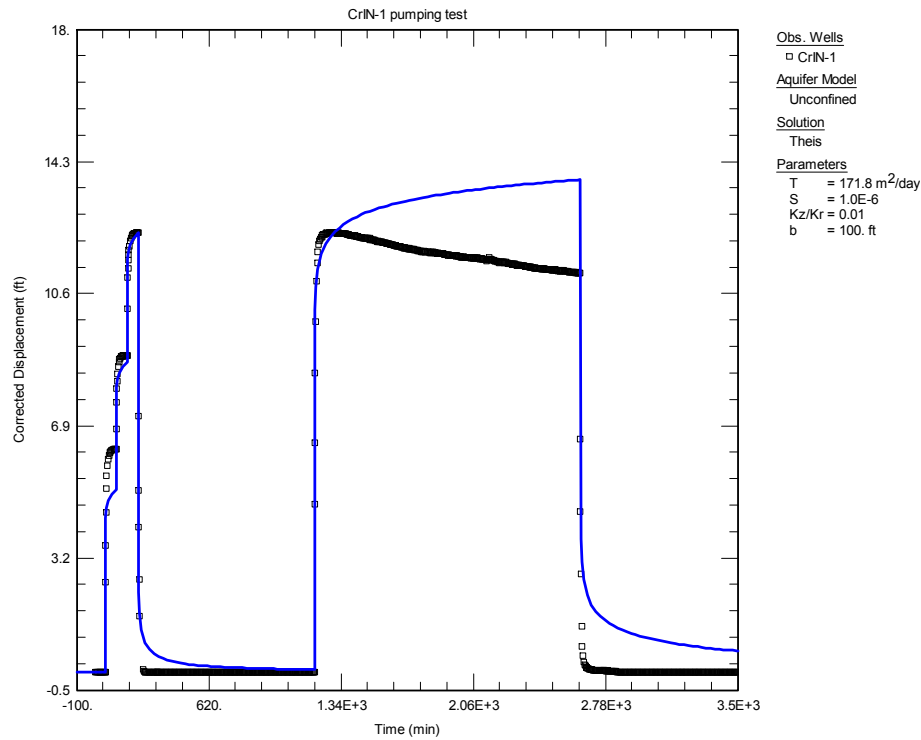


**Figure D-3** Matching observed drawdowns (black dots) during the four-step CrIN-1 test using the Theis model (blue line)

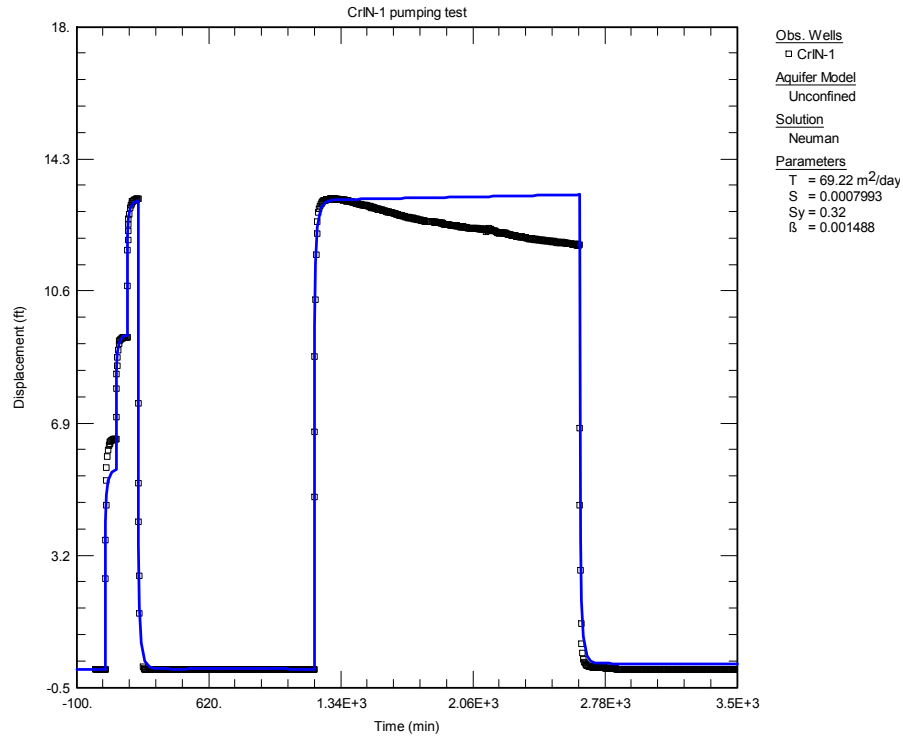


**Figure D-4** Matching observed drawdowns (black dots) during the four-step CrIN-1 test using the Neuman model (blue line)

### D-3.0 CRIN-2

The pumping test at CrIN-2 was conducted from May 31 to June 3, 2016, and the pump was run at multiple steps with various constant pumping rates (Figure D-5). The pump was started at 12:01 on May 31 at a rate of 30 gpm for 1 h. At 13:00, the pump was stopped for about 1 h of recovery, after which it was restarted at a rate of 50 gpm for an additional 1 h. The pump was then stopped for about 1.5 h to observe the water-level recovery. During the third step, the pump was restarted with a rate of 70 gpm for 1 h. After 3 h of three-step pumping, the pump was stopped for a 16.5-h recovery period, and the water levels were monitored until 10:00 on June 1. The pump was restarted with a constant rate of 58 gpm for 24 h and then stopped for a 25-h recovery period (see Figure D-5).

Figure D-6 (left) shows some spikes in the observed water-level-depth data at the pump starting stages that are not representative of the actual pumping test drawdowns. When the spikes were manually located and removed, the data look clean and reasonable (Figure D-6, right). Additional details can be found in Rasmussen and Crawford (1997, 094014) and Spaine (2002, 602105). The observed multistep water depths were converted to corrected displacements or drawdowns (in feet) and then used for parameter estimation (Figure D-7).

First, the variable-rate Theis model was used to fit the multistep observation data. The multistep variable pumping rates and parameter estimation results are shown in Tables D-4 and D-5. The estimated hydraulic conductivity is 8.55 m/d, and the storage coefficient is  $10^{-6}$ . The computed drawdowns during the first three steps and recovery time do not fit the observation data well (Figure D-8).

Next, the variable-rate Neuman model was used to fit the observation data. By considering the delayed gravity response of the unconfined aquifer, the Neuman model can simulate well the multistep pumping test processes and the computed drawdowns fit the observation data better. The estimated parameters are listed in Table D-6: conductivity is 3.26 m/d, storage coefficient is 0.00116, and specific yield is 0.32 (specific yield is during the parameter estimation process is limited to the expected maximum porosity of the Puye Formation, which is equal to 0.32). The parameter  $\beta$  coefficient is 0.003434, and in this model, the ratio of  $\frac{K_z}{K_r}$  is equal to 0.536. The objective function (or sum of squares) is reduced from 227.2, which was obtained from the Theis model, to 79.2.

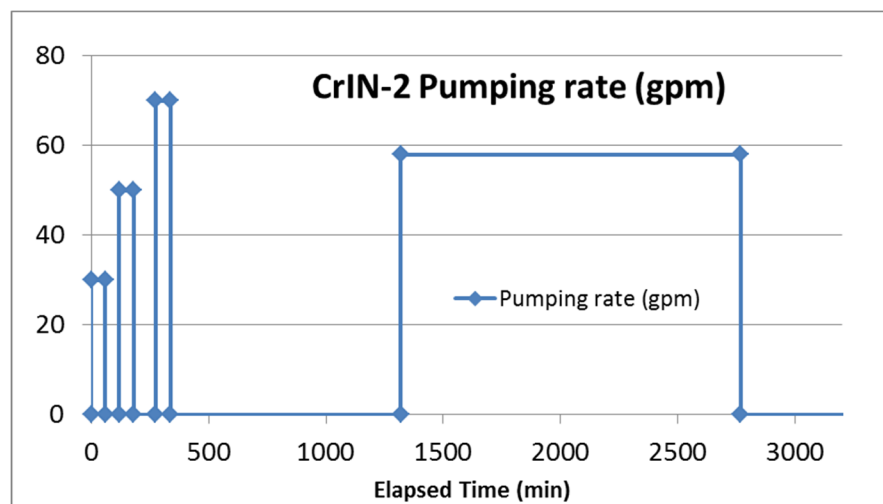
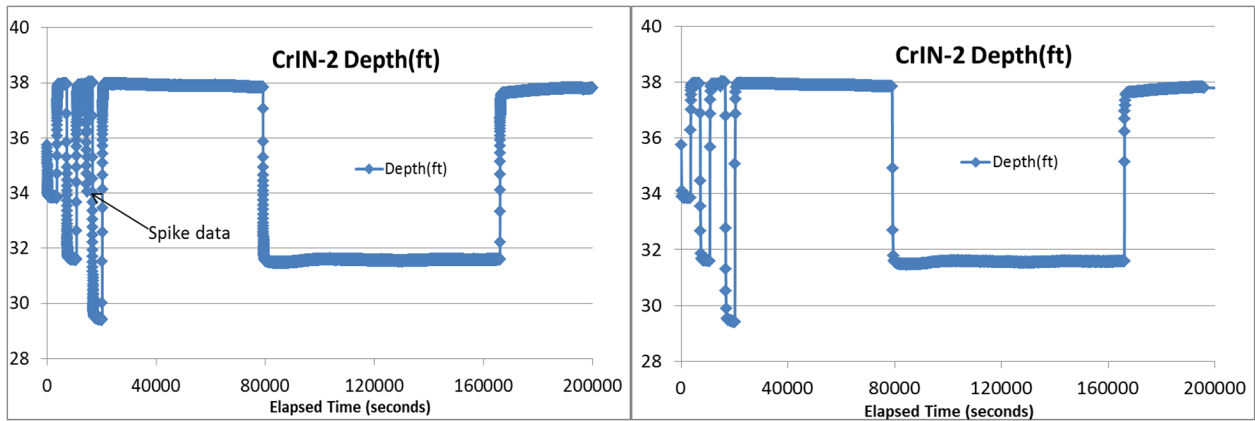
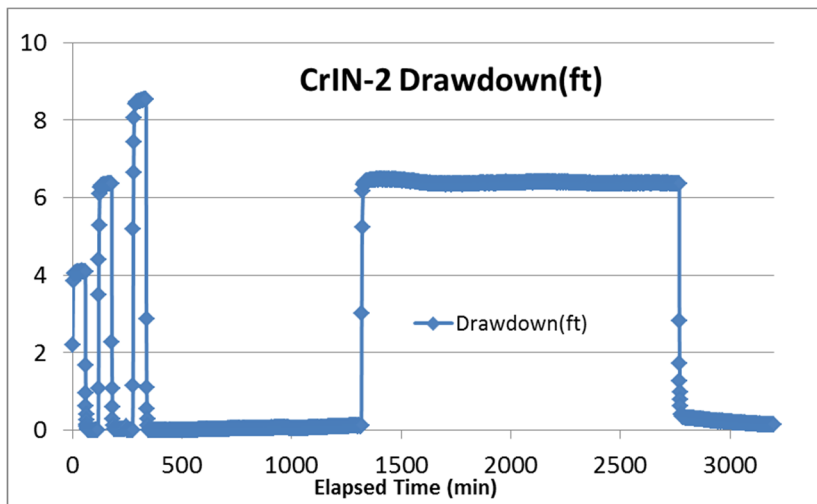


Figure D-5 Variable pumping rates for the test at well CrIN-2



**Figure D-6** Measured water-depth data with spikes (left) and corrected water-depth data (right) from the pumping test of well CrIN-2



**Figure D-7** Corrected drawdown data from the pumping test of well CrIN-2



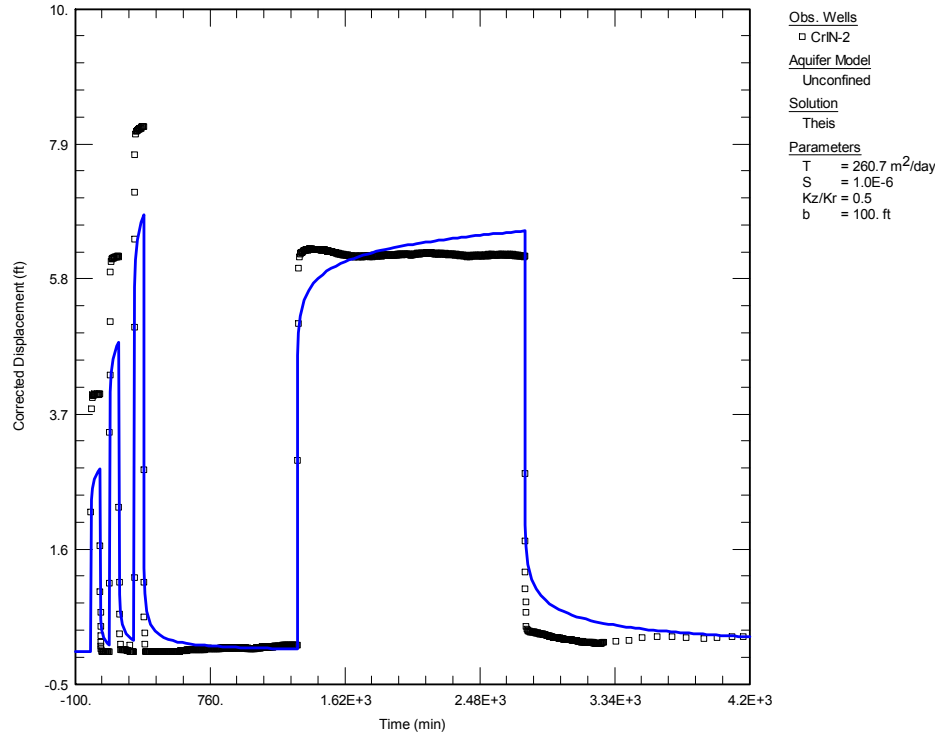


**Figure D-8 Matching observed drawdowns (black dots) during the four-step CrIN-2 test using the Theis model (blue line)**

**Table D-4  
CrIN-2 Well Structure and Pumping Test Data Applied in the Pumping Test Analyses**

Data Set: E:\EP2016\AquiferTest\CrIN\CrIN-2-Theis1.aqt Date: 09/14/16 Time: 18:04:07																																			
<b>PROJECT INFORMATION</b>																																			
Company: LANL Client: zd Project: ep Location: Puye Test Date: 2016 Test Well: CrIN-2																																			
<b>AQUIFER DATA</b>																																			
Saturated Thickness: 100. ft Anisotropy Ratio (Kz/Kr): 0.5																																			
<b>PUMPING WELL DATA</b>																																			
No. of pumping wells: 1																																			
Pumping Well No. 1: CrIN-2																																			
X Location: 0. ft																																			
Y Location: 0. ft																																			
Casing Radius: 8.625 ft																																			
Well Radius: 8. ft																																			
Partially Penetrating Well																																			
Depth to Top of Screen: 36. ft																																			
Depth to Bottom of Screen: 86. ft																																			
No. of pumping periods: 9																																			
<table border="1"> <thead> <tr> <th colspan="2"></th> <th colspan="2">Pumping Period Data</th> <th colspan="2"></th> </tr> <tr> <th>Time (min)</th> <th>Rate (gal/min)</th> <th>Time (min)</th> <th>Rate (gal/min)</th> <th>Time (min)</th> <th>Rate (gal/min)</th> </tr> </thead> <tbody> <tr> <td>0.</td> <td>30.</td> <td>179.2</td> <td>0.</td> <td>1318.</td> <td>58.</td> </tr> <tr> <td>59.17</td> <td>0.</td> <td>274.</td> <td>70.</td> <td>2768.3</td> <td>0.</td> </tr> <tr> <td>119.3</td> <td>50.</td> <td>336.2</td> <td>0.</td> <td>4271.</td> <td>0.</td> </tr> </tbody> </table>								Pumping Period Data				Time (min)	Rate (gal/min)	Time (min)	Rate (gal/min)	Time (min)	Rate (gal/min)	0.	30.	179.2	0.	1318.	58.	59.17	0.	274.	70.	2768.3	0.	119.3	50.	336.2	0.	4271.	0.
		Pumping Period Data																																	
Time (min)	Rate (gal/min)	Time (min)	Rate (gal/min)	Time (min)	Rate (gal/min)																														
0.	30.	179.2	0.	1318.	58.																														
59.17	0.	274.	70.	2768.3	0.																														
119.3	50.	336.2	0.	4271.	0.																														
<b>OBSERVATION WELL DATA</b>																																			
No. of observation wells: 1																																			
Observation Well No. 1: CrIN-2																																			
X Location: 0. ft																																			
Y Location: 0. ft																																			
Radial distance from CrIN-2: 0. ft																																			
Partially Penetrating Well																																			
Depth to Top of Screen: 36. ft																																			

**Table D-5**  
**Estimated Parameters Using the Theis Model for CrIN-2**

Aquifer Model: Unconfined					
Solution Method: Theis					
<u>Estimated Parameters</u>					
<u>Parameter</u>	<u>Estimate</u>	<u>Std. Error</u>	<u>Approx. C.I.</u>	<u>t-Ratio</u>	
T	260.7	9.26	+/- 18.18	28.15	m <sup>2</sup> /day
S	1.0E-6	3.266E-6	+/- 6.412E-6	0.3062	
Kz/Kr	0.5	2.16	+/- 4.241	0.2314	
b	100.	not estimated			ft
C.I. is approximate 95% confidence interval for parameter					
t-ratio = estimate/std. error					
No estimation window					
K = T/b = 8.552 m/day (0.009898 cm/sec)					
Ss = S/b = 1.0E-8 1/ft					
<u>Parameter Correlations</u>					
	<u>T</u>	<u>S</u>	<u>Kz/Kr</u>		
T	1.00	0.15	-0.33		
S	0.15	1.00	-0.98		
Kz/Kr	-0.33	-0.98	1.00		
<u>Residual Statistics</u>					
for weighted residuals					
Sum of Squares	....	227.2	ft <sup>2</sup>		
Variance	.....	0.2744	ft <sup>2</sup>		
Std. Deviation	.....	0.5238	ft		
Mean	.....	-0.06096	ft		
No. of Residuals	....	831			
No. of Estimates	....	3			

**Table D-6  
Estimated Parameters Using the Neuman Model for CrIN-2**

Aquifer Model: Unconfined Solution Method: Neuman					
<u>Estimated Parameters</u>					
<u>Parameter</u>	<u>Estimate</u>	<u>Std. Error</u>	<u>Approx. C.I.</u>	<u>t-Ratio</u>	m <sup>2</sup> /day
T	99.28	14.05	+/- 27.57	7.069	
S	0.00116	0.0003273	+/- 0.0006425	3.544	
Sy	0.32	0.2009	+/- 0.3943	1.593	
β	0.003434	0.002067	+/- 0.004058	1.661	
C.I. is approximate 95% confidence interval for parameter t-ratio = estimate/std. error No estimation window					
K = T/b = 3.257 m/day (0.00377 cm/sec) Ss = S/b = 1.16E-5 1/ft					
<u>Parameter Correlations</u>					
	T	S	Sy	β	
T	1.00	-0.97	-0.99	-1.00	
S	-0.97	1.00	0.97	0.97	
Sy	-0.99	0.97	1.00	0.99	
β	-1.00	0.97	0.99	1.00	
<u>Residual Statistics</u>					
for weighted residuals					
Sum of Squares . . . . 79.19 ft <sup>2</sup>					
Variance . . . . . 0.09576 ft <sup>2</sup>					
Std. Deviation . . . . . 0.3094 ft					
Mean . . . . . -0.01445 ft					
No. of Residuals . . . . 831					
No. of Estimates . . . . 4					

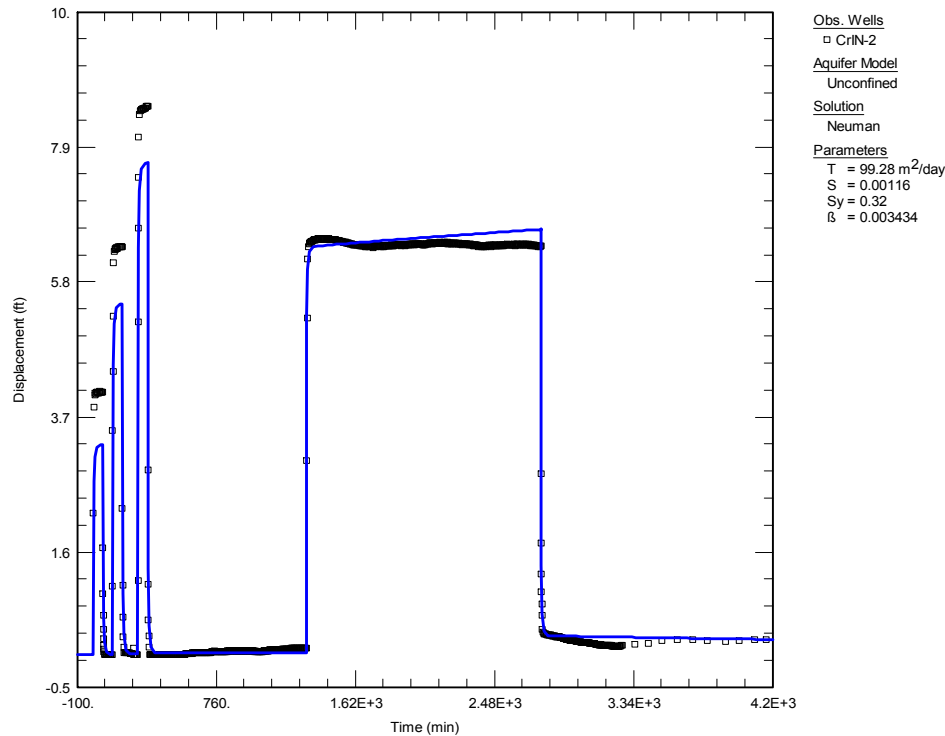


**Figure D-9** Matching of the observed drawdowns (black dots) during the four-step CrIN-2 test using the Neuman model (blue line)

#### D-4.0 CRIN-3

The pumping test at CrIN-3 was conducted from September 8 to 11, 2016 (the latest test in a series of five pumping tests), and the pump was run at multiple steps with various constant pumping rates. This well was drilled with an angle of 17 degrees vertically. The contact depths for the stratigraphy and screen are in linear feet along borehole length (the actual depths can be estimated by accounting for the well angle). During the test, detailed pumping rate observations were recorded with a about 5-min frequency (Figure D-10). The pump was started from 7:43 on September 8 at rates varying from 46 to 55 gpm for about 1 h (step 1); at 8:46, the rate increased to about 55–64 gpm for about 1 h (step 2), and then at 9:46, the pumping went to step 3. The rates increased continuously to about 71–82 gpm for another hour. At 10:46, the pump was stopped for about 4 h of recovery and was restarted with a nearly constant rate of 81 gpm for 24 h. Finally, the pump was stopped for about 1.5 d of recovery (Figure D-10).

Figure D-11 (left) shows some artificial spikes in the observation data at the pump starting stage. The spikes were located and removed and the cleaned-up water-level data are shown in Figure D-11 (right). The observed multistep water depths were converted to corrected displacements or drawdowns (in feet) and used to estimate the parameter (Figure D-12).

First, the variable-rate Theis model was used to fit the multistep observation data. The multistep variable pumping rates and parameter estimation results are shown in Tables D-7 and D-8. The estimated hydraulic conductivity is 31.56 m/d and the storage coefficient is  $10^{-6}$ . The computed drawdowns during the first three pumping steps and the recovery period are shown in Figure D-13.

Next, the variable-rate Neuman model was used to estimate the parameter based on the observation data (Figure D-14). By considering the delayed gravity response of the unconfined aquifer, the Neuman model can simulate well the multistep pumping test processes, and the computed drawdowns fit the observation data slightly better. The estimated parameters are listed in Table D-9: conductivity is 14.87 m/d, storage coefficient is 0.0102, and specific yield is  $p$  (specific yield is during the parameter estimation process is limited to the expected maximum porosity of the Puye Formation, which is equal to 0.32). The parameter  $\beta$  coefficient is 0.00064, and in this model, the ratio of  $\frac{K_z}{K_r}$  is equal to 0.1. The objective function (or sum of squares) is reduced from 29.56, which was obtained from the Theis model, to 24.92.

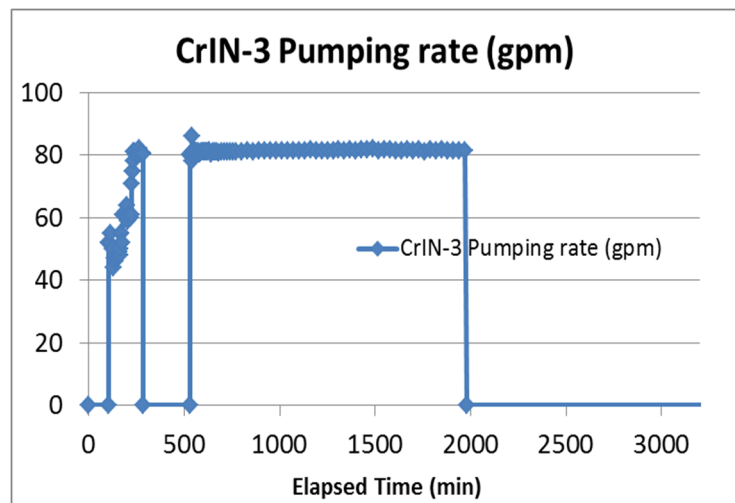


Figure D-10 Variable pumping rates for the test at well CrIN-3

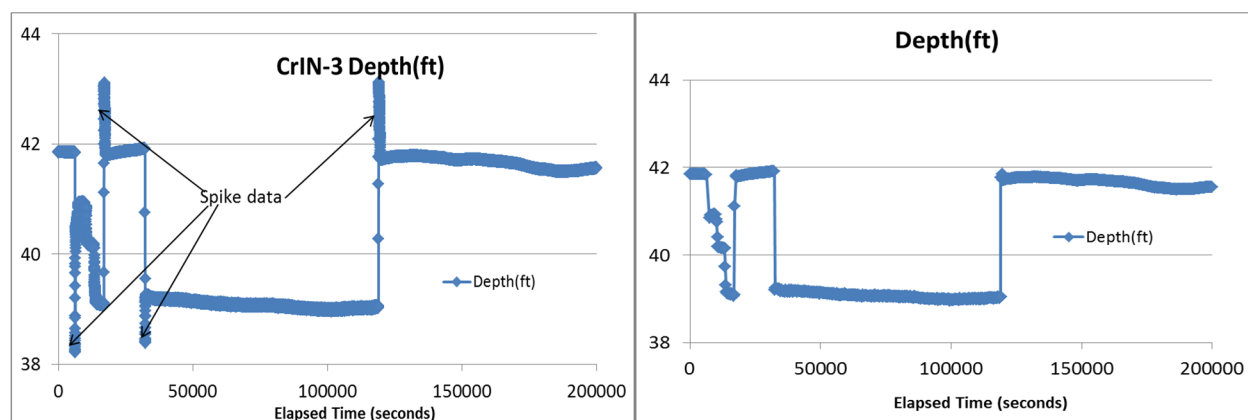


Figure D-11 Measured water-depth data with spikes (left) and corrected water-depth data (right) from the pumping test of well CrIN-3

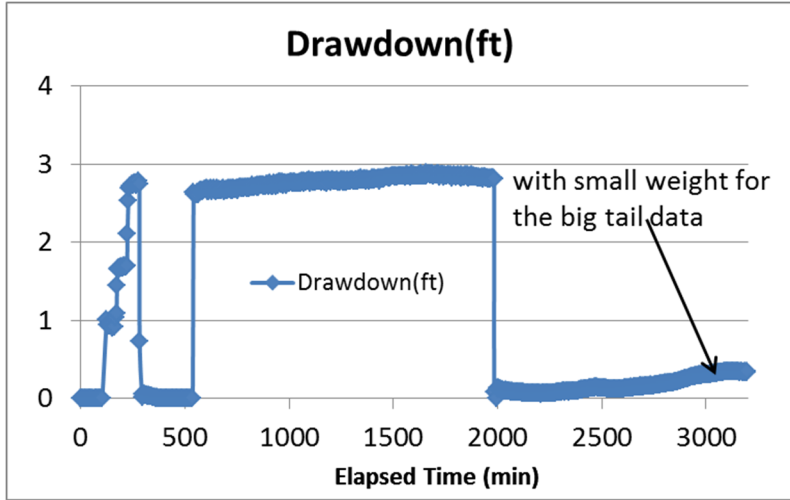


Figure D-12 Corrected drawdown data from the pumping test of well CrIN-3

**Table D-7  
CrIN-3 Well Structure and Pumping Test Data Applied in the Pumping Test Analyses**

Data Set: E:\EP2016\AquiferTest\CrIN\CrIN-3-Theis1.aqt Title: CrIN-3 Pumping Test Date: 11/01/16 Time: 14:29:14					
<b>PROJECT INFORMATION</b>					
Company: LANL Client: zd Project: ep Location: Puye Test Date: 2016 Test Well: CrIN-3					
<b>AQUIFER DATA</b>					
Saturated Thickness: 100. ft Anisotropy Ratio (Kz/Kr): 0.1					
<b>PUMPING WELL DATA</b>					
No. of pumping wells: 1					
Pumping Well No. 1: CrIN-3					
X Location: 0. ft Y Location: 0. ft					
Casing Radius: 8.625 ft Well Radius: 8. ft					
Partially Penetrating Well Depth to Top of Screen: 36. ft Depth to Bottom of Screen: 86. ft					
No. of pumping periods: 142					
<b>Pumping Period Data</b>					
<u>Time (min)</u>	<u>Rate (gal/min)</u>	<u>Time (min)</u>	<u>Rate (gal/min)</u>	<u>Time (min)</u>	<u>Rate (gal/min)</u>
0.	1.0E-8	283.1	0.	725.	81.2
0.	1.0E-9	527.9	0.	740.	81.1
103.	1.0E-9	528.	80.	755.	81.1
103.	0.	530.	80.	770.	81.1
105.	0.	531.	80.	800.	81.2
108.	52.	532.5	80.	830.	81.3
116.	55.	533.	80.	860.	81.2
122.	50.	534.	80.	890.	81.4
128.	44.	535.	80.	920.	81.3
135.	47.	536.	80.	950.	81.3
140.	46.	537.	80.	980.	81.5
145.	47.	538.	80.	1010.	81.5
150.	48.	539.	86.	1040.	81.4
155.	48.	540.	78.	1070.	81.6
160.	49.	541.	80.	1100.	81.4
165.	48.	542.	80.	1130.	81.6
166.	50.	543.	80.	1160.	81.7
167.	55.	544.	81.	1190.	81.6
168.	55.	545.	81.	1220.	81.6
171.	55.	547.	80.5	1250.	81.5
175.	52.	549.	81.	1280.	81.6
176.	52.	551.	80.5	1310.	81.7
178.	61.	553.	80.	1340.	81.4



**Table D-8**  
**Estimated Parameters Using the Theis Model for CrIN-3**

Aquifer Model: Unconfined					
Solution Method: Theis					
<u>Estimated Parameters</u>					
<u>Parameter</u>	<u>Estimate</u>	<u>Std. Error</u>	<u>Approx. C.I.</u>	<u>t-Ratio</u>	
T	961.8	45.16	+/- 88.65	21.3	m <sup>2</sup> /day
S	1.0E-6	0.05029	+/- 0.09872	1.989E-5	
Kz/Kr	0.1	5570.7	+/- 1.094E+4	1.795E-5	
b	100.	not estimated			ft
C.I. is approximate 95% confidence interval for parameter					
t-ratio = estimate/std. error					
No estimation window					
K = T/b = 31.56 m/day (0.03652 cm/sec)					
Ss = S/b = 1.0E-8 1/ft					
<u>Parameter Correlations</u>					
	<u>T</u>	<u>S</u>	<u>Kz/Kr</u>		
T	1.00	-0.24	0.24		
S	-0.24	1.00	-1.00		
Kz/Kr	0.24	-1.00	1.00		
<u>Residual Statistics</u>					
for weighted residuals					
Sum of Squares	....	29.56	ft <sup>2</sup>		
Variance	.....	0.03863	ft <sup>2</sup>		
Std. Deviation	.....	0.1966	ft		
Mean	.....	-0.04677	ft		
No. of Residuals	....	768			
No. of Estimates	....	3			

**Table D-9  
Estimated Parameters Using the Neuman Model for CrIN-3**

Aquifer Model: Unconfined Solution Method: Neuman					
<u>Estimated Parameters</u>					
<u>Parameter</u>	<u>Estimate</u>	<u>Std. Error</u>	<u>Approx. C.I.</u>	<u>t-Ratio</u>	m <sup>2</sup> /day
T	453.3	2.237	+/- 4.392	202.6	
S	0.01019	0.001035	+/- 0.002033	9.84	
Sy	0.32	0.07128	+/- 0.1399	4.489	
β	0.00064	not estimated			
C.I. is approximate 95% confidence interval for parameter t-ratio = estimate/std. error No estimation window  K = T/b = 14.87 m/day (0.01721 cm/sec) Ss = S/b = 0.0001019 1/ft					
<u>Parameter Correlations</u>					
	<u>T</u>	<u>S</u>	<u>Sy</u>		
T	1.00	-0.50	-0.68		
S	-0.50	1.00	0.45		
Sy	-0.68	0.45	1.00		
<u>Residual Statistics</u>					
for weighted residuals					
Sum of Squares . . . . 24.92 ft <sup>2</sup>					
Variance . . . . . 0.03258 ft <sup>2</sup>					
Std. Deviation . . . . . 0.1805 ft					
Mean . . . . . -0.03723 ft					
No. of Residuals . . . . 768					
No. of Estimates . . . . 3					

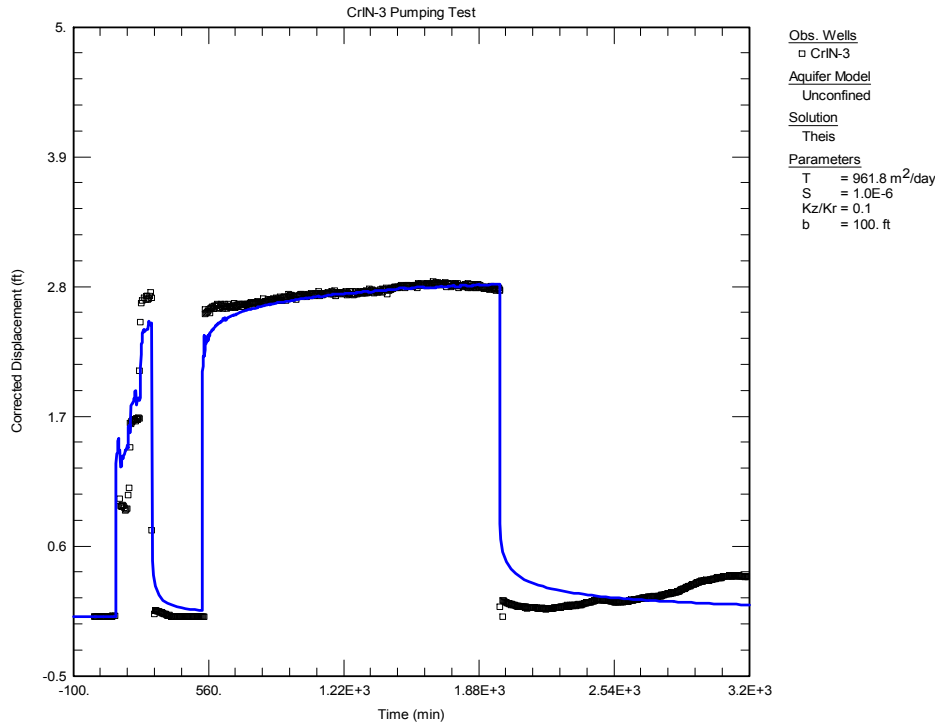


**Figure D-13 Matching observed drawdowns (black dots) during the four-step CrIN-3 test using the Theis model (blue line)**

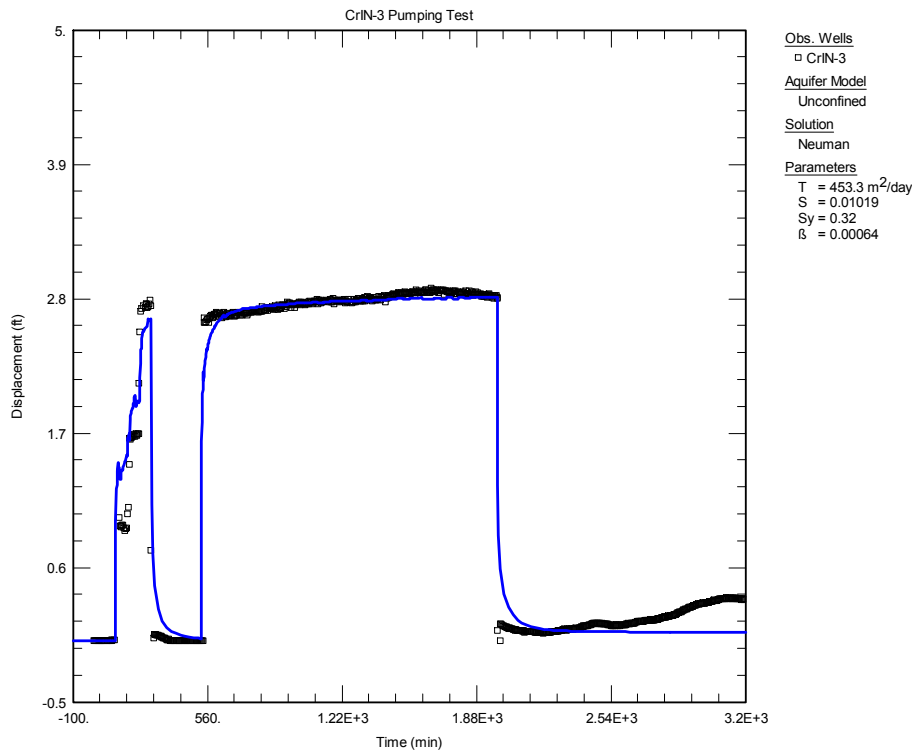


**Figure D-14 Matching observed drawdowns (black dots) during the four-step CrIN-3 test using the Neuman model (blue line)**

### D-5.0 CRIN-4

The observation at CrIN-4 occurred from June 21 to 23, 2016, and multistep pumping was started at 9:58 am on June 21 with a pumping rate of 38 gpm for about 1 h, after which the rate was increased to 60 gpm for another hour and to 75 gpm for another hour. The pump was then stopped for a recovery of 2 h. The pump was restarted with a constant rate of 62 gpm for 24 h. Finally, the pump was stopped for a recovery of about 1 d until 14:58 on June 23. The pumping and recovery processes are shown in Figure D-15.

Figure D-16 (left) shows some artificial spikes in the observation data at the pump starting and stopping stages. The spikes were located and removed, and the corrected water-depth data are shown in Figure D-16 (right). The corrected water depths were converted to displacements or drawdowns (in feet) and were used for parameter estimation (Figure D-17).

It should be noted that this well was drilled with an angle of 11 degrees vertically. The contact depths for the stratigraphy and screen are in linear feet along borehole length. The screen was designed from depth 1083 ft to 1133 ft bgs with a length of 50 ft. When the well angle is taken into account, the depths below ground surface can be used to compute the actual vertical depths below the ground surface.

The variable-rate Theis model was used to simulate the multistep pumping test. The multistep variable pumping rates and parameter estimation results are shown in Tables D-10 and D-11. The estimated hydraulic conductivity is 15.61 m/d and the storage coefficient is  $10^{-6}$ . The computed drawdowns during the first three steps and the recovery time do not fit the observation data very well (with an objective function value or sum of squares of 128.1) (Figure D-18).

The variable-rate Neuman model was used to fit the observation data (Figure D-19). By considering the delayed gravity response of the unconfined aquifer, the Neuman model can simulate well the multistep pumping test processes and the computed drawdowns fit the observation data better. The estimated parameters are listed in Table D-12, in which the conductivity is 5.84 m/d, storage coefficient is 0.00656, and specific yield is 0.32 (specific yield is during the parameter estimation process is limited to the expected maximum porosity of the Puye Formation, which is equal to 0.32). The parameter  $\beta$  coefficient is 0.002449, and in this model, the ratio of  $\frac{K_z}{K_r}$  is equal to 0.383. The objective function is reduced from 128.1, which was obtained from the Theis model, to 75.2.

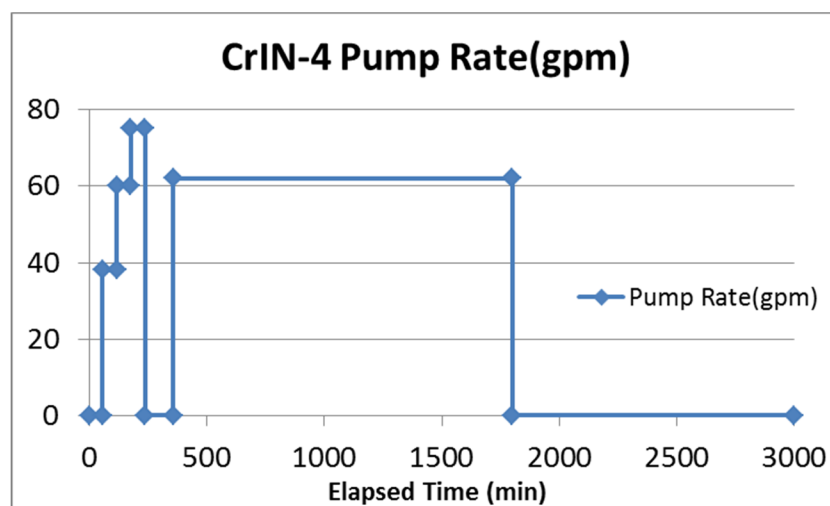
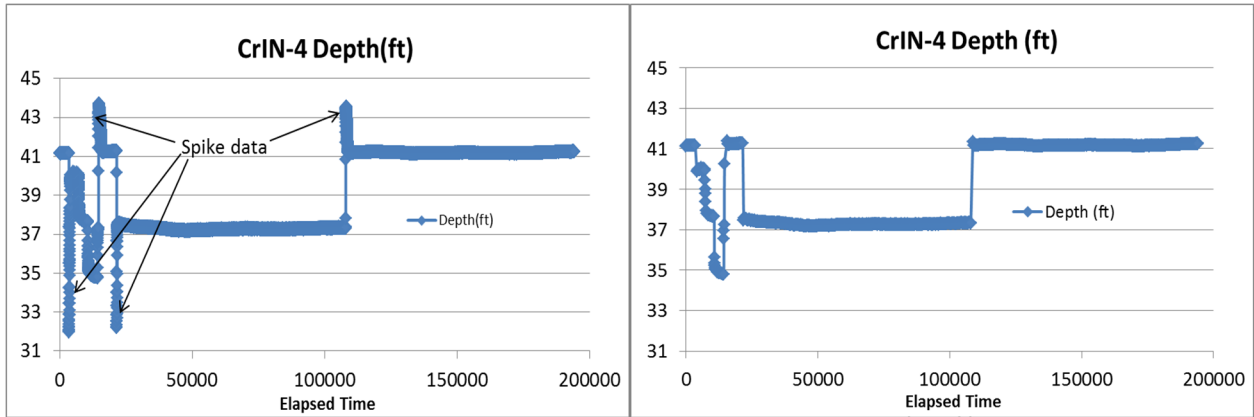
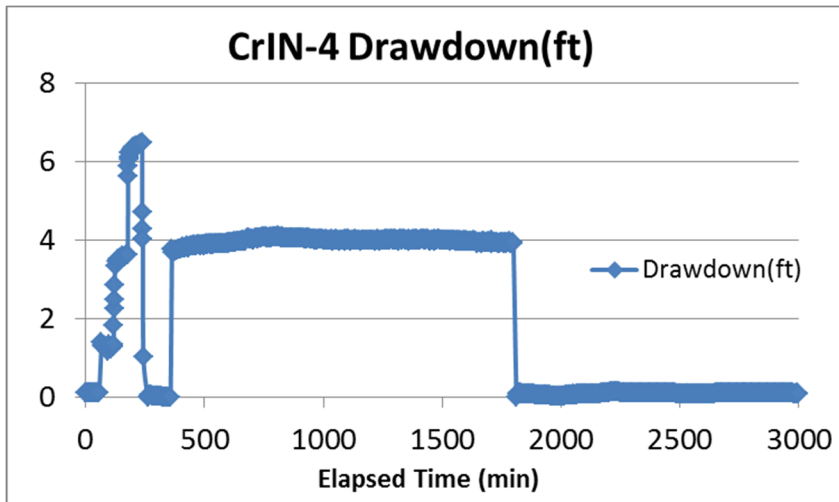


Figure D-15 Variable pumping rates for the test at well CrIN-4



**Figure D-16** Measured water-depth data with spikes (left) and corrected water-depth data (right) from the pumping test of well CrIN-4 (elapsed time = seconds)



**Figure D-17** Corrected drawdown data from the pumping test of well CrIN-4

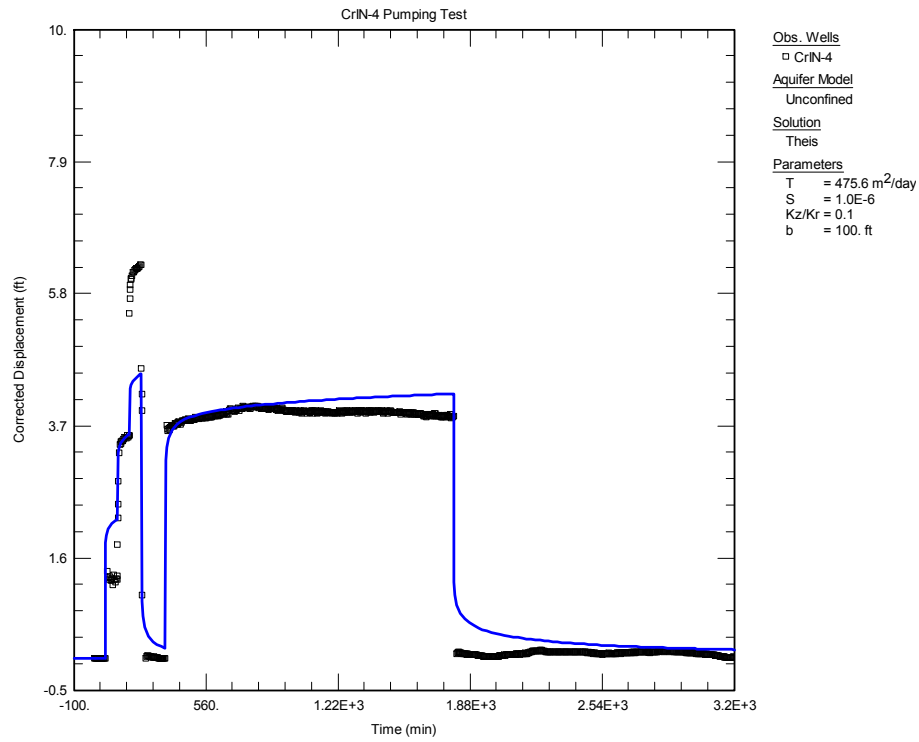


**Figure D-18** Matching of the observed drawdowns (black dots) during the four-step CrIN-4 test using the Theis model (blue line)

**Table D-10  
CrIN-4 Well Structure and Pumping Test Data Applied in the Pumping Test Analyses**

Data Set: E:\EP2016\AquiferTest\CrIN\CrIN-4-Theis1.aqt Title: CrIN-4 Pumping Test Date: 10/06/16 Time: 10:31:22					
<u>PROJECT INFORMATION</u>					
Company: LANL Client: zd Project: ep Location: Puye Test Date: 2016 Test Well: CrIN-4					
<u>AQUIFER DATA</u>					
Saturated Thickness: 100. ft Anisotropy Ratio (Kz/Kr): 0.1					
<u>PUMPING WELL DATA</u>					
No. of pumping wells: 1					
<u>Pumping Well No. 1: CrIN-4</u>					
X Location: 0. ft Y Location: 0. ft					
Casing Radius: 8.625 ft Well Radius: 8. ft					
Partially Penetrating Well Depth to Top of Screen: 36. ft Depth to Bottom of Screen: 86. ft					
No. of pumping periods: 13					
<u>Pumping Period Data</u>					
<u>Time (min)</u>	<u>Rate (gal/min)</u>	<u>Time (min)</u>	<u>Rate (gal/min)</u>	<u>Time (min)</u>	<u>Rate (gal/min)</u>
0.	1.0E-8	177.7	60.	357.5	62.
57.4	0.	177.7	75.	1799.3	0.
57.5	38.	237.8	75.	3000.	0.
118.2	38.	237.8	0.		
118.2	60.	357.4	0.		
<u>OBSERVATION WELL DATA</u>					
No. of observation wells: 1					
<u>Observation Well No. 1: CrIN-4</u>					
X Location: 0. ft Y Location: 0. ft					
Radial distance from CrIN-4: 0. ft					
Partially Penetrating Well Depth to Top of Screen: 36. ft Depth to Bottom of Screen: 86. ft					

**Table D-11  
Estimated Parameters Using the Theis Model for CrIN-4**

Aquifer Model: Unconfined Solution Method: Theis					
<u>VISUAL ESTIMATION RESULTS</u>					
<u>Estimated Parameters</u>					
<u>Parameter</u>	<u>Estimate</u>				
T	474.3	m <sup>2</sup> /day			
S	1.0E-6				
Kz/Kr	0.1				
b	100.	ft			
K = T/b = 15.56 m/day (0.01801 cm/sec) Ss = S/b = 1.0E-8 1/ft					
<u>AUTOMATIC ESTIMATION RESULTS</u>					
<u>Estimated Parameters</u>					
<u>Parameter</u>	<u>Estimate</u>	<u>Std. Error</u>	<u>Approx. C.I.</u>	<u>t-Ratio</u>	
T	475.6	32.2	+/- 63.21	14.77	m <sup>2</sup> /day
S	1.0E-6	0.2609	+/- 0.5121	3.833E-6	
Kz/Kr	0.1	2.89E+4	+/- 5.673E+4	3.46E-6	
b	100.	not estimated			ft
C.I. is approximate 95% confidence interval for parameter t-ratio = estimate/std. error No estimation window  K = T/b = 15.61 m/day (0.01806 cm/sec) Ss = S/b = 1.0E-8 1/ft					
<u>Parameter Correlations</u>					
	<u>T</u>	<u>S</u>	<u>Kz/Kr</u>		
T	1.00	-0.36	0.36		
S	-0.36	1.00	-1.00		
Kz/Kr	0.36	-1.00	1.00		
<u>Residual Statistics</u>					
for weighted residuals					
Sum of Squares . . . . 128.1 ft <sup>2</sup>					
Variance . . . . . 0.1924 ft <sup>2</sup>					
Std. Deviation . . . . . 0.4386 ft					
Mean . . . . . -0.09789 ft					
No. of Residuals . . . . 669					
No. of Estimates . . . . 3					



**Table D-12**  
**Estimated Parameters Using the Neuman Model for CrIN-4**

Aquifer Model: Unconfined Solution Method: Neuman					
<u>Estimated Parameters</u>					
<u>Parameter</u>	<u>Estimate</u>	<u>Std. Error</u>	<u>Approx. C.I.</u>	<u>t-Ratio</u>	<u>m<sup>2</sup>/day</u>
T	178.	23.36	+/- 45.85	7.621	
S	0.006561	0.0019	+/- 0.00373	3.452	
Sy	0.32	0.2017	+/- 0.396	1.586	
β	0.002449	0.00147	+/- 0.002886	1.666	
C.I. is approximate 95% confidence interval for parameter t-ratio = estimate/std. error No estimation window					
K = T/b = 5.839 m/day (0.006759 cm/sec) Ss = S/b = 6.561E-5 1/ft					
<u>Parameter Correlations</u>					
	<u>T</u>	<u>S</u>	<u>Sy</u>	<u>β</u>	
T	1.00	-0.92	-0.98	-1.00	
S	-0.92	1.00	0.91	0.91	
Sy	-0.98	0.91	1.00	0.98	
β	-1.00	0.91	0.98	1.00	
<u>Residual Statistics</u>					
for weighted residuals					
Sum of Squares . . . . 75.23 ft <sup>2</sup>					
Variance . . . . . 0.1131 ft <sup>2</sup>					
Std. Deviation . . . . . 0.3363 ft					
Mean . . . . . -0.09209 ft					
No. of Residuals . . . . 669					
No. of Estimates . . . . 4					

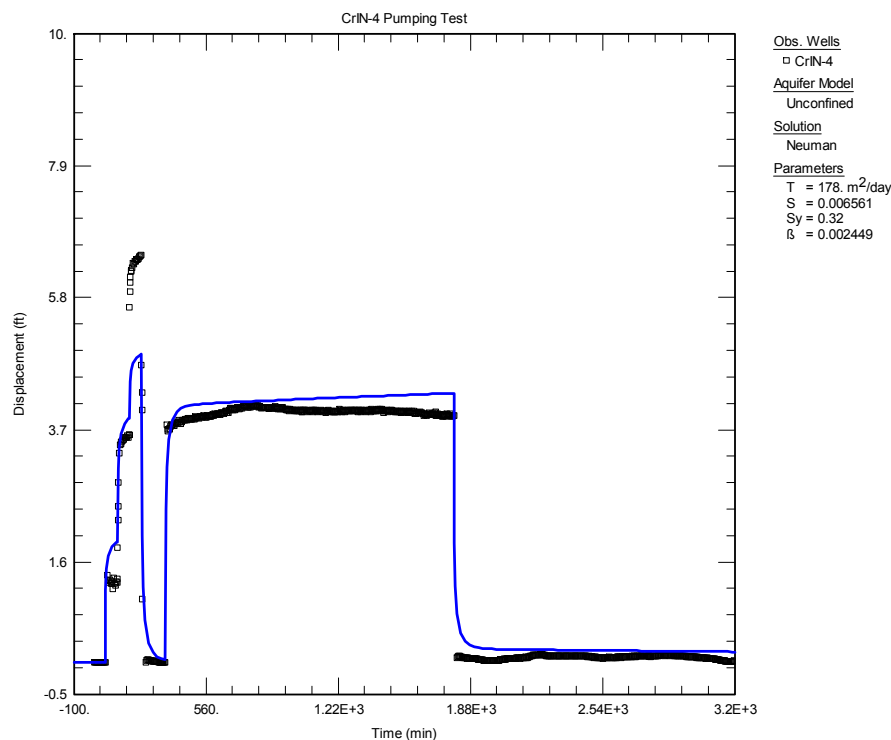


**Figure D-19 Matching observed drawdowns (black dots) during the four-step CrIN-4 test using the Neuman model (blue line)**

### D-6.0 CRIN-5

The well CrIN-5 was drilled with an angle of 25 degrees vertically. The screen was placed within the Puye Formation from 1162 to 1222 ft bgs with a length of 60 ft. Taking into account the well angle, the below ground surface depths can be applied to compute the actual vertical depths below the ground surface. The observation at CrIN-5 occurred from August 3 to 5, 2016, and the multistep pumping was started at 9:59 on August 3, with a pumping rate of 32 gpm for about 1 h, after which the rate increased to 50 gpm for another hour and 68 gpm for another hour. The pump was then stopped for a recovery of 2 h. The pump was restarted with a constant rate of 61 gpm for 24 h and was finally stopped for a recovery of about 1 d until 13:01 on August 5. The pumping and recovery processes are shown in Figure D-20.

Figure D-21 (left) shows some artificial spikes in the observation data at the pump starting and stopping stages. The spikes were located and removed, and the corrected data are presented in Figure D-21 (right). The observed water depths were converted to corrected displacements or drawdowns (in feet) and then used for parameter estimation (Figure D-22).

The variable-rate Theis model is used to simulate approximately the multistep pumping test. The multistep variable pumping rates and parameter estimation results are shown in Tables D-13 and D-14. The estimated hydraulic conductivity is 11.87 m/d and the storage coefficient is  $10^{-6}$ . The computed drawdowns during the first three steps and recovery time do not fit the observation data very well (with an objective function value or sum of squares of 166.7) (Figure D-23).

The variable-rate Neuman model was then used to estimate the hydraulic parameters and to fit the observation data (Figure D-24). By considering the delayed gravity response of the unconfined aquifer,

the Neuman model can simulate well the multistep pumping test processes and the computed drawdowns match the observation data better. The estimated parameters are listed in Table D-15: conductivity is 5.97 m/d, storage coefficient is 0.000014, and specific yield is 0.23. The parameter  $\beta$  coefficient is 0.00034, and in this model, the ratio of  $\frac{K_z}{K_r}$  is equal to 0.05. The objective function is reduced more than half from 166.7, which was obtained from the Theis model, to 76.3.

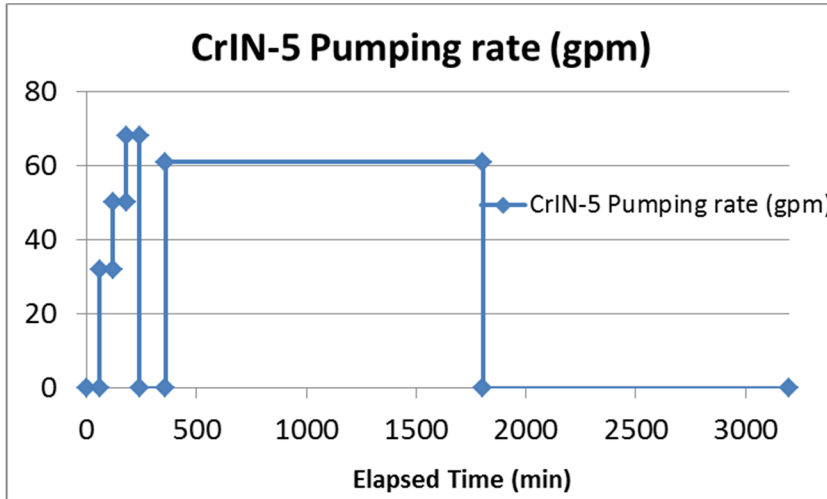


Figure D-20 Variable pumping rates for the test at well CrIN-5

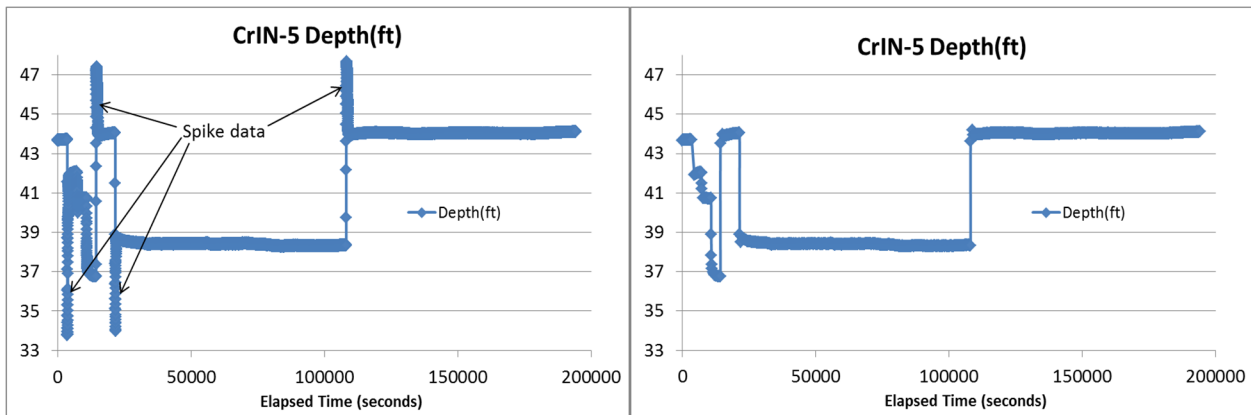


Figure D-21 Measured water-depth data with spikes (left) and corrected water-depth data (right) from the pumping test of well CrIN-5

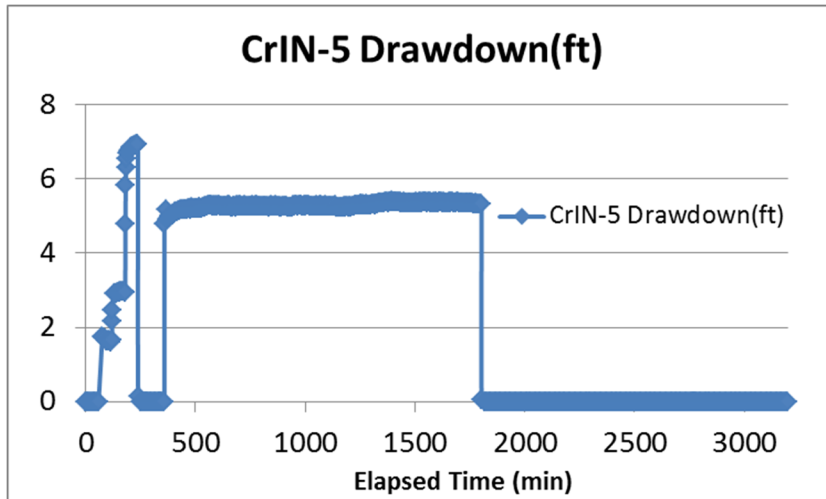


Figure D-22 Corrected drawdown data from the pumping test of well CrIN-5

**Table D-13**  
**CrIN-5 Well Structure and Pumping Test Data Applied in the Pumping Test Analyses**

Data Set: E:\EP2016\AquiferTest\CrIN\CrIN-5-Theis1.aqt Title: CrIN-5 Pumping Test Date: 10/07/16 Time: 15:14:21					
<u>PROJECT INFORMATION</u>					
Company: LANL Client: zd Project: ep Location: Puye Test Date: 2016 Test Well: CrIN-4					
<u>AQUIFER DATA</u>					
Saturated Thickness: 100. ft Anisotropy Ratio (Kz/Kr): 0.01					
<u>PUMPING WELL DATA</u>					
No. of pumping wells: 1					
Pumping Well No. 1: CrIN-5					
X Location: 0. ft					
Y Location: 0. ft					
Casing Radius: 8.625 ft					
Well Radius: 8. ft					
Partially Penetrating Well					
Depth to Top of Screen: 36. ft					
Depth to Bottom of Screen: 96. ft					
No. of pumping periods: 14					
<u>Pumping Period Data</u>					
<u>Time (min)</u>	<u>Rate (gal/min)</u>	<u>Time (min)</u>	<u>Rate (gal/min)</u>	<u>Time (min)</u>	<u>Rate (gal/min)</u>
0.	1.0E-8	180.3	50.	358.8	61.
58.8	0.	180.3	68.	1802.8	61.
58.83	32.	238.8	68.	1802.8	0.
120.1	32.	238.8	0.	3200.	0.
120.2	50.	358.8	0.		
<u>OBSERVATION WELL DATA</u>					
No. of observation wells: 1					
Observation Well No. 1: CrIN-5					
X Location: 0. ft					
Y Location: 0. ft					
Radial distance from CrIN-5: 0. ft					
Partially Penetrating Well					
Depth to Top of Screen: 36. ft					
Depth to Bottom of Screen: 96. ft					

**Table D-14  
Estimated Parameters with the Theis Model for CrIN-5**

Aquifer Model: Unconfined					
Solution Method: Theis					
<u>VISUAL ESTIMATION RESULTS</u>					
<u>Estimated Parameters</u>					
<u>Parameter</u>	<u>Estimate</u>				
T	355.1	m <sup>2</sup> /day			
S	1.0E-6				
Kz/Kr	0.01				
b	100.	ft			
K = T/b = 11.65 m/day (0.01349 cm/sec)					
Ss = S/b = 1.0E-8 1/ft					
<u>AUTOMATIC ESTIMATION RESULTS</u>					
<u>Estimated Parameters</u>					
<u>Parameter</u>	<u>Estimate</u>	<u>Std. Error</u>	<u>Approx. C.I.</u>	<u>t-Ratio</u>	
T	361.7	13.08	+/- 25.69	27.65	m <sup>2</sup> /day
S	1.0E-6	3.652E-7	+/- 7.172E-7	2.738	
Kz/Kr	0.01	0.005662	+/- 0.01112	1.766	
b	100.	not estimated			ft
C.I. is approximate 95% confidence interval for parameter					
t-ratio = estimate/std. error					
No estimation window					
K = T/b = 11.87 m/day (0.01374 cm/sec)					
Ss = S/b = 1.0E-8 1/ft					
<u>Parameter Correlations</u>					
	<u>T</u>	<u>S</u>	<u>Kz/Kr</u>		
T	1.00	-1.00	-1.00		
S	-1.00	1.00	1.00		
Kz/Kr	-1.00	1.00	1.00		
<u>Residual Statistics</u>					
for weighted residuals					
Sum of Squares . . . . 166.7 ft <sup>2</sup>					
Variance . . . . . 0.258 ft <sup>2</sup>					
Std. Deviation . . . . . 0.5079 ft					
Mean . . . . . -0.2307 ft					
No. of Residuals . . . . 649					
No. of Estimates . . . . 3					

**Table D-15**  
**Estimated Parameters Using the Neuman Model for CrIN-5**

Aquifer Model: Unconfined Solution Method: Neuman					
<u>VISUAL ESTIMATION RESULTS</u>					
<u>Estimated Parameters</u>					
<u>Parameter</u>	<u>Estimate</u>				
T	361.7	m <sup>2</sup> /day			
S	1.0E-6				
Sy	0.2407				
β	0.0003374				
K = T/b = 11.87 m/day (0.01374 cm/sec)					
Ss = S/b = 1.0E-8 1/ft					
<u>AUTOMATIC ESTIMATION RESULTS</u>					
<u>Estimated Parameters</u>					
<u>Parameter</u>	<u>Estimate</u>	<u>Std. Error</u>	<u>Approx. C.I.</u>	<u>t-Ratio</u>	
T	181.9	0.1375	+/- 0.2701	1322.5	m <sup>2</sup> /day
S	1.365E-5	2.165E-6	+/- 4.252E-6	6.305	
Sy	0.2288	0.09752	+/- 0.1915	2.346	
β	0.0003398	1.848E-6	+/- 3.63E-6	183.8	
C.I. is approximate 95% confidence interval for parameter					
t-ratio = estimate/std. error					
No estimation window					
K = T/b = 5.967 m/day (0.006906 cm/sec)					
Ss = S/b = 1.365E-7 1/ft					
<u>Parameter Correlations</u>					
	<u>T</u>	<u>S</u>	<u>Sy</u>	<u>β</u>	
T	1.00	-0.03	-0.55	1.00	
S	-0.03	1.00	0.02	-0.09	
Sy	-0.55	0.02	1.00	-0.59	
β	1.00	-0.09	-0.59	1.00	
<u>Residual Statistics</u>					
for weighted residuals					
Sum of Squares . . . . 76.31 ft <sup>2</sup>					
Variance . . . . . 0.1183 ft <sup>2</sup>					
Std. Deviation . . . . . 0.344 ft					
Mean . . . . . -0.04854 ft					
No. of Residuals . . . . 649					
No. of Estimates . . . . 4					

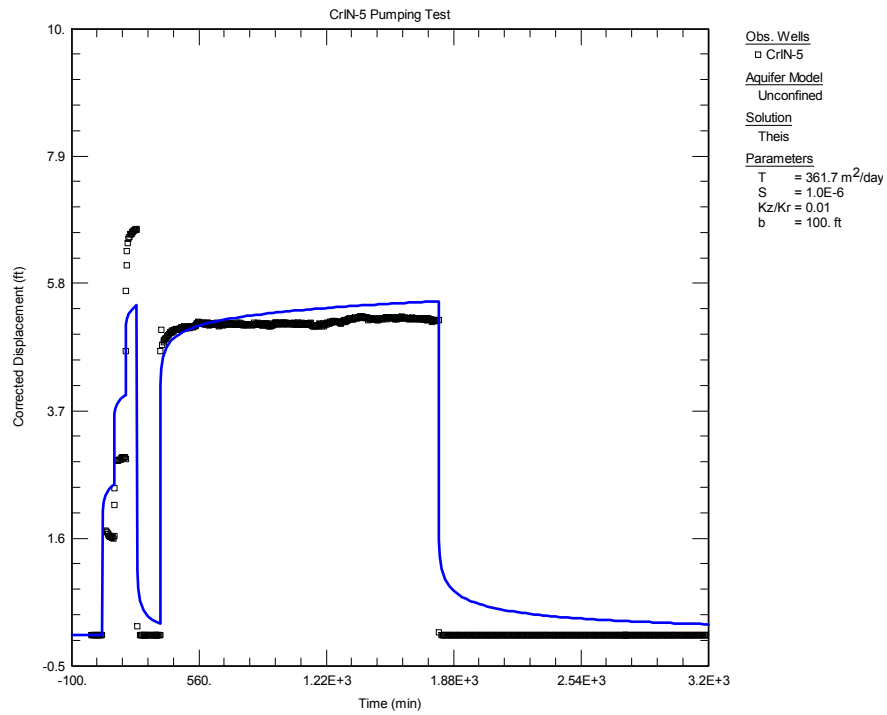


**Figure D-23** Matching observed drawdowns (black dots) during the four-step CrIN-5 test using the Theis model (blue line)

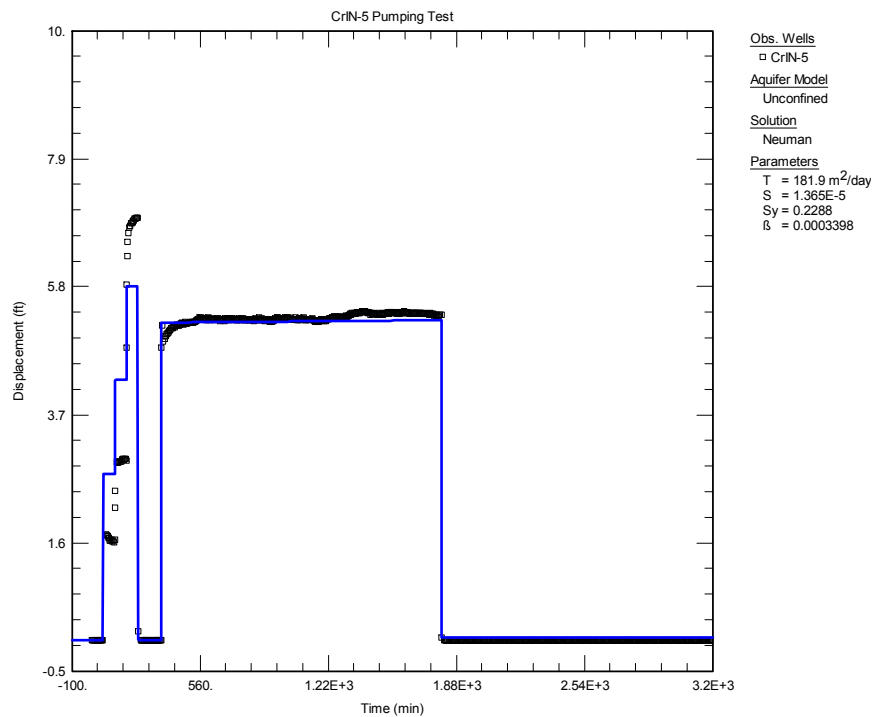


**Figure D-24** Matching of the observed drawdowns (black dots) during the four-step CrIN-5 test using the Neuman model (blue line)



## D-7.0 SUMMARY

A series of pumping tests were conducted on wells CrIN-1, CrIN-2, CrIN-3, CrIN-4, and CrIN-5 at the Laboratory's Chromium site to (1) characterize pumping/injection capabilities of these wells and (2) to gain an understanding of the hydraulic characteristics of the regional aquifer. All the wells are screened in the saturated portion of the Puye Formation. These five sets of pumping test data were used for parameter estimations with two analytical models: the Theis and the Neuman. The estimated parameters from the five tests are summarized in Table D-16.

The aquifer transmissivity estimated using the Theis model are more consistent with previous pumping tests conducted at the site. The aquifer transmissivity estimated using the Neuman model are lower than the Theis estimates primarily because the Neuman model accounts for delayed yield effect from the vadose zone, which causes some aquifer recharge during the pumping tests.

The estimated hydraulic conductivities derived from using the Theis model are consistently smaller than those from using the Neuman model. The estimated average hydraulic conductivities are 14.7 and 6.4 m/d for the Theis and Neuman models, respectively. However, determining hydraulic conductivity of the aquifer materials based on the estimated aquifer transmissivity is uncertain because the effective aquifer thickness during is not known.

The anisotropy factors estimated by both models are similar. The anisotropy factors for the Theis and Neuman models are 0.23 and 0.26, respectively.

The storage coefficients estimated with Theis model are very small ( $10^{-6}$ ), and they are not considered to be realistic because they are based on single-well pumping test analyses.

The specific yield estimates obtained using the Neuman model are uncertain; this parameter was constrained not to exceed the expected maximum porosity of the Puye Formation, which is equal to 0.32; in most of the Neuman analyses the specific yield was close to this maximum value (Table D-16).

The storage coefficients estimated with Neuman model are reasonable (with an average of 0.0037).

Because the Neuman model considers the delayed gravity response of the unconfined aquifer, the computed drawdowns for the five tests match the observation data better than those computed from the Theis model.

The regional water levels reached almost complete recovery at all the CrIN wells after the 24-h pumping was terminated.

**Table D-16**  
**Summary of the Estimated Parameters Using the Theis and Neuman Models**

<b>Model</b>	<b>Parameter</b>	<b>CrIN-1</b>	<b>CrIN-2</b>	<b>CrIN-3</b>	<b>CrIN-4</b>	<b>CrIN-5</b>	<b>Average</b>
	24 h-pumping rate (gpm)	70	58	81.5	62	61	—*
	Drawdown (ft)	13.2	6.4	2.8	4	5.3	—
	Specific capacity (gpm/ft)	5.3	9.1	29.1	15.5	11.5	14.1
Theis (with unconfined correction)	Hydraulic conductivity (m/d)	5.6	8.6	31.6	15.6	11.9	14.7
	Transmissivity (m <sup>2</sup> /d)	172	261	962	476	362	446
	Storage coefficient (-)	10 <sup>-6</sup>	10 <sup>-6</sup>	10 <sup>-6</sup>	10 <sup>-6</sup>	10 <sup>-6</sup>	10 <sup>-6</sup>
	Anisotropy ratio Kz/Kr (-)	0.20	0.50	0.1	0.30	0.05	0.23
Neuman (unconfined)	Hydraulic conductivity (m/d)	2.3	3.3	14.9	5.8	6.0	6.4
	Transmissivity (m <sup>2</sup> /d)	69.2	99.3	453.	178.	182.	196
	Storage coefficient (-)	0.0008	0.00116	0.0102	0.00656	0.000014	0.0037
	Anisotropy ratio Kz/Kr (-)	0.23	0.54	0.1	0.383	0.05	0.26
	Specific yield (-)	0.32	0.32	0.32	0.32	0.23	0.30

\*— = Not calculated.

## D-8.0 REFERENCES

*The following list includes all documents cited in this appendix. Parenthetical information following each reference provides the author(s), publication date, and ERID or ESHID. This information is also included in text citations. ERIDs were assigned by the Environmental Programs Directorate's Records Processing Facility (IDs through 599999), and ESHIDs are assigned by the Environment, Safety, and Health (ESH) Directorate (IDs 600000 and above). IDs are used to locate documents in the Laboratory's Electronic Document Management System and, where applicable, in the master reference set.*

*Copies of the master reference set are maintained at the NMED Hazardous Waste Bureau and the ESH Directorate. The set was developed to ensure that the administrative authority has all material needed to review this document, and it is updated with every document submitted to the administrative authority. Documents previously submitted to the administrative authority are not included.*

Duffield, G.M., June 16, 2007. "AQTESOLV for Windows, Version 4.5, User's Guide," HydroSOLVE, Inc., Reston, Virginia. (Duffield 2007, 601723)

Hantush, M.S., July 1961. "Drawdown around a Partially Penetrating Well," Journal of the Hydraulics Division, Proceedings of the American Society of Civil Engineers, Vol. 87, No. HY 4, pp. 83-98. (Hantush 1961, 098237)

Hantush, M.S., September 1961. "Aquifer Tests on Partially Penetrating Wells," Journal of the Hydraulics Division, Proceedings of the American Society of Civil Engineers, pp. 171-195. (Hantush 1961, 106003)

Neuman, S.P., April 1974. "Effect of Partial Penetration on Flow in Unconfined Aquifers Considering Delayed Gravity Response," Water Resources Research, Vol. 10, No. 2, pp. 303-312. (Neuman 1974, 085421)

Rasmussen, T.C., and L.A. Crawford, 1997. "Identifying and Removing Barometric Pressure Effects in Confined and Unconfined Aquifers," Ground Water, Vol. 35, No. 3, pp. 502-511. (Rasmussen and Crawford 1997, 094014)

Spane, F.A., 2002. "Considering Barometric Pressure in Groundwater Flow Investigations," Water Resources Research, Vol. 38, No. 6, pp. 1-18. (Spane 2002, 602105)

Theis, C.V., 1934-1935. "The Relation Between the Lowering of the Piezometric Surface and the Rate and Duration of Discharge of a Well Using Ground-Water Storage," American Geophysical Union Transactions, Vol. 15-16, pp. 519-524. (Theis 1934-1935, 098241)

